

https://dspace.org/

Hydrogeological study of geological features in the groundwater system of Tweefontein 360KT farm, Limpopo Province

Dalasile, Piwo-kuhle

2018

https://hdl.handle.net/10539/26863

Dalasile, Piwo-kuhle (2018) Hydrogeological study of geological features in the groundwater system of Tweefontein 360KT farm, Limpopo province, University of the Witwatersrand, Johannesburg, https://hdl.handle.net/10539/26863

Downloaded from a DSpace repository. https://dspace.org/

Hydrogeological study of geological features in the groundwater system of Tweefontein 360KT farm, Limpopo Province

Piwo-kuhle Dalasile

Student number: 602304



Submitted in partial fulfillment for the degree of

Master of Science in Hydrogeology

School of Geosciences, Faculty of Science, University of the Witwatersrand

Johannesburg

Supervisor: Prof. Tamiru Abiye (Wits)

July 2018

DECLARATION

I Piwo-kuhle Dalasile declare that ***Hydrogeological study of geological features in the groundwater system of Tweefontein 360KT farm, Limpopo Province*** is my own investigation and covers no section copied in whole or in part from any source unless it is clearly acknowledged in quotation marks and with detailed, complete and precise referencing. Further, the report has not been submitted before for any degree or examination at any university.

…….. (Signature) …… (Date)

ABSTRACT

A hydrogeological study was conducted to investigate the possible influence of geological structures on the groundwater flow (regime) and dynamics at the Tweefontein farm 360KT, near Steelpoort, Limpopo Province. The aim of the investigation was to understand the groundwater system, as well as to devise appropriate measures that promote proper groundwater resource management, which will allow for prediction and mitigation of possible groundwater ingress into underground workings. Field observations, cross sections, borehole data, chemical analyses and environmental stable isotopes were used to understand the influence of geological features on flow dynamics in Tweefontein farm.

Geological features, faults and dykes were found to enhance groundwater flow due to the presence of interconnected cross-cutting joints. Furthermore, weathering was also found to enhance groundwater flow within these structures. Calcrete and ferricrete within the weathered zone can act as a barrier or limit vertical flow of groundwater to the fractured zone, and this can enhance the formation of later flows which may contribute to formation of springs. There is no major ingress of groundwater into existing underground workings near a prominent NE-striking faulted shear zone that is partly overlain by a river. It can be postulated, based on the documentary evidence collected in this study that the inability of water to ingress underground workings overlain by rivers is attributed to depth, as well as the infilling within the prominent NE-striking geological features. Groundwater within the study area shows a Ca-Mg-HCO_3^-dominated water type indicative of fresh, shallow circulating groundwater. However, there also is a chloride-dominated facies showing the strong effect of evaporation within the shallow weathered zone aquifer. The enrichment in Ca and Mg ions may be attributed to weathering of ferromagnesian silicate minerals of the Bushveld Igneous Complex. Highly enriched stable isotope (δ^2H and $\delta^{18}O$) signatures on surface-water and shallow groundwater suggest the presence of evaporation prior to infiltration. Water from mine fissures plot on the local meteoric water line suggesting direct and preferential recharge through geological structures during periods of rainfall in the summer and winter months. Groundwater in deep mine fissures shows a highly depleted isotopic signature compared to water in the shallow weathered aquifer, which suggests limited vertical hydraulic connection.

DEDICATIONS

I would like to send my dedications to the Lord Jesus Christ for His continued guidance and support throughout all this work. I would also like to thank my family, friends and colleagues for their continued support and encouragements during the course of this work.

ACKNOWLEDGEMENTS

I would like to send a big thanks to Samancor Eastern Chrome Mines for granting me the opportunity to use mine data and equipment in writing this report. I also would like to thank all the private owners for making borehole data available for such studies to be done.

I would like to thank Groundwater Resource Information Project (GRIP), Limpopo for making borehole data available. I also thank the Department of Rural Development and Land Reform for providing the GIS data for this work.

I would like to thank my supervisor Prof. Tamiru Abiye for his patience and guidance throughout this project and for imparting very beneficial knowledge.

I also would like to thank all my colleagues for the motivation and for allowing me to undertake this work amidst a busy schedule.

TABLE OF CONTENTS

DECLARATION.....i

ABSTRACT.....ii

DEDICATIONS.....iii

ACKNOWLEDGEMENTS.....iv

CHAPTER 1 1

INTRODUCTION 1

1.1. General Introduction 1

1.2. Background 3

1.3. Hypothesis 5

1.4. Research Question 5

1.5. Aims and Objectives 5

1.6. Structure of the Thesis 6

CHAPTER 2 7

LITERATURE REVIEW 7

2.1. Introduction 7

2.2. The Literature review on Faults and Dykes 7

2.3. Crystalline Basement Rock Aquifers of the Semi-Arid Regions of Southern Africa 11

2.4. Stress-field orientation of the Bushveld Igneous Complex 14

2.5. Hydrogeological Overview of the Bushveld Igneous Complex 16

2.6. Case Studies within the Bushveld Igneous Complex 19

CHAPTER 3 21

STUDY SITE 21

3.1. Description of the study area 21

3.2. Physiography 22

3.3. Climate 25

3.4. Drainage 26

3.5. Regional Geology of the Bushveld Igneous Complex 28

3.6. Geology of the Study Area 32

3.7. Hydrogeology of the study area 39

CHAPTER 4 40

MATERIALS AND METHODS 40

4.1. Introduction 40

4.2. Desktop Research 40

4.3. Field Work 40

4.4. Geological Cross Sections 41
4.5. Borehole Data 41
4.6. Water Chemistry 41
4.7. Environmental Isotopes 44
CHAPTER 5 45
RESULTS AND DISCUSSION 45
5.1. Field Work 45
5.2. Borehole Data 56
5.3. Hydrogeochemistry 71
5.4. Environmental Isotopes 77
5.5. Conceptual Model 80
Chapter 6 82
CONCLUSION AND RECOMMENDATIONS 82
Conclusion 82
Recommendations 84
References 85
Appendices 89

LIST OF FIGURES

Figure 1: The Olifants (East) Basin in Limpopo Province with the study area (Modified after Rashleigh, 2009). 3
Figure 2: Illustrates permeability variations (conduit and barrier effect) within faults (Source: Bense et al., 2013). 9
Figure 3: Illustration of the variations in permeability in the damaged and core zones (Source: Bense et al., 2013). 10
Figure 4: A conceptual cross-section of a basement aquifer (Source: Chilton and Foster (1995)..... 13
Figure 5: Alluvial overburden on a dry tributary near the Steelpoort River (Approximately 12m thick). 17
Figure 6: An aerial photograph showing surface erosion with associated wash-off near Steelpoort River (Source: Google Earth, 2017). 22
Figure 7: Shows the physiography of Tweefontein farm and with the surrounding areas. 23
Figure 8: Surface topography of Tweefontein farm. 24
Figure 9: A graph showing average monthly rainfall and S-Pan evaporation around the town of Steelpoort (Source: Golder Associates, 2006). 25
Figure 10: Annual and monthly volume chart for the Dwars River, from gauge station number B4H009 from October 1967 to October 2011 (Source: Modified after Holland and Witthüser, 2012). 27
Figure 11: Simplified geological map of the Bushveld Large Igneous Province, which includes the Rustenburg Layered Suite, the Rooiberg volcanics and the Lebowa Granites Suite (Source: Kinnaird et al., 2002). 28
Figure 12: Geological map of the Eastern Limb of the Bushveld Igneous Complex, indicating the study area (Source: Viljoen and Schurmann, 1998). 30
Figure 13: Map showing farms in the Steelpoort area, with Tweefontein in the centre, and also illustrating the general geology of the underlying rocks (Source: Seabrook, 2005). 31
Figure 14: Geological map of the southern portion of the Steelpoort linearment, SW of the town of Steelpoort (Source: Beukes et al., 2013). 34
Figure 15: Geological map of Tweefontein farm. 35
Figure 16: A rose diagram showing the orientation of joints in the Tweefontein Farm (Source: Samancor ECM, 2014). 38
Figure 17: The orientation of principal stresses in the Tweefontein farm. 38
Figure 19: A highly weathered dolerite dyke located in the central portion of Tweefontein farm..... 45
Figure 20: Highly jointed and fractured dolerite dyke outcrop in the Tweefontein farm. 46
Figure 21: Highly fractured dolerite dyke outcrop in the Tweefontein farm. 46
Figure 22: A major fault with calcium carbonate infill, observed in the field at Tweefontein farm..... 47
Figure 23: Major joints striking in an N-S direction on the Tweefontein farm, the joint on the right has secondary mineral infill (biotite and chlorite). 49
Figure 24: A fold structure near the contact with Bushveld rocks on a road cut north of Tweefontein farm. 50
Figure 25: The upper reaches of the Dwars River, with transported alluvium on top of anorthosites. 51
Figure 26: The middle portion of the Dwars River, showing alluvium on the river banks. 52
Figure 27: Regolith seen from the erosional surfaces on the central part of the Tweefontein farm... 53
Figure 28: A trench showing the regolith and weathered aquifers in the Tweefontein farm. 53
Figure 29: Regolith, calcrete and norite in the vicinity of Dwars River, in the Tweefontein farm..... 55
Figure 30: Shows ferricrete exposed to the surface on the reaches of the Dwars River in the extreme north of the Tweefontein farm. 55
Figure 31: Aquifer units exposed in an opencast high wall in Tweefontein farm..... 56
Figure 32: Water-level contours and flow direction within the wider Tweefontein area. 58

Figure 33: Water-level contours and localised flow direction within the Tweefontein farm. 59
Figure 34: Exploration borehole T240 with lithological and hydrogeological units. 60
Figure 35: Borehole T322 with lithological and hydrogeological units. 61
Figure 36: Borehole T320 with lithological and hydrogeological units. 62
Figure 37: Fracture frequencies within the core samples (boreholes T240, T320 and T322) from Tweefontein farm 63
Table 1:Fracture frequencies in percentages for surface exploration boreholes. 63
Figure 38: Underground borehole TWF029 drilled horizontally through the shear zone, showing intersected geological units and structures. 64
Figure 39: Borehole TWF029 core sample showing intersected geological units and structures. 65
Figure 40: Tweefontein geology map, with cross-section profiles. 67
Figure 41: A cross section A-B, showing flow directions and geological units within Tweefontein farm. 68
Figure 42: A cross section C-D showing flow directions and geological units within Tweefontein farm. 69
Figure 43: A cross section E-F showing flow directions and geological units within Tweefontein farm 70
Table 2:Surface and borehole water samples collected in Tweefontein farm. 74
Figure 44: A Piper plot for both surface and borehole water samples collected in Tweefontein farm. 76
Figure 45: The oxygen 18 vs deuterium plot for the Tweefontein samples. 78
Table 3: The oxygen 18 vs deuterium isotope results for Tweefontein farm. 79
Figure 46: A conceptual model showing the aquifer system and groundwater flow directions. 80

LIST OF TABLES

Table 1:Fracture frequencies in percentages for surface exploration boreholes. 63
Table 2:Surface and borehole water samples collected in Tweefontein farm. 74
Table 3: The oxygen 18 vs deuterium isotope results for Tweefontein farm. 79

CHAPTER 1

INTRODUCTION

1.1. General Introduction

Proper understanding of groundwater systems is essential for efficient and sustainable groundwater resource management. A groundwater system entails a geological medium where groundwater occurs which is characterised by flow boundaries and recharge and discharge zones (Alley et al., 2002). Groundwater as a source of water has some advantages compared to surface water, in that it usually has better quality, less prone to pollution due to its protected nature, and is minimally affected by fluxes which are related to seasonal changes and it has widespread occurrence – even in areas that have limited surface-water resources (UNESCO, 2004). The groundwater system is intrinsically linked to other environmental constituents such as the hydrological cycle, such that any change in precipitation would directly affect the system both quantitatively and qualitatively (Alley et al., 2002; UNESCO, 2004).

Within the African context, groundwater is pivotal for socio-economic development, and, as a result, the implementation of irrigation systems has been carried out in vast areas that are underlain by both regional and local aquifers. Largely in Africa, groundwater occurrence in alluvial, lacustrine, basaltic and weathered aquifers presents the most favourable sources, while unweathered crystalline rocks present less favourable groundwater sources – with the water mostly used for subsistence farming and domestic use (UNESCO, 2004). However, extensive weathering, favourable geological medium, and presence of geological structures tend to present zones of high transmissivity within crystalline rock aquifers (Chilton and Foster, 1995; Taylor and Howard, 2000). Crystalline rock aquifers usually develop on the weathered zone and the underlying fractured zone of crystalline rocks (Wright, 1992). In rural, tropical and subtropical Africa, crystalline basement aquifers cover large areas, and, as a result, they are particularly important water sources due to limited surface water resources (Wright, 1992, as cited in Tessema et al., 2014).

The southern African region falls within the arid to semi-arid climate and is characterised by limited surface water resources. This makes crystalline rock aquifers an alternative source for water supply especially in rural communities. In this region, crystalline basement aquifers are quite extensive – occupying about 55% of the land (UNEP and WRC, 2008; Titus et al., 2009). As a result most rural and subsistence farming activities rely on water from crystalline basement aquifers (Titus et al., 2009). These aquifers are largely controlled by geological structures, thus making understanding of the orientation of the structures and principal stresses paramount for proper borehole sighting (Sami, 2009). These aquifers have also been found to be very complex, and, as a result, they present a challenge in the development of a sustainable water supply for rural communities. This could be due to the highly variable nature of groundwater occurrence, particularly when there is a thin layer of the weathered overburden (Adams, 2009; Holland, 2011).

In South Africa, crystalline rocks host some of the world's biggest mineral deposits like the Bushveld Igneous Complex. Thus, mining forms part of socio-economic development. This makes proper understanding of groundwater systems in such crystalline rock aquifers very important in and around mining operations – since mining has potential to disturb the groundwater resource and its distribution. During the process of mining, groundwater can also pose a threat to underground mining operations where mine ingress through fissures can flood mines, thus affecting production and possibly injuring personnel. This, in turn, can affect the livelihood of the communities surrounding these operations. South Africa is a water scarce country, which further makes proper management and understanding of groundwater, as it relates to mining, very important.

The present study focuses on the understanding of the groundwater flow regime in a crystalline rock aquifer within the Eastern Limb of the Bushveld Igneous Complex at Tweefontein farm, near Steelpoort. Furthermore, the study seeks to provide a better understanding of the potential consequences of the planned extension of mining operations by Samancor Eastern Chrome Mines with regards to activity taking place underneath the Dwars River.

1.2. Background

The study area is located approximately 22 km south of the Steelpoort town, near the border between the Limpopo and Mpumalanga Provinces (Figure 1). The area is characterised with rugged mountains, hills and gentle undulating slopes. A series of fairly broad alluvial valleys are carved by the Steelpoort and Dwars Rivers, together with their associated tributaries. Within the Steelpoort area, there are several platinum and chrome mines which use groundwater resources to supplement their surface water supplies, for mining processes.

The major aquifers in the area are weathered bedrock aquifer, fractured zone aquifer, and the alluvial aquifer in areas that are adjacent to streams (Titus et al., 2009; Gebrekristos and Cheshire, 2012). Groundwater plays a crucial role in the study area, and is used for domestic activities, small industries and various mining processes. Local small-scale farmers in and around the Tweefontein mine area have domestic and agricultural water-supply boreholes. Several boreholes tap into these aquifers to meet the water demands for socio-economic development within the greater Tweefontein area.

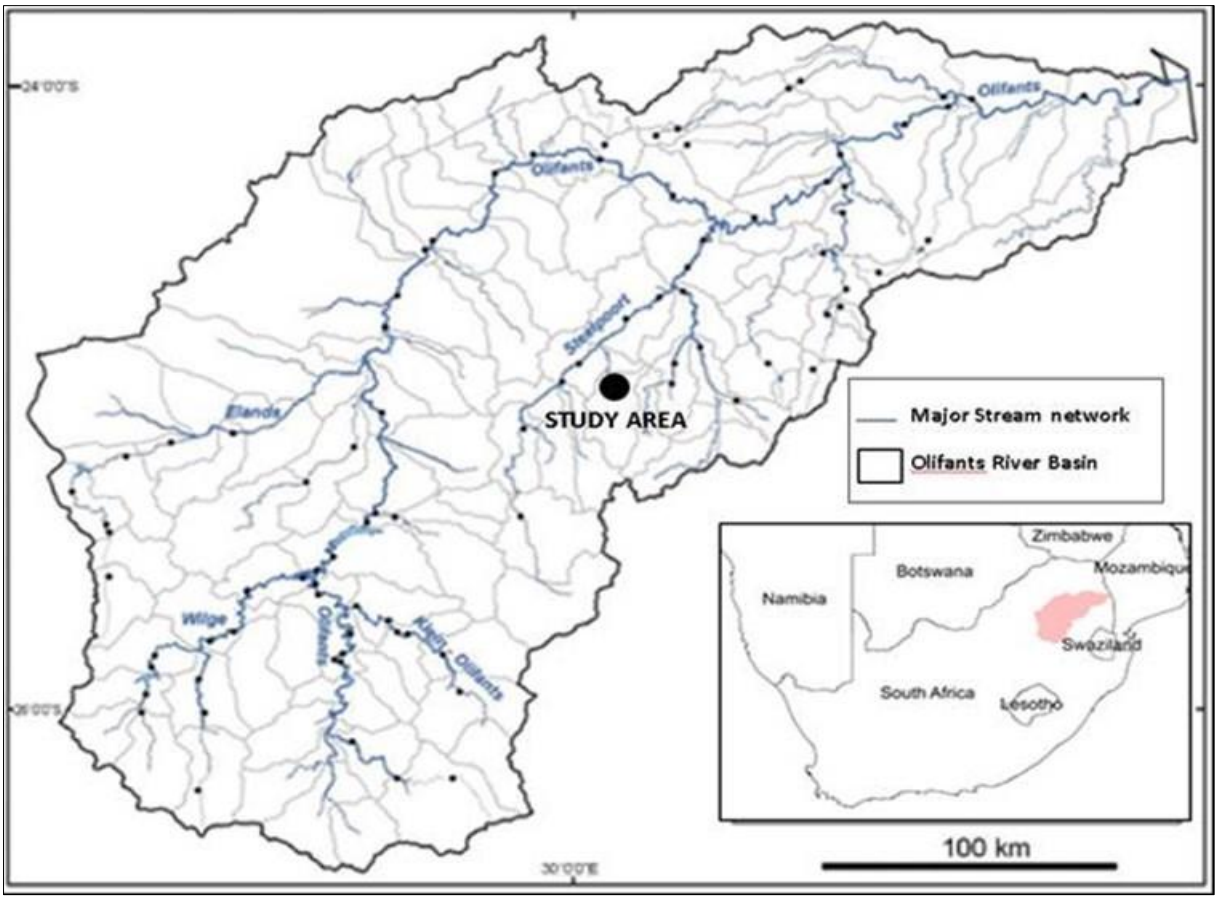


Figure 1: The Olifants (East) Basin in Limpopo Province with the study area (Modified after Rashleigh, 2009).

The area around Steelpoort is structurally complex and is characterised by extensive mining activities of platinum and chrome ore. It has been shown through other studies that geological structures such as faults and dykes can act as barriers to groundwater flow or as conduits (Sami, 2009; Titus et al., 2009).

The Tweefontein mining operation, located within the Tweefontein 360KT farm, has been extracting the Middle Group chromitite seams of the Critical Zone since the 1970s. The Middle Group chromitites consist of four seams, designated MG1 to MG4, which may locally bifurcated (split). These chromitite layers are hosted within a crystalline feldspathic pyroxenite. Samancor Eastern Chrome mines currently operates three underground operations within the Eastern Limb: Tweefontein, Lannex and Doornbosch. The Tweefontein Mine is currently mining the deeply situated MG1 and MG2 chromitite layers primarily from underground, while the remaining shallow Middle Group chromitite layers are mined from opencast mining operations. Locally, at Tweefontein farm, the MG1 chromitite layer has an average thickness of 1.65 m, while the MG2 package has an average thickness of 2m.

At Tweefontein farm, there has not been considerable work done to establish the influence of prominent geological structures on the groundwater system. The presence of prominent geological structures such as the Dwars River fault system and dolerite dykes near the mine has prompted the need to understand the influence of these structures on the flow of groundwater within the farm. Titus et al. (2009) noted the importance of detecting major water bearing structures in advance as this could help predict groundwater ingress and with the design of appropriate interventions such as sealing and the changing of mining layouts. Thus, the findings of this study will be useful for decision-makers in evaluating the viability of future mining within the Tweefontein farm.

Furthermore, future underground mining within the farm has been earmarked to extend to areas directly underlying the Dwars River. The Dwars River is a perennial river cutting through the farm in a north-south trend, and is a major tributary of the Steelpoort River, which itself is a tributary of the Olifants River.

The present study seeks to understand the influence of geological structures on the groundwater flow within the Tweefontein farm, near the town of Steelpoort in Limpopo Province.

1.3. Hypothesis

The hypothesis of the study is that better understanding of the flow regime will enable proper management of the groundwater resource, and allow for predictions and mitigation with regard to possible mine ingress.

1.4. Research Question

The study is guided by the following three key research questions:

- What are the factors that control the ability geological structures to transmit water?
- What are the prominent geological structures governing groundwater flow?
- What are the impacts of mining on the groundwater flow regime within the Tweefontein farm?

1.5. Aims and Objectives

The aim of the study is to provide a site-specific understanding of the influence of geological structures on the groundwater system, which understanding will enable and/ or promote proper management of the groundwater resource as well as to allow prediction and mitigation with regard to possible mine ingress. With this in focus, the following pertinent objectives are pursued:

- To investigate the influence of the prominent geological structures on the groundwater flow pattern system(s) at the Tweefontein farm.
- To investigate whether these structures act as barriers to groundwater flow or as conduits.
- To further investigate the potential influences of these structures to the proposed underground extension under the Dwars River.

1.6. Structure of the Thesis

Chapter 1*:* Reviews preliminary aspects of the study, the background, and provide the study objectives.

Chapter 2*:* Overviews previous work done on the influence of faults and dykes on the groundwater system, and also discusses the geology of the Bushveld Igneous Complex. Thereafter, the crystalline rock aquifers of Southern Africa are discussed, also with the stress field orientation of the Bushveld Igneous Complex. Finally, an overview of the hydrogeology of the Bushveld Igneous Complex is presented together with corresponding case studies.

Chapter 3*:* Outlines the environmental setting of the research area, with a particular focus on its physiographic, climatic and drainage aspects. The chapter concludes with detail on the local geology and hydrogeology of Tweefontein farm.

Chapter 4*:* Outlines the steps followed with data collection and the interpretation thereof.

Chapter 5*:* Presents and interprets all field evidence in an attempt to answer the aims and objectives of the study, which are to understand the influence of geological structures on the groundwater system. To achieve this, all borehole data are presented with all corresponding interpretation. The geological cross sections are also presented, with both hydrochemical and isotope data. The chapter concludes with a hydrogeological conceptual model to provide visual understanding.

Chapter 6*:* Concludes with the major research findings and provides recommendations for future work in Tweefontein farm. References and appendices follow chapter 6.

CHAPTER 2

LITERATURE REVIEW

2.1. Introduction

Geological features can greatly influence the flow and distribution of groundwater, and thus can act as both barriers and conduits to flow (Anna, 1986; Nakhwa, 2005). This makes the understanding of the occurrence of these structures, as well as their spatial relation to groundwater paramount for effective groundwater management. According to Roberts (1982), the major geological structures that tend to have an influence on the groundwater system are mainly fractures and folds. Since these structures can influence the groundwater occurrence, understanding them becomes imperative to properly comprehend the hydrogeology of a given area.

In this section, the literature is reviewed, with an objective to understand the regional and local geology and hydrogeology the study area. Previous work on faults and dykes which has focused on the general aspects of how these structures influence groundwater flow is reviewed. The geological setting of the Bushveld Igneous Complex is discussed, with more emphasis on the Eastern Limb where the project area is situated. Thereafter, the occurrence and the significance of the crystalline aquifers of Southern Africa is discussed, together with the stress-field orientation of the Bushveld Igneous Complex. The last section of the chapter provides an overview of the hydrogeology of the Bushveld Igneous Complex accompanied by corresponding case studies.

2.2. The Literature review on Faults and Dykes

Dykes

Within the Bushveld Igneous Complex, the presence of faults and the intrusion of dolerite dykes are thought to have occurred due to the breakup of Gondwana (Seabrook, 2005). Generally, two sets of dykes have been identified – generally striking NNE and WNW (Seabrook, 2005). Furthermore, highly jointed dykes act as conduits to groundwater flow, while unjointed dykes inhibit groundwater flow, as they act as no-flow (impermeable) boundary, and thus redirect the direction of groundwater movement (Cook, 2003).

Bromley et al. (1994) conducted a study in Botswana where they applied airborne geophysics to investigate the influence of dykes on the groundwater systems.

Multiple dykes ranging from 10-40 m were identified. Pumping tests and water-level data used as part of the study showed that dykes with a thickness greater that 10 m were most likely to act as a no-flow impermeable boundary, while dykes less than 10 m were permeable due to the development of hydraulic continuity with the country rock which occurs through the cooling of joints and fractures.

Laboratory studies by Gudmundsson et al. (2003) revealed the instances where fractures can develop in the country rock due to the intrusion of dykes, which can then lead to conduits forming parallel to the contact. In contrast, Engel et al. (1989) reported that dykes can lead to the salinisation of groundwater, where dykes act as an impermeable boundary. As a result, they inhibit the lateral movement of groundwater while increasing groundwater levels, which will favour evaporation, causing the residual to be highly saline due to evaporation.

Engel et al. (1989) further noted, in groundwater investigations conducted within the Witwatersrand Basin where there are north-south trending dolerite dykes ranging in thickness from 6 to 60 m, that the dykes compartmentalise the aquifer. The Basin is recharged by rain water and is discharged through a spring located at the contact between the dolomite and the dykes.

Faults

In the Eastern Limb of the Bushveld Igneous Complex, major faults trend in a similar direction to the dykes (Maynard, 2007). The Eastern Limb of the Bushveld Igneous Complex is subdivided into three sectors by major faults, namely the Steelpoort fault and Wonderkop fault striking in a NNE to NE direction (Lea, 1996). Several synthetic faults exist which are related and are connected to the major regional faults. Sheared and broken faults with little or weathered infill have also been found to be most likely permeable to groundwater flow, while faults with a thin layer of gouge can be impermeable to flow (Freeze and Cherry, 1979).

Within the study area, underground mapping has revealed the presence of a thick faulted shear zone associated with the Dwars River fault system, which eventually connects with the bigger Steelpoort fault. This shear zone has a thickness of 20m. Hammond et al. (2002) noted that faults can have shared conduit-barrier systems. This can take place at the time of their formation, and at a later stage due to infilling that sometimes occurs over time – and these changes in turn affect the hydrogeology of the area (Figure 2).

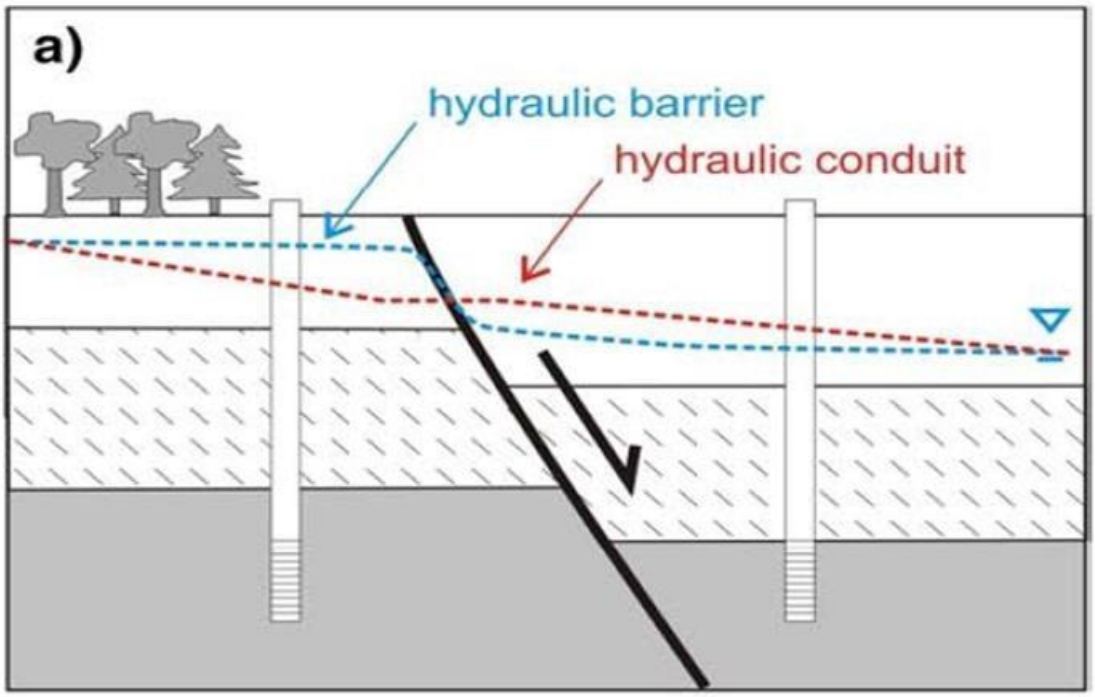


Figure 2: Illustrates permeability variations (conduit and barrier effect) within faults (Source: Bense et al., 2013).

Faults zones are usually categorised into the fault core and a damaged zone. The fault core is usually in the centre, is where most displacement occurs, and where there is intense strain. Within the damaged zone there are usually secondary structures such as smaller faults and joints (Figure 3). In cases where there are unconsolidated sediments, a third zone (the mixed zone) can develop, where there is mixing of sediments (Banse et al., 2013).

Elucidating evidence on faulted core can be found in the work of Evans et al. (1997). Their experimental work showed that developed damaged zones in crystalline rocks have better water flow within the region that is parallel to the fault, while the fault core tends to act as a barrier – thus preventing groundwater movement across the fault in crystalline rocks. The work of Evans et al. (1997) was corroborated by Banse et al. (2013), who did experimental work on crystalline rocks to assess the permeability of orientated core samples. Their findings revealed that the damaged zone acts as a high permeability zone – while the core has lower permeability (Figure 3).

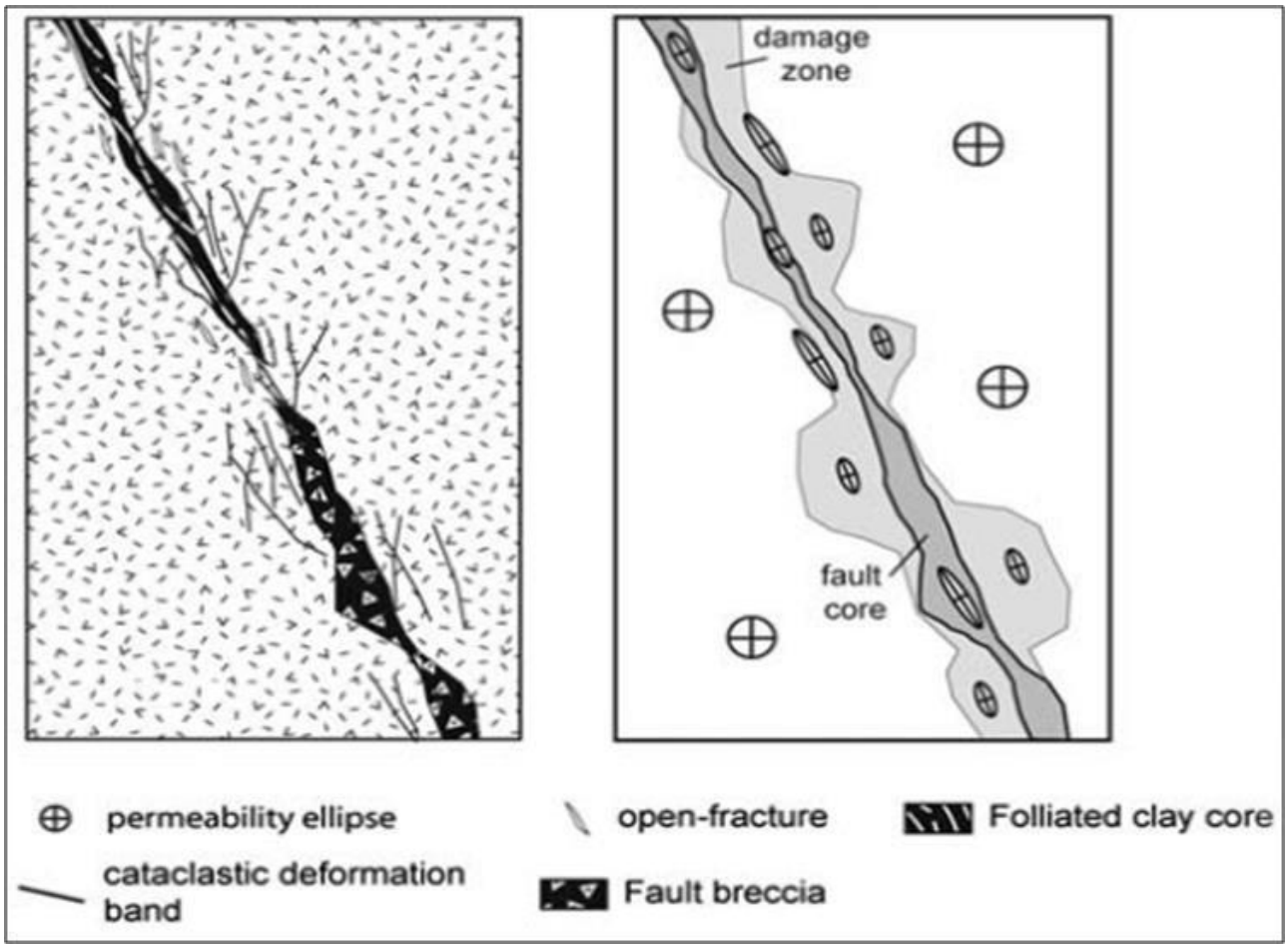


Figure 3: Illustration of the variations in permeability in the damaged and core zones (Source: Bense et al., 2013).

A study conducted by Anna (1986) in northern United States revealed that faults, shear zones and fractures have an influence in shaping secondary water-transmitting properties within rocks and that tensional structures are likely to form parallel to the direction of a major stress in the rocks.. On the other hand, Faunt (1997) noted that the opposite tended to occur with compressional geological structures which are orientated perpendicular to tensional structures.

The ability of faults or fractures to conduct water changes with the change in the *in-situ* stress field of the area. This makes it important to understand the local and regional patterns of fractures, and also the orientation of the stresses and their magnitude (Braathen and Henriksen, 2006). Tensional stress tends to form geological features such as normal faults, while compressional stress tends to form geological features such as thrusts and reverse faults. Features formed due to tensional stress can improve secondary porosity and permeability, and thus enhance

the flow of water along these features (Anna, 1986; Dettinger, 1989). These openings that have been formed within and around the fault zones, can also act as reservoirs for water storage (Faunt, 1997). However, compressional features tend to lead to lower secondary porosity and permeability, and this could lead to these features forming barriers to flow or to minimizing flow (Anna, 1986).

Faunt (1997) distinguished four modes which influence how faults can allow water to flow when it has been subjected to deformation: the frequency of fracturing, material within the fault, the amount of displacement, and the stress regime. However, the impact of these will be greatly influenced by the degree of deformation and rock type, and thus there is always a relationship between geological structures and stratigraphy. Therefore geological structures and stratigraphy should not be isolated when comprehensive studies are done on groundwater systems.

2.3. Crystalline Basement Rock Aquifers of the Semi-Arid Regions of Southern Africa

In Southern Africa, crystalline basement aquifers play an important role in domestic water supply and subsistence farming. Even though they are considered to be minor, they are widespread in the region and large rural communities rely on these aquifers for water supply (Adams, 2009). Between 60% and 90% of these rural populations survive on groundwater, with much of it coming from crystalline basement rock aquifers (Braune and Mutheiwana, 2009).

Crystalline basement aquifers in Southern Africa are difficult to develop as a dependable water supply, due to thinner weathered zone, owing to arid to semi-arid conditions and the highly variable nature of the aquifers (Adams, 2009; Holland, 2011). Works done in Malawi and Zimbabwe attest to the highly variable nature of these aquifers. In Malawi the weathered zone aquifer was well developed and is thus a reliable water source (Chilton and Smith-Carington, 1984; Wright, 1992). However, in Zimbabwe the fractured zone aquifer proved to be more productive, due to a thinner weathered zone (Wright, 1992).

In South Africa, crystalline rock outcrops are estimated to cover about 15% of the land, but nevertheless most of the country is underlain by crystalline basement rocks (Holland, 2011). Crystalline basement rock aquifers normally occur in the weathered zone of the rocks and in the fractured zone – and such rocks are dated to the Precambrian Period (Wright, 1992).

Adams (2009) stated that the weathered zone in crystalline basement aquifers in arid to semi-arid areas of Southern Africa, are usually shallower or thinner compared to those in humid areas. However, Titus et al. (2009) reported that the crystalline basement rock aquifer in Namaqualand has a thick weathered zone of up to 80 m – despite the area being an arid to semi-arid region. Titus et al. (2009) attributed the deep weathered zone to climatic cycles throughout geological history.

In a regolith aquifer the porosity tends to be higher, while permeability tends to be lower, and this can be attributed to the presence of high clay content (Figure 4) (Acworth, 1987). Porosity reduces with increasing depth until unweathered rocks are reached (Holland, 2011). Fractures within the underlying fractured aquifer tend to decrease with increasing depth, and this reduction is attributed to stress conditions that relate to magma cooling processes and tectonic-related stresses (Houston and Lewis, 1988).

Normally, the top weathered zone of a rock feeds, under gravity, to the underlying fractured aquifer due to its ability to store water (Adams, 2009). Also, pumping from the fractured aquifer can cause vertical leakage from the overlying weathered zone aquifer. The process of estimating recharge from the weathered zone to the fractured zone is difficult, since it depends on hydraulic conditions at the boundary between the weathered and fractured aquifers (Howard and Karandu, 1992; Holland, 2011).

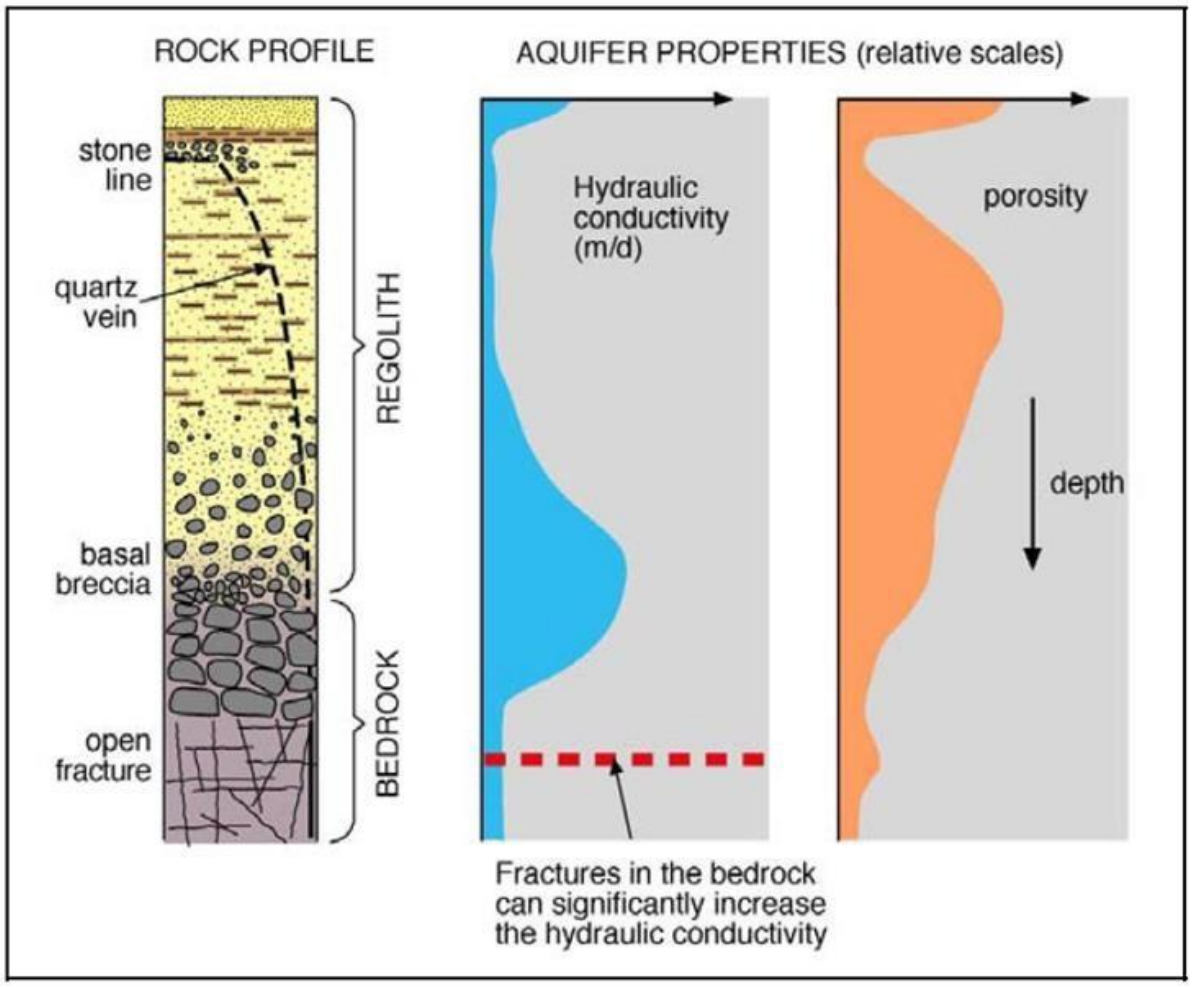


Figure 4: A conceptual cross-section of a basement aquifer (Source: Chilton and Foster (1995)

Fractures in crystalline rocks occur due to a variety of reasons. Firstly, fractures may form as a result of decompression – which generally forms sub-horizontal joints, usually at 40-50 m below the surface. Secondly, fractures may form due to tectonic activity which tends to generate near vertical joints (Houston, 1992).

Faunt (1997) distinguished four modes, which influence how faults allow water to pass through: the frequency of fracturing, material within the fault, the amount of offset, and stress relationships. Furthermore, in order for these fractures to be able to transmit water, the following should prevail: (i) numerous interconnections within the fractures, (ii) open apertures, (iii) being parallel to gravitational gradient, and (iv) being under pressure (Bisson and Lehr, 2004).

Fracturing tends to be intense along lineaments, and rivers tend to flow along these zones of weakness; thus, lineaments are usually sought after in groundwater exploration (Adams, 2009). This is the case in the study area, were major rivers such as the Steelpoort and Dwars Rivers tend to flow along the strike of the faults. However, Sami, (2009) showed the importance of understanding the prevailing stress

conditions in groundwater exploration within the basement rock aquifers of Southern Africa, with the aim of identifying extensional features since they are associated with high-yielding boreholes.

Holland and Witthüser (2009) conducted a study to understand the factors that influence borehole yield in basement rock aquifers in the Limpopo Province, South Africa. They discovered that there are multiple factors that tend to influence borehole productivity on a regional scale. They noted that boreholes on gneiss, granitic contacts and alluvium tend to have high yields. The study further revealed that variations in the aquifers tend to have a dominant influence, rather than small-scale geological features like faults on borehole productivity.

One of the present challenges associated with crystalline aquifers in Southern Africa is pollution. Due to their shallow and unconfined nature, most aquifers are prone to extensive pollution. Linn (2009) noted in Botswana that the shallow groundwater in basement aquifers is vulnerable to pollution, which is primarily caused by human activities. Higher nitrate levels were found, which rendered most of the waters to be beyond acceptable drinking standards (Linn, 2009).

2.4. Stress-field orientation of the Bushveld Igneous Complex

When dealing with fractured crystalline rocks such as the Bushveld Igneous Complex it is important to consider the structural and tectonic history of the area, and also the impact of geomorphic processes on the nature and degree of weathering (Sami, 2009; Holland, 2011). This is because the hydraulic properties of crystalline rocks are also greatly influenced by the geometry and mechanical properties of fractures. The fracture formation can be due to multiple deformational events and, these processes affect both fracture orientations their properties (NRC, 1996; Braathen, 1999). Thus, it is paramount to understand the prevailing stress regime and the deformational history of an area.

The Precambrian crystalline rocks have undergone multiple tectonic episodes under different stress conditions as a result of complex deformational settings closer to the surface of the Earth’s crust (Lloyd, 1999). Titus et al. (2009) reported that fractures that are closer to the surface to the depth of 100 m, are in a tensional state which would be favourable for the movement of groundwater.

Petzer (2009), however, argued that in areas where there have been a series of deformational events, some, all or none of the geological features may be linked to the current prevailing stress regime. Sami (2009), on the other hand, noted that from a hydrogeological point of view the current prevailing stress regime and its influence on the geological structures are more significant.

Sami (2009) studied the Eastern Limb of the Bushveld Igneous Complex, on an area located north of the current study area. According to the findings, the Bushveld Igneous Complex underwent an E–W compression, which was related to its emplacement and post-emplacement isostatic changes, and thereafter there was sagging under tensional conditions. These processes led to a change in the orientation of stresses, and the process of sagging gave rise to strike-slip stresses and NNE-orientated wrenching. As a result, wrench faults were formed orientated in a concomitant NNE direction. The NNE wrenching would thus be associated with NNW-N extensional stress, which would give rise to ENE extensional structures and NE and ESE shear structures. Furthermore, stress that was due to downwarping on the Lebombo Monocline axis after the emplacement Karoo sediments, led to an E-W extension – and this resulted in N-S oriented structures. This event also led to reactivation of older structures which are NNE and NNW orientated (Sami, 2009).

Sami (2009) concluded that the area underwent several periods of extension in different directions (namely: W, NNW and ENE) after the emplacement of the Bushveld Igneous Complex and Karoo sediments. This gave rise to extensional structures orientated in N-S, ENE and NNW. The structures orientated ENE and W manifest the current stress orientation in the area, which is related to the Lobombo down warping. Thus, N-S and NNW orientated structures would be the most favourable for groundwater exploration, since they formed an extensional regime. Titus et al. (2009) made similar observations within the Namaqualand basement rocks, where extensional fractures orientated in a NNW direction were most productive, while structures orientated in a NE and NNE direction formed due to compression and are shear structures. These would be a less favourable target for groundwater exploration given their shear origin. Most dolerite dykes in the study area are orientated in a NE direction and fewer dykes are orientated in an ESE direction. The dykes are believed to have intruded into the near vertical shear structures, which are orientated in the same direction (Sami, 2009).

2.5. Hydrogeological Overview of the Bushveld Igneous Complex

The Bushveld Igneous Complex is composed of crystalline mafic to ultramafic rocks, and also felsic granites (Kinnaird et al., 2002). Crystalline rocks of Southern Africa occur within an arid to semi-arid environment where areas like the Bushveld Igneous Complex are characterised by low storage capacity, while in some areas where there is co-existence of geological structures – weathering and favourable lithology features such as aquifers can be or are favourable water sources (Chilton and Foster, 1995; Adams, 2009).

Aquifers

Aquifers within the Bushveld Igneous Complex can be generally divided into three (Gebrekristos and Cheshire, 2012): an alluvial aquifer on the banks of rivers and streams; a shallow, weathered bedrock aquifer; and a deep, fractured bedrock aquifer.

Alluvial aquifers are almost entirely restricted to near river and stream channels, and comprises of sand, silt, clay and gravel. These vary greatly in thickness and have high yields due to their linkages with surface water, and since sand and gravels tend to have high permeability. However, low yields have also been encountered in areas where there is much clay and silt contents (Gebrekristos and Cheshire, 2012). The thickness of the alluvial aquifers varies greatly, but is thicker when they are adjacent to major river channels. Field observations of the alluvium on the reaches of the Steelpoort River reveal thicknesses of up to 12 m (Figure 5).



Figure 5: Alluvial overburden on a dry tributary near the Steelpoort River (Approximately 12m thick).

The weathered bedrock aquifer within the Bushveld Igneous Complex is perched with a thickness of 12 to 50 m and the degree of weathering increases from high to low lying areas. The overburden aquifer is generally composed of both saprolite and saprock. The composition of the overburden is greatly influenced by the underlying rocks since it is formed due to *in-situ* weathering, and the colour tends to vary from brown to greenish for pyroxenites, through to yellowish brown to yellowish white soil (Titus et al., 2009). The Bushveld Igneous Complex is situated in a semi-arid environment, and, as a result, much of the weathered overburden aquifer is thinner, whereas aquifers in highly weathered crystalline terrains occur when the bedrock is subject to the geomorphic activity of meteoric water – primarily deep weathering and stripping (Taylor and Howard, 2000; Titus et al., 2009).

The deeper aquifer represents crystalline bedrock that has not been weathered, with the matrix having negligible hydraulic conductivity and the fractures with high hydraulic conductivities. Within this aquifer, fractures control the existence and flow of groundwater. Fractures that are connected allow movement of groundwater from the deep fractured aquifer to the overlying weathered aquifer. The fractures have been found to be variable, with changing apertures and continuity (Titus et al., 2009).

Hydraulic Characteristics

The weathered zone aquifer within the Critical Zone usually comprises alternating layers of weathered norites, anorthosites and pyroxenites. Hurbet and van Rensburg (2003) reported the transmissivity values of 6 m^2/d within the cycle of norites and anorthosites on the Clapham and Forest Hill farms within the Eastern Limb. Test yields of 2.0 ℓ/s within the weathered zone aquifer were also reported. These yields are consistent with the average yield values reported by Barnard (2000) for the Rustenburg Layered Suite of 2.0 ℓ/s for gabbro, norite, chromitite and magnetite rocks.

Titus et al. (2009) reported transmissivity values of 3-8 m^2/d within the weathered zone. Storativity values were found to vary greatly within the weathered zone from E-04 to E03. There were a limited number of borehole transmissivities of up to 500 m^2/d, and with storativity up to 0.15. This abnormally high value was recorded in shallow and deep aquifers in weathered and faulted zones.

In the fractured rock aquifers, low porosity and high conductivity exist when fractures are intersected. As a result, it is difficult or problematic to estimate the hydraulic properties of the unweathered crystalline rocks of the Bushveld Igneous Complex – due to the heterogeneity associated with the fractures in these rocks and the lack of deep boreholes. However, conductivity values ranging between E03-E01 have been reported, especially near fault zones (Titus et al., 2009).

Gebrekristos and Cheshire (2012) reported highly variable hydraulic properties for pyroxenites within the Critical Zone of the Western Limb. However, borehole yields varying from 0.7 ℓ/s for deeper boreholes to 12.8 ℓ/s for shallow boreholes, were recorded. Transmissivity values of 1 m^2/d were recorded within the fractured aquifer at 50 m depth, while transmissivity values of 10 m^2/d were recorded at 40 m depth. Such high yields and high transmissivity values at shallow depths were attributed to intense weathering near the surface, and the degree of weathering decreases with increasing depth.

Hydrogeochemistry

There are several projects that have been conducted on the groundwater chemistry of the Bushveld Igneous Complex rocks. The following water facies were identified for shallow groundwaters: Mg-Ca-HCO_3 and Ca-Mg-Cl (Titus et al., 2009). The Mg-Ca-HCO_3 type has been attributed to the presence of ferro-magnesian minerals within the Bushveld Igneous Complex rocks, which are generally high in calcium and

magnesium. The Mg-Ca-HCO_3 facies has been found to represent shallow groundwater that has been recently recharged, while the Ca-Mg-Cl facies and Mg-HCO_3 have been linked to irrigation return-water flows, which tend to be high in chlorine (Titus et al., 2009)

Deep circulating groundwaters within fractures have been found to be dominated by a Na-Ca-Cl or Ca-Na-Cl water facies. Such waters are characterised by relatively high TDS values – varying from 350-1000 mg/ℓ. Elevated TDS values have been attributed to longer residence time, which favours water rock interaction (Titus et al., 2009).

2.6. Case Studies within the Bushveld Igneous Complex

Various case studies on the Bushveld Igneous Complex aquifers were done by Titus et al. (2009), Sami (2009) and Gebrekristos and Cheshire (2012). The case studies all sought to establish comprehensive understanding of the properties of the aquifer. Even though limited work has been done on the EasternLimb, most work has been done on the Western Limb of the Bushveld Igneous Complex, and the findings are present below. The studies are limited to the Critical Zone, since mining is focussed on this zone.

UG2 Weathered Pyroxenite Aquifer

Gebrekristos and Cheshire (2012) conducted some work on the western limb of the Bushveld Igneous Complex within the upper Critical Zone. They found that the weathered pyroxenites that host the UG2 chromitite seam are prone to weather differently from anorthosites and norites. The pyroxenites were found to weather more deeply, up to three times higher than the surrounding anorthosites and norites, thus rendering it a pivotal aquifer, and groundwater ingress into underground workings has been reported from this unit.

The deeper weathering on the pyroxenite was attributed to the presence of bedding planes within the pyroxenite unit and also to the composition of the major rock-forming minerals such as pyroxene. This would result in differential weathering in the near surface environment. Sami (2009) also found similar conditions on the Eastern Limb where proneness to weathering within the rocks increased with an increase in pyroxene minerals.

Marikana Open Pit (Western Limb)

Numerical models reported by Titus et al. (2009) in the Marikana area, showed that about 30 ℓ/s of long-term mine ingress into an open pit should be expected as the weathered aquifer is disturbed. However, the authors cautioned that this could be an underestimate when comparing with present ingress rates. This difficulty in predicting reliable inflow rate estimates was attributed to the presence of fractures within the aquifer, which can also contribute to increased inflows into the pit. The inflow rates could only be determined by measuring dewatering rates.

Mining in Highly Faulted Zones

In a study by Titus et al. (2009) in the Brits area, where there is the Brits graben fault system, high groundwater ingress rates were noted in a decline shaft within the weathered zone. These inflows were related to the Brits graben system. Large volumes of water were intersected at the boundary between the weathered zone and the underlying fractured zone.

Transmissivity values of 285 m^2/d were reported, with hydraulic conductivity values of 5.7 m/d for long-term pumping. On the other hand, numerical models predicted transmissivity values of 40 m^2/d and hydraulic conductivity values of 2 m/d. This discrepancy was attributed to the fact that the models averaged the parameters for the whole aquifer. However, underground workings in the vicinity of the graben system at depths of about 200 m, did not experience similar challenges of high water ingress (Titus et al., 2009).

Open Pit (Eastern Limb)

An open cast mine within the Steelpoort area did not experience water ingress challenges. The aquifers were found to differ widely in terms of thickness and hydraulic properties. Borehole yields of less than 2 ℓ/s were noted for most boreholes, while 10 ℓ/s were recorded in the reaches of rivers, and these are associated with the alluvial aquifer (Titus et al., 2009).

From these case studies it can be observed that there is much inconsistency with regard to Bushveld aquifers. Parameters cannot be generalised as they vary from place to place, and these are directly related to prevailing geological conditions and the degree of weathering.

CHAPTER 3

STUDY SITE

3.1. Description of the study area

The Tweefontein 360KT farm is located approximately 22 km south of the town of Steelpoort on the border between Limpopo Province and Mpumalanga Province within the Olifants (east) basin. The area falls under the Greater Tubatse Local Municipality, which is part of Sekhukhune District Municipality in Limpopo Province (Figure 1).

The area is mainly used for residential purposes and partly for farming – as it is located within a low rainfall region. Farming is typically done during the summer months, but the main activity in the area is in fact mining. The Steelpoort River is a major tributary of the Olifants River (Tertiary Drainage Region B41), and originates on the Highveld plateau and flows for approximately 250 km before reaching its confluence with the Olifants River near Kromellenboog.

Most of the rural communities are located on the northern side of the Steelpoort River, occupying roughly the area from Kennedy's Vale to Steelpoort. Owing mainly to overgrazing and a high density of population, these areas have poor vegetation cover and hence are prone to surface erosion with associated wash-off of sediment into the Steelpoort River and its tributaries (Figure 6). The Steelpoort River is, therefore, characterised by a high silt load and associated river channel sedimentation – especially within the middle portion (Golder Associates, 2006).

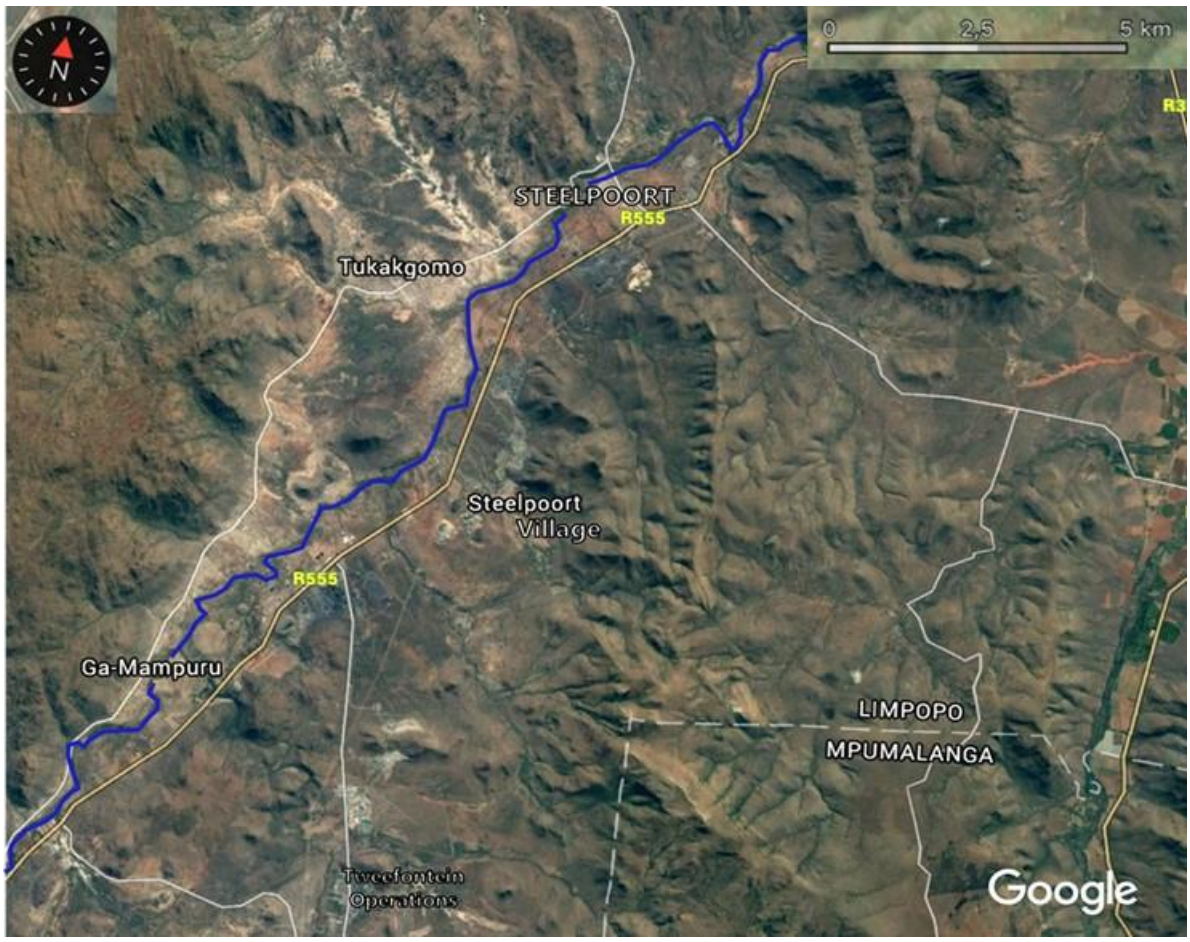


Figure 6: An aerial photograph showing surface erosion with associated wash-off near Steelpoort River (Source: Google Earth, 2017).

3.2. Physiography

Holland and Witthüser (2012) described the study area as having rough mountains, hills and gentle undulating surfaces. A series of fairly broad alluvial valleys are curved by the Steelpoort and the Dwars Rivers with their associated tributaries.

The area is covered by the Bushveld Igneous Complex, which generally forms a mountainous terrain with altitudes that range from 1200 to 1600 m above mean sea level. These elevated areas slope steeply towards the flatter south central portion of the farm where mine infrastructure is located. In the far-east, Transvaal rocks can be seen in the background (Figures 7 and 8).

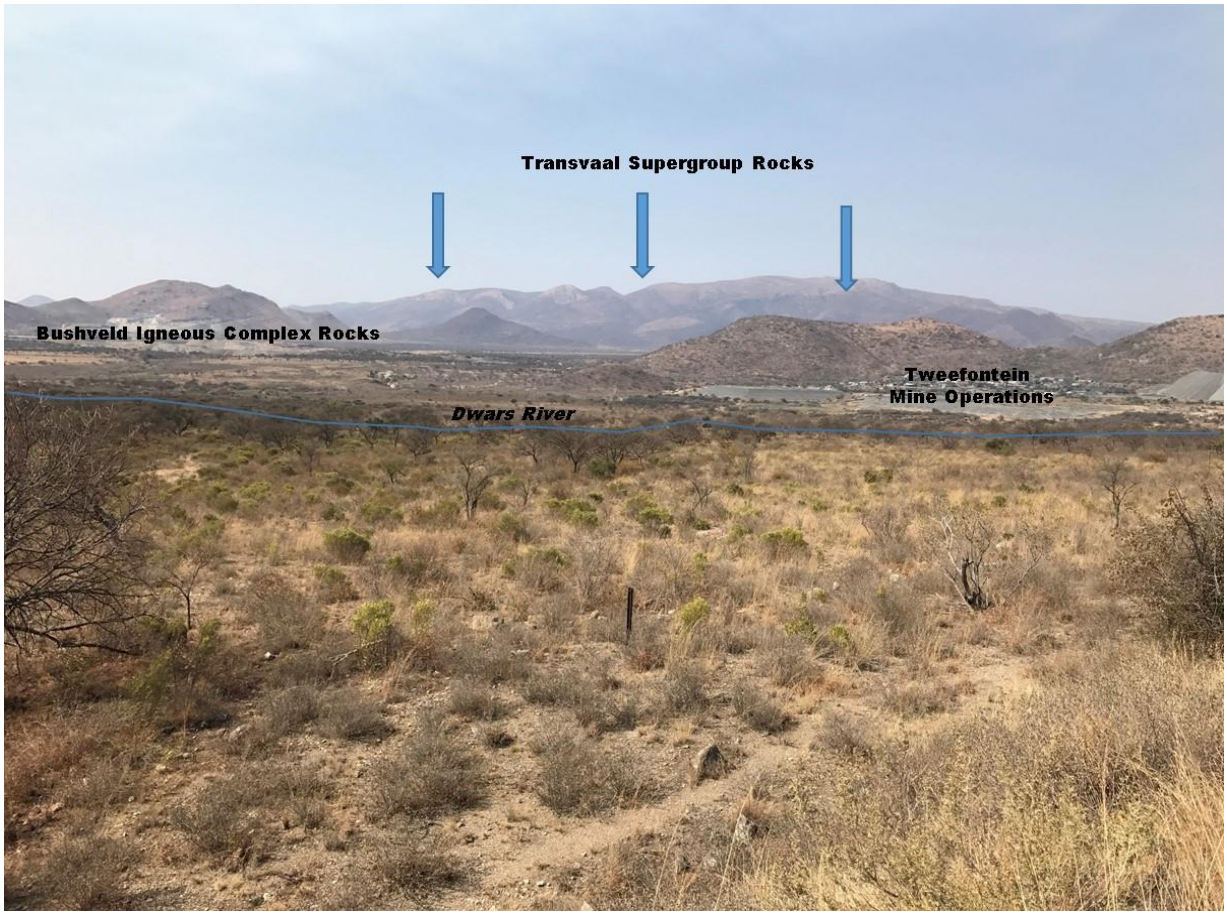


Figure 7: Shows the physiography of Tweefontein farm and with the surrounding areas.

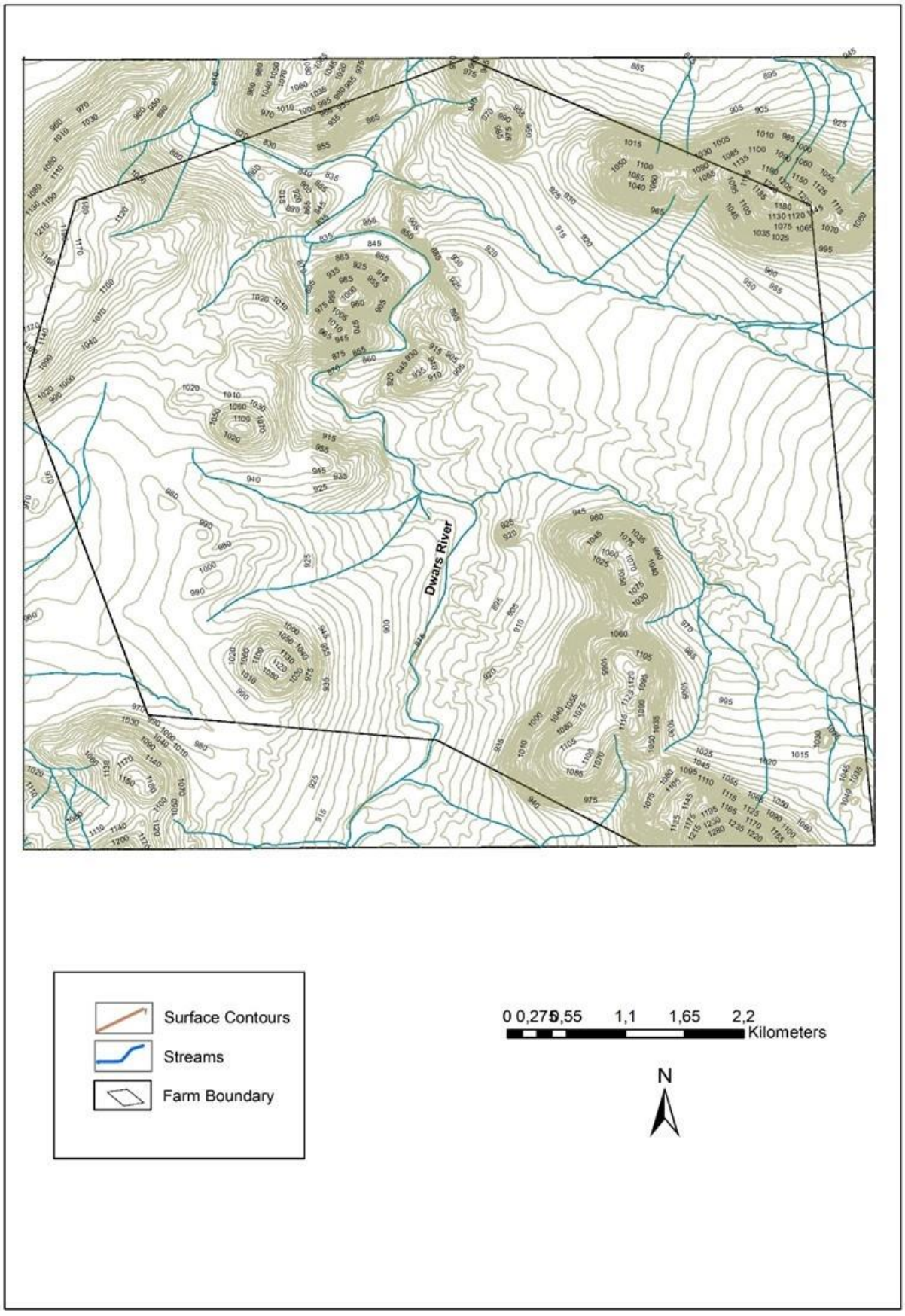


Figure 8: Surface topography of Tweefontein farm.

3.3. Climate

The study area is characterised by climatic conditions that are arid to semi-arid with summer rainfall and cold-dry winter. Midgley et al. (1990) reported the mean annual precipitation (MAP) of 553 mm and mean annual evaporation (MAE) of 1550 mm for the Steelpoort River area. The rainfall data were collected near Steelpoort Town on station number 0593 376, and the record runs from March 1904 to August 2000 (a total of 35 427 days which equals to 97 years) (Figure 9). Hence, on average, evaporation exceeds precipitation by about 1 000 mm per year. Mean annual runoff of 31.4 Mm^3 was also determined for quaternary catchment B41H (BKS, 2008).

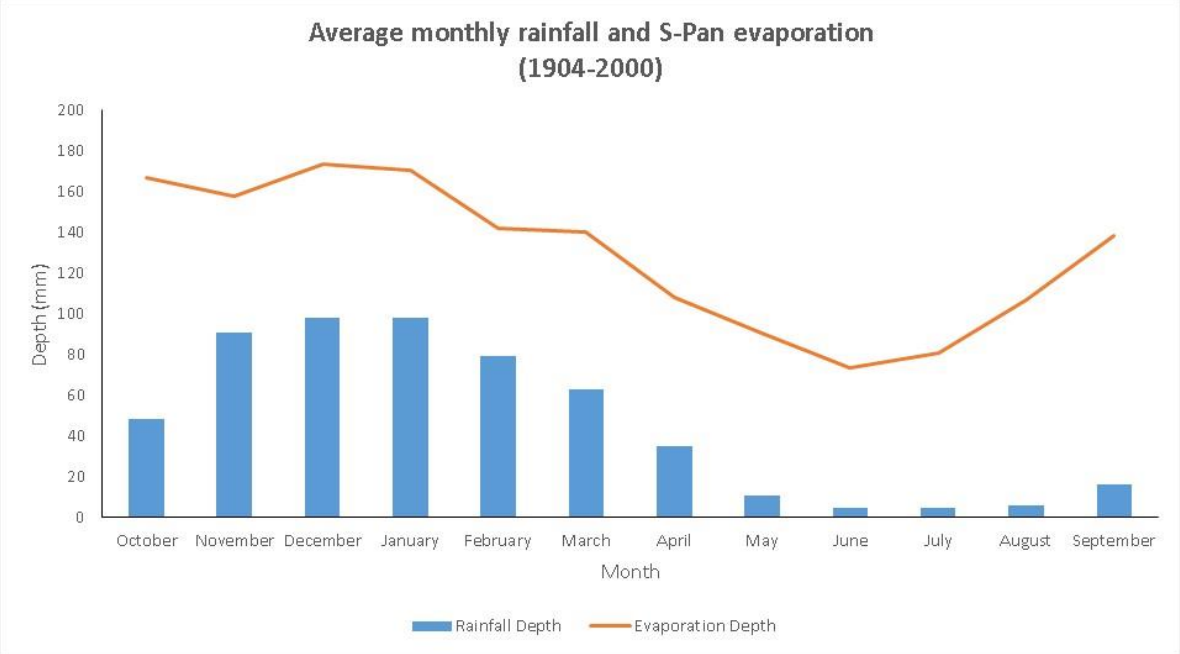


Figure 9: A graph showing average monthly rainfall and S-Pan evaporation around the town of Steelpoort (Source: Golder Associates, 2006).

The area around Tweefontein operations receives summer rainfall, with over 70% of the annual rainfall occurring during the months of October to February, and there is little or no rainfall during winter.The mean temperature varies from 19–30°C in summer and 13–19 °C in winter (Holland and Witthüser, 2012).

3.4. Drainage

The Dwars River, a major tributary of the Steelpoort River, joins the latter at Kennedy's Vale about 20 km upstream of the town of Steelpoort. The Dwars River mainly drains the high ground of the Lebalelo mountain range, which consists predominantly of mountain veld and commercial farm areas (Golder Associates, 2006).

The Tweefontein Mine is situated within the Dwars River catchment area, which has approximately 510 km^2 in the areal extent. Ephemeral streams flow from the steeper slopes toward the flatter areas and ultimately the perennial Dwars River which is flowing westward of Tweefontein operations (Figure 8).

Golder Associates (2006), reported mean annual runoff of the Dwars River catchment of approximately 36 x 10^6 m^3, with peak flow periods typically occurring during the summer months from December to February. The average monthly discharge rates provided by the Department of Water and Sanitation are highly variable from gauging station BH4H009 (Figure 10). This shows strong seasonal and cyclic variations in discharge volumes (Holland and Witthüser, 2012).

The data from station B4H009 was loaded in on an excel based program called Time-plot to estimate the mean annual base flow of the Dwars River, the program uses a single parameter recursive method (Nathan and MacMahan, 1990). The mean annual base flow was estimated to be 3.50 million cubic meters (Figure 10).

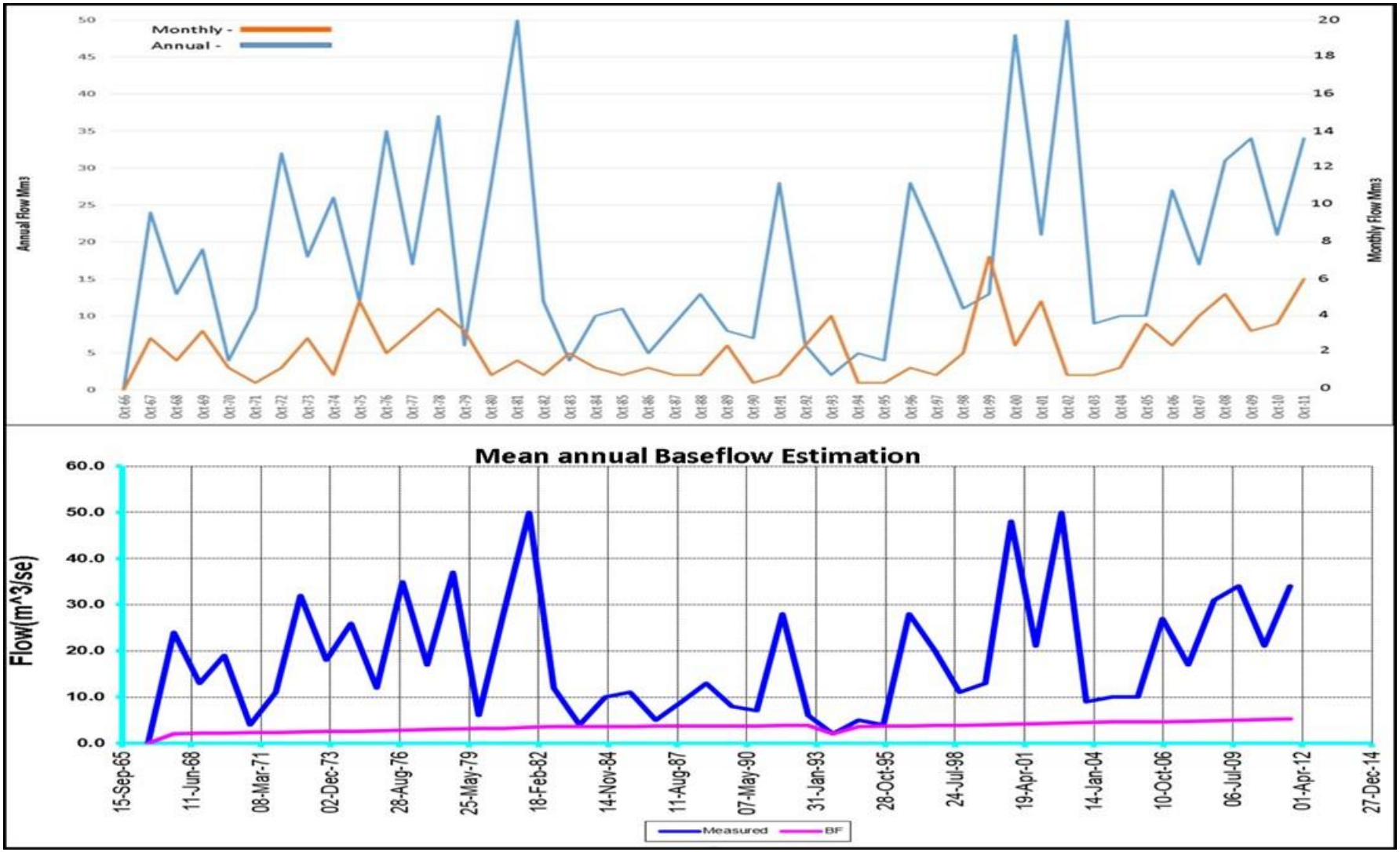


Figure 10: Annual and monthly volume chart for the Dwars River, from gauge station number B4H009 from October 1967 to October 2011 (Source: Modified after Holland and Witthüser, 2012).

3.5. Regional Geology of the Bushveld Igneous Complex

The Bushveld Igneous Complex is a layered intrusion which was intruded into the Transvaal sediments approximately two billion years ago (Cawthorn et al., 2006). It occupies an area measuring approximately 65 000 km^2, and is 450 km in width (Eales and Cawthorn, 1996). The sediments of the Pretoria Group and the volcanic rocks of the Rooiberg Group form the floor and the roof of the Bushveld Complex, respectively (Cawthorn, 2002). A large magmatic body such as the Bushveld complex displays various rocks of variable compositions, ranging from basic to ultra-basic and felsic rocks (SACS,1980) (Figure 11).

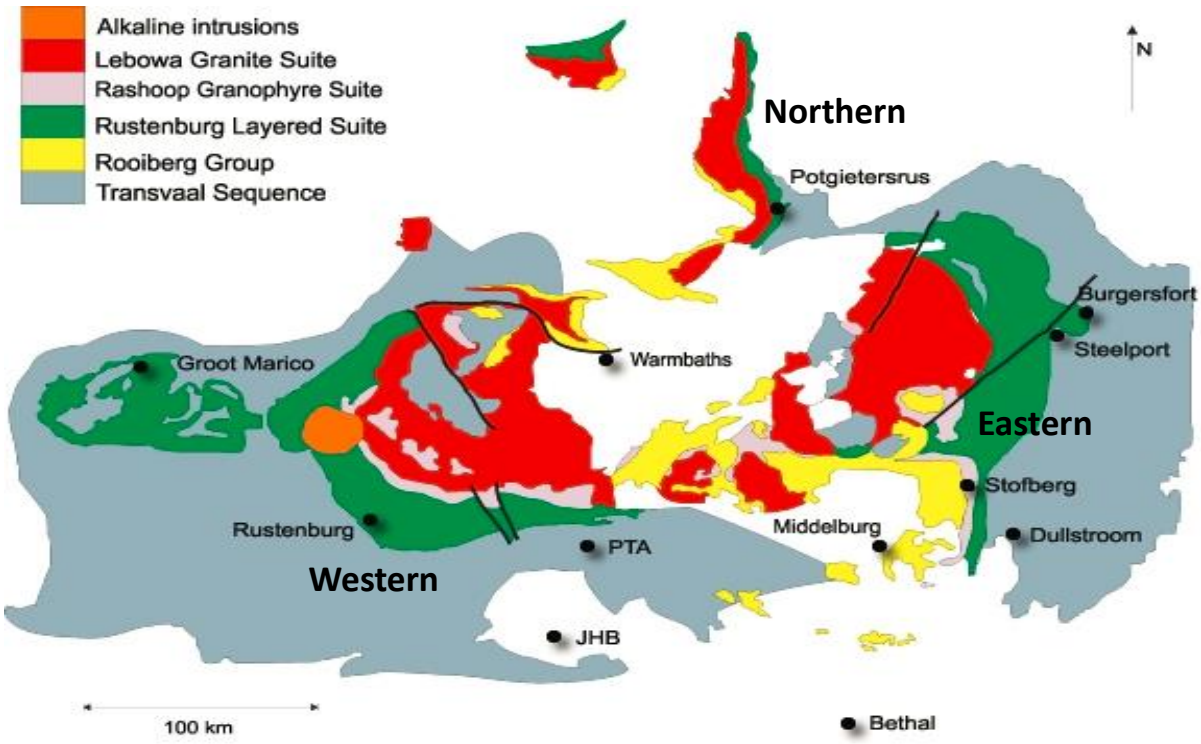


Figure 11: Simplified geological map of the Bushveld Large Igneous Province, which includes the Rustenburg Layered Suite, the Rooiberg volcanics and the Lebowa Granites Suite (Source: Kinnaird et al., 2002).

The Bushveld Igneous Complex rocks are divided into three main stratigraphic groups: the Rustenburg Layered Suite, the Lebowa Granite Suite and the Rushoop Granophyre Suite. The ultramafic-mafic layered rocks outcrop in four main limbs – the Western, Far Western, Eastern and Northern limbs (Cawthorn, 1999). The ultramafic-mafic sequences are divided, from bottom up, into the Marginal Zone, Critical Zone, Main Zone, and Upper Zone (Maynard, 2007).

The Eastern Limb has been further sub-divided into three: the western sector, the central sector, and the southern sector (Hatton and von Gruenewaldt, 1987). These sectors are separated by major geological structures; the central and western sectors are divided by the Steelpoort fault and Wonderkop fault, while the Steelpoort fault is divided into the central sector and southern sector (Figure 12) (Lea, 1996).

The southern sector of the Bushveld Igneous Complex has a structure that tends to be reflected on the geomorphology of the area. Generally, hill slopes are parallel to the igneous layers, and dolerite dykes and faults led to the formation of sharp valleys, with also some breaks in slopes. The presence of dolerite dykes and faults in the region is attributed to disintegration of the Eastern edge of Gondwanaland. The general trend of the dykes is NNE and WNW (Seabrook, 2005)

The Critical Zone is further sub-divided into the Upper Critical Zone, composed of cyclical sequences of anorthosite and norites, and the Lower Critical Zone that is dominated by pyroxenites. Chromite layers occur in both the Upper and Lower Critical Zones. The mineralogy of the layers is simple: essentially chromite with interstitial pyroxene and plagioclase and a minor amount of sulphides (Hulbert and von Gruenewaldt, 1985).

During the emplacement of the Bushveld Igneous Complex, Holzer et al. (1999) suggested that the Kaapvaal Craton had collided with the Zimbabwe Craton, and as a result of the collision the Kaapvaal experienced a NW-SE compression. The Bushveld magmas were later deposited on an extensional regime whereby the faults that were reactivated – such as the Thabazimbi-Murchison or Crocodile River and Steelpoort faults (Cawthorn et al., 2002; Silver et al., 2004)

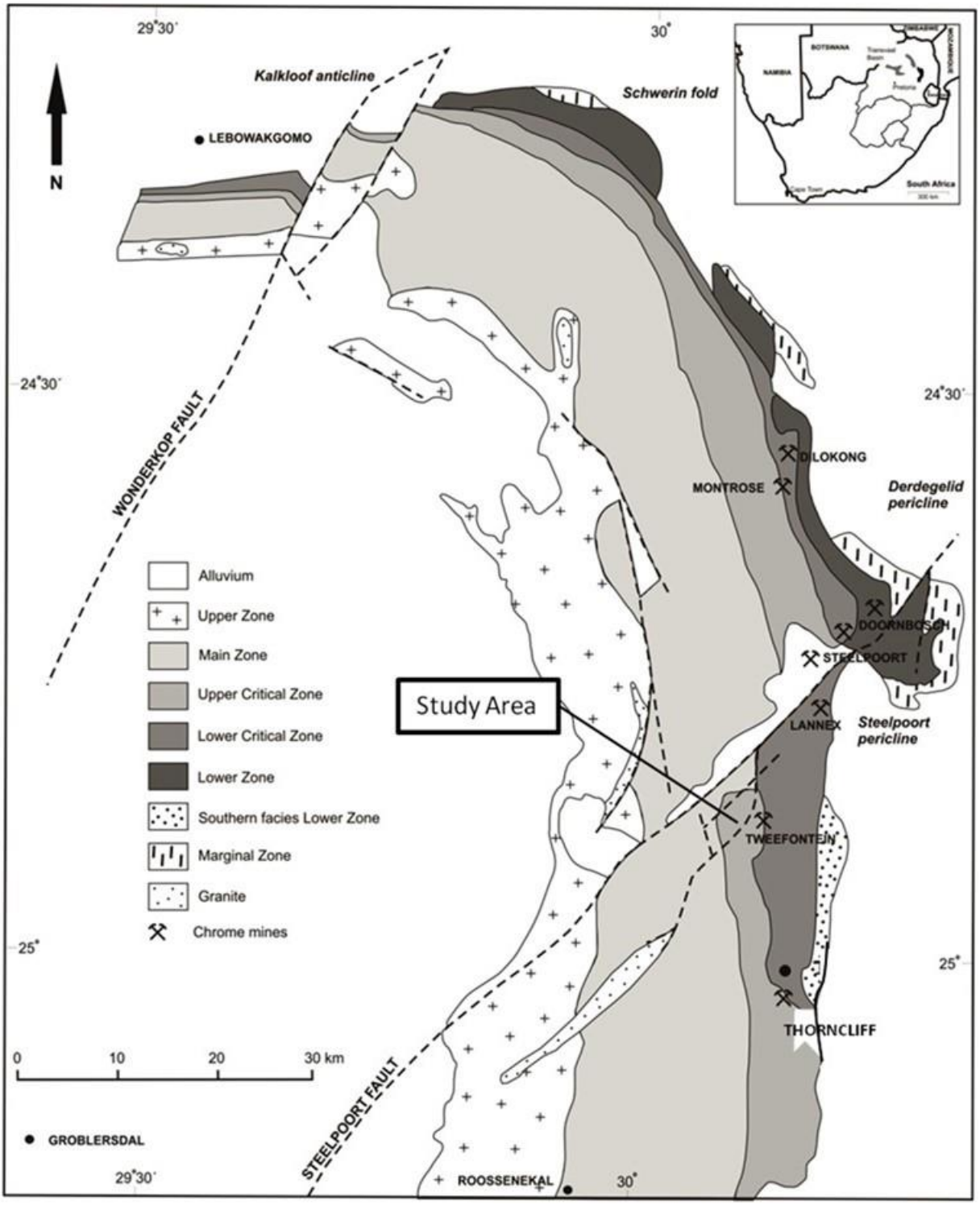


Figure 12: Geological map of the Eastern Limb of the Bushveld Igneous Complex, indicating the study area (Source: Viljoen and Schurmann, 1998).

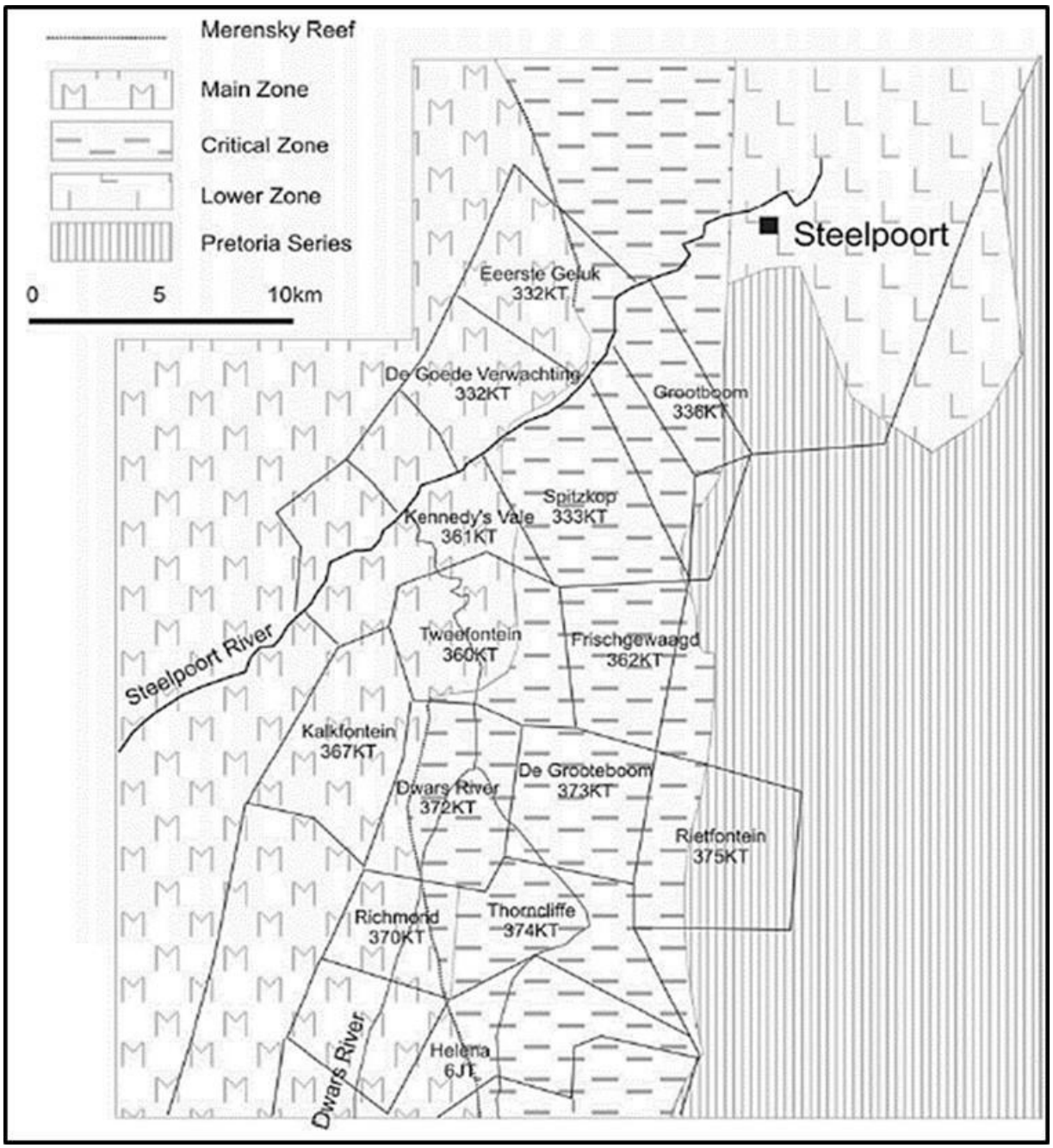


Figure 13: Map showing farms in the Steelpoort area, with Tweefontein in the centre, and also illustrating the general geology of the underlying rocks (Source: Seabrook, 2005).

The Steelpoort Fault is a prominent structural feature in the southern part of the Eastern Limb (Figures 12 and 13). This lineament postdates the emplacements of the Bushveld Igneous Complex (Beukes et al., 2013). Stratigraphic variations, in the development of rock sequences, in the north and south of the lineament have been documented by Cameron (1964). The variations are attributed to the Steelpoort lineament being a feeder to the Bushveld (Cawthorn, 2003).

For example, south of the Steelpoort lineament, where the study area is located, the Lower Group Chromitites (LG) of the Lower Critical Zone are absent or occur as thinner successions, while the Middle Group Chromitites (MG) occur as thicker successions. North of the Steelpoort lineament the opposite occurs, where the Middle Group Chromitites are thinner successions and the Lower Group Chromitites occur as thicker successions. As a result, much of the chromitite mining south of the lineament is restricted to the middle group chromitites, and in the north the lower group chromitites – primarily the LG6 package – are exploited. The Upper Group Chromitite (UG) sequences occur on both sides of the lineament as thicker successions, but tend to be much thicker toward the south (Kinnaird et al., 2002; Scoon and Teigler, 1995; Seabrook, 2005).

3.6. Geology of the Study Area

Stratigraphy

Tweefontein farm mostly lies within rocks of the Rustenburg Layered Suite within the Critical Zone of the Bushveld Igneous Complex, and includes anorthosites, norites, pyroxenites and chromitites. Quaternary deposits consist mainly of a thin layer of colluvial and alluvial deposits which overlie this sequence (Golder Associates, 2006).

Mining within the farm is entirely restricted to the Critical Zone. The Critical Zone rocks are ultramafic and are categorised into two subzones: the lower subzone and the upper subzone. The lower subzone has a thick sequence of orthopyroxenitic cumulates, while the upper subzone has suites of chromitite, harzburgite, pyroxenite, through norite to anorthosite (Kinnaird et al., 2002). The rock type that surrounds the presently mined chromitite seams, is pyroxenite and anorthosite.

Quartzites of the Magaliesberg formation (Transvaal Super Group) outcrop in the far eastern part of the area. The Magaliesberg quartzite forms part of an anticlinal overfold structure, which was developed prior to or during the emplacement of the Bushveld magma (Samancor ECM, 2013). Within the western portion of the farm is a large mass of altered sediments called the “Dwars River Fragment” – which form part of the Transvaal Supergroup. This fragment is bounded by two fault systems: the Kalkfontein fault in the west and Dwars fault in the east (van Rensburg, 1965). Beyond the Dwars River Fragment in the far western portion of the farm occurs Main Zone gabbro-norites (Figures 14 and 15).

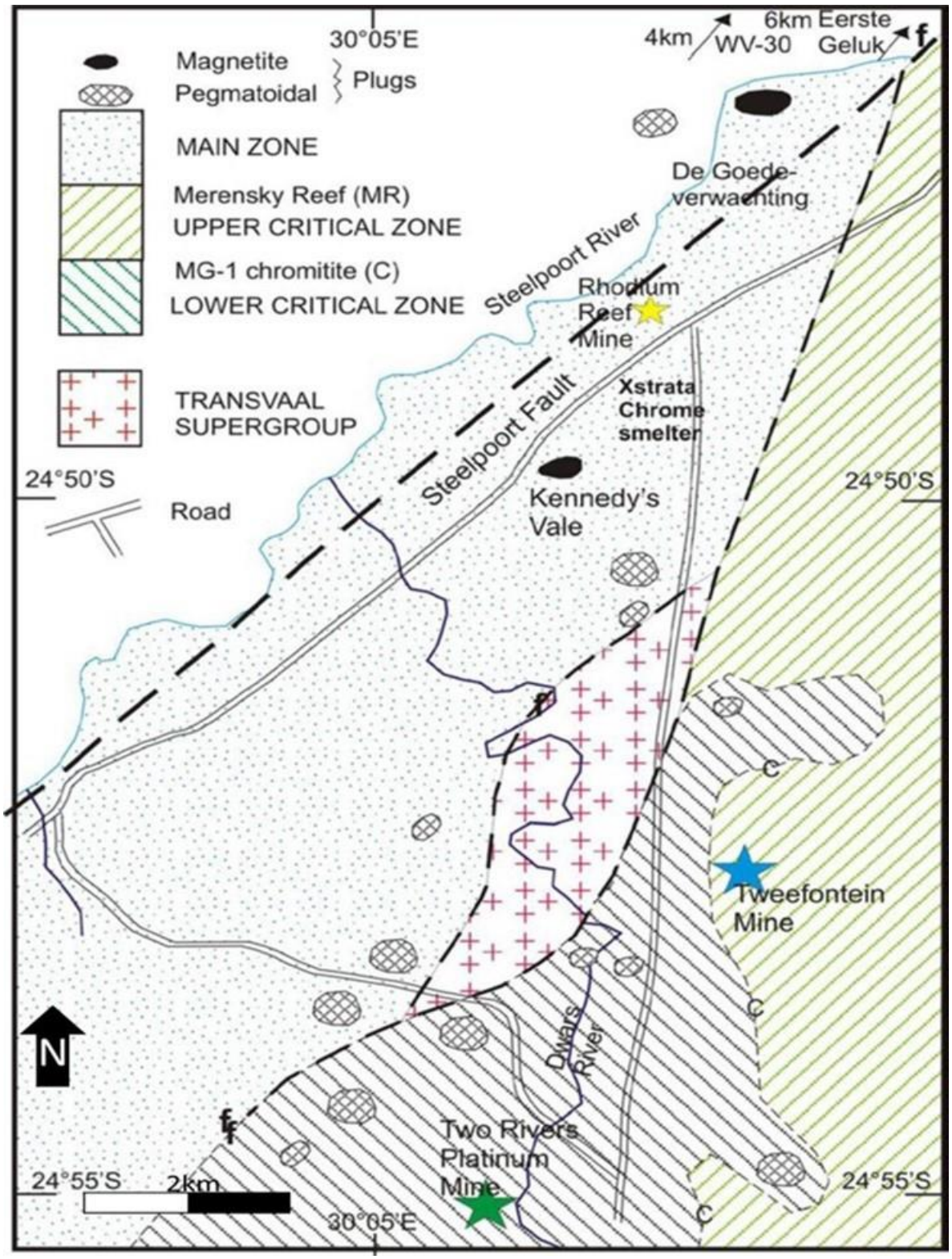


Figure 10: Geological map of the southern portion of the Steelpoort linearment, SW of the town of Steelpoort (Source: Beukes et al., 2013).

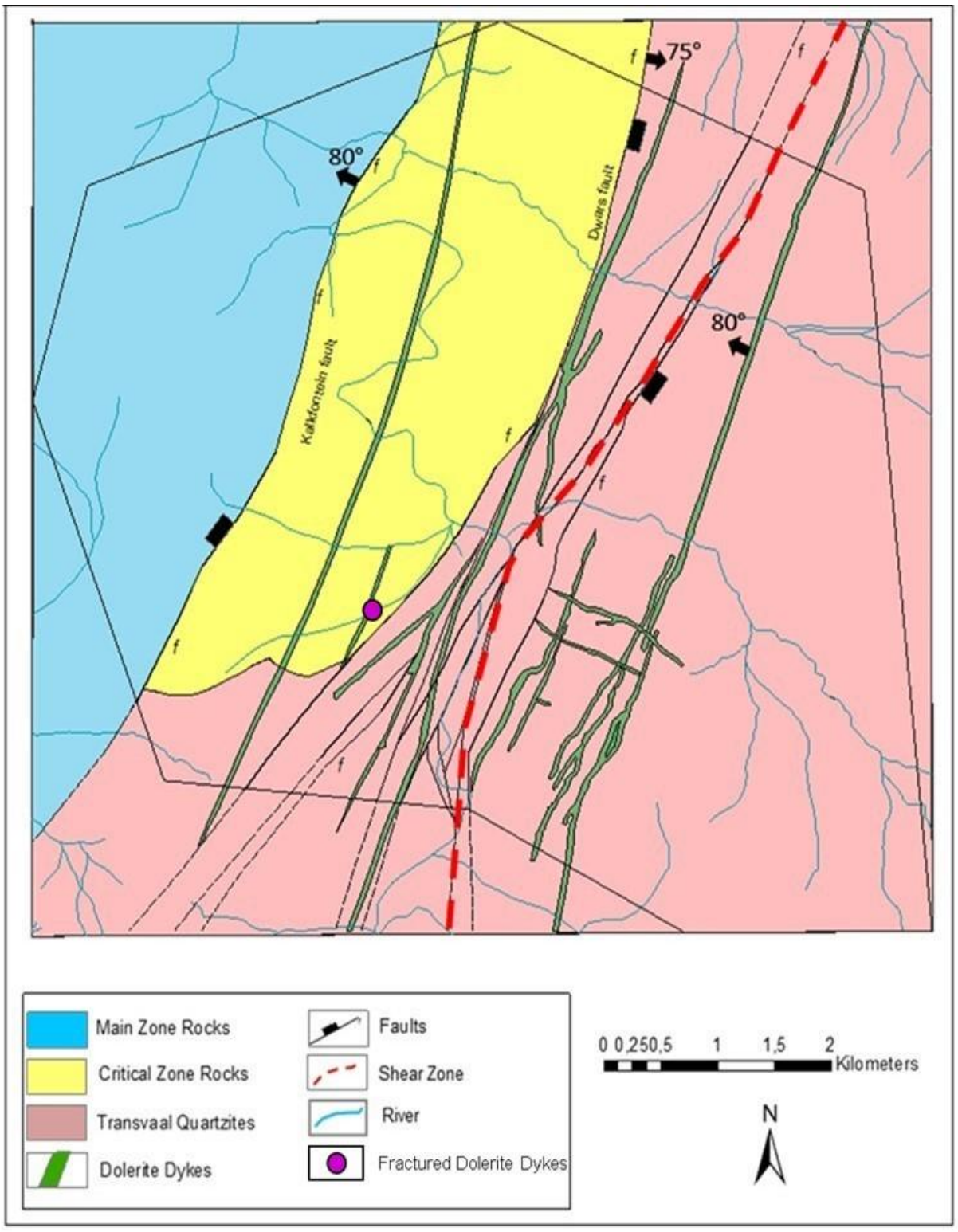


Figure 15: Geological map of Tweefontein farm.

Geological Structures

Faults

The Bushveld magmas were emplaced along a restricted transpressional extension within the faults that were reactivated – such as the Thabazimbi-Murchison, Crocodile River and Steelpoort faults (Cawthorn et al., 2002; Silver et al., 2004). This means that the Steelpoort lineament is a pre-Bushveld structure, and an extensional regime was at play when it was emplaced. The Dwars River faults system, on the other hand, is post-Bushveld since the faults cut through the Bushveld rocks and may be related to a later tectonic event such as the breakup of the Gondwana supercontinent.

The Steelpoort fault zone is 200–250 m wide, while the regional structural trend seems to be sub-parallel to the northeast-southwest trending Steelpoort Fault (Figure 16). Extensive weathering and fracturing are reported with minor lateral shearing at the intersection of the Steelpoort and Dwars River faults, and also at the intersection points with the River (Golder Associates, 2006).

The Dwars River faults are a system of successive normal faults that terminate against the Transvaal quartzite fragment on the western parts of the farm – meaning that the area underwent extension. These faults form subparallel to the dolerite dykes and strike in a NNE-SSW direction.

Joints

The prominent joint orientation in Tweefontein farm is NNE-SSW and NW-SE. The NNE-SSW orientated joints are parallel to sub-parallel to the main faults and dykes in the area, which are also NE-SW and NNE-SSW orientated. Another major set of joints is NW-SE orientated, and this set is sub-parallel to the fewer NW-SE orientated dykes. A third set is orientated in a NNW-SSE direction and the fourth set is WSW-ENE orientated (Figure 16).

Dykes

In the area around Tweefontein and neighbouring farms, dominant NE-SW striking faults and a swarm of regional dolerite dykes which run sub-parallel to the faults, are present. The dykes steeply dip between 75° and 85° SW. A secondary set of dykes is also present, which generally strikes NW-SE. Regional field work revealed that the area has been compartmentalised by dykes (Mills, 1980; Maynard, 2007). Previous

work on the farm does not show any evidence of post-dyke faulting (Mills, 1979). This suggests that all the faults are older than the dykes, since there is no visible displacement with the dykes.

Stress Field Orientation

The area was subjected to multiple deformational events, and, as a result, various prevailing geological structures exist. The NE and ESE-orientated structures are of shear origin related to earlier NNE wrenching, but these structures were re-activated afterward by post-Karoo extensional stress (Sami, 2009). The ENE and W extension gave rise to NNW and N-S orientated structures in the area. The NNW and N-S structures show the current stress orientation in the area, which is related to the Lobombo downwarping (Sami, 2009). Thus, sigma 1 in the area should be normal to the surface, while sigma 2 is orientated sub-parallel to the NE-SW trending structures and sigma 3 is orientated in a NW-SE direction (Figure 17).

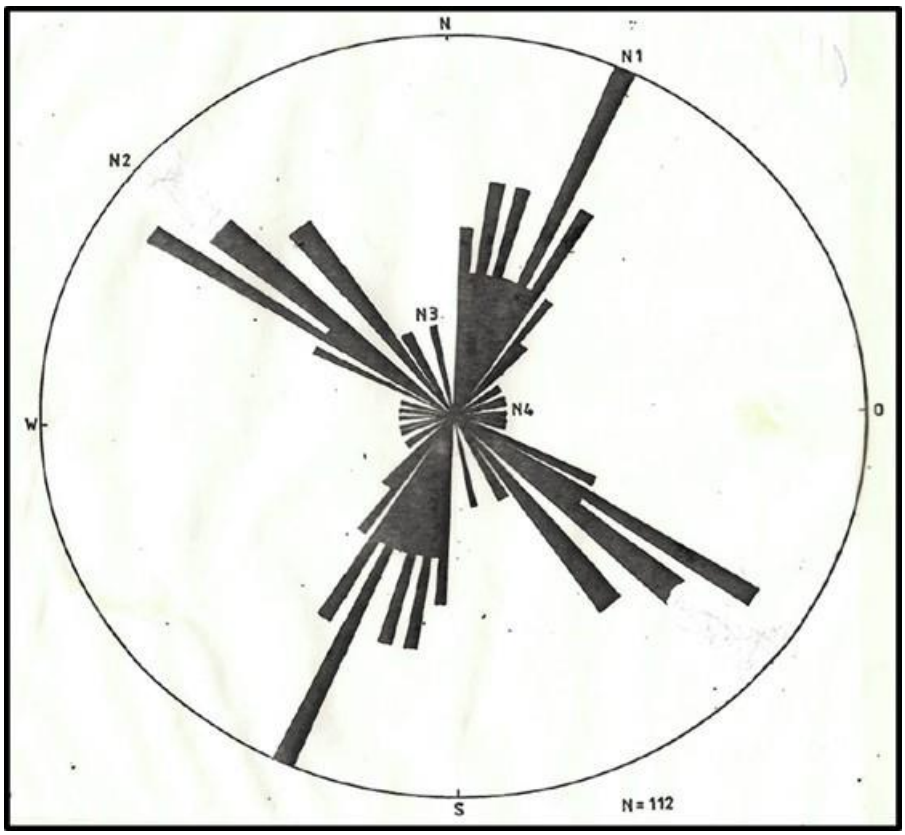


Figure 11: A rose diagram showing the orientation of joints in the Tweefontein Farm (Source: Samancor ECM, 2014).

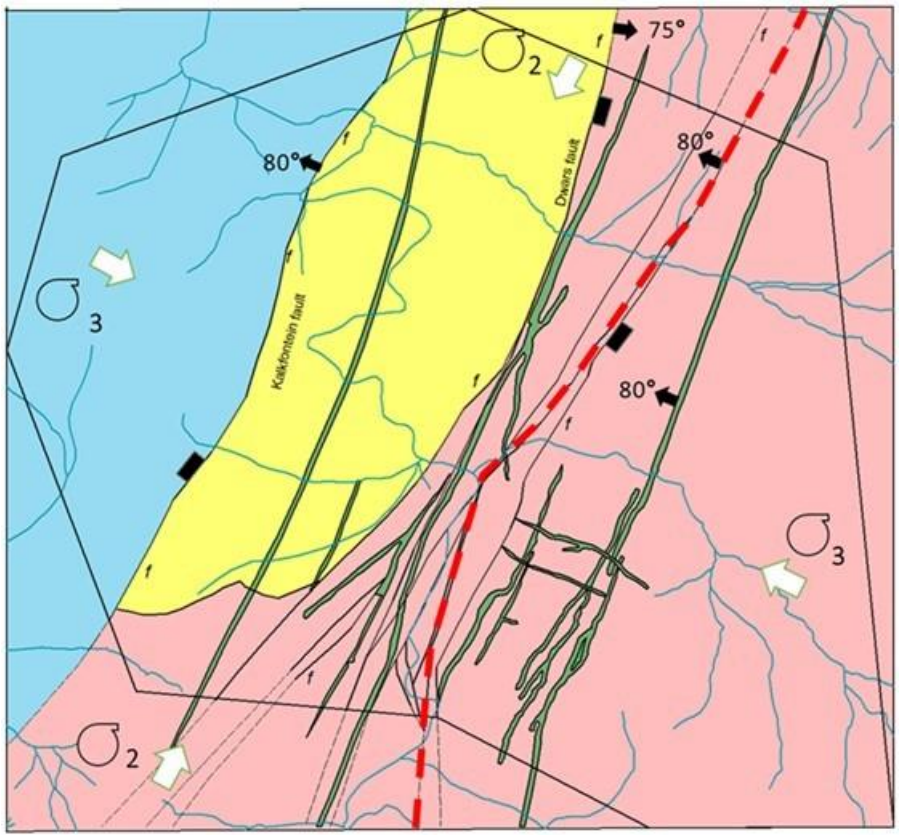


Figure 12: The orientation of principal stresses in the Tweefontein farm.

3.7. Hydrogeology of the study area

Tweefontein farm is underlain by mafic rocks of the Rustenburg Layered Suite of the Bushveld Igneous Complex. This comprises a sequence of pyroxenite, norite and anorthosite assemblages. Later recent deposits consist mainly of a thin layer of colluvial and alluvial deposits that overlie the Bushveld rocks. The colluvium comprises sandy and clayey hill wash covering the valley floor with alluvial sand and pebbles along the edge of Steelpoort River. The lateral extent of the alluvium is not greater than 50 m on either side of the River channel (Golder Associates, 2006).

Water Strike Depths and Water Levels

Within the area, water strikes generally vary from dry to 16–30 m from selected boreholes. Water levels were found to vary with topography from 4–30 m below the surface (Holland and Witthüser, 2012).

Groundwater Yield

Blowing yields from monitoring boreholes were 3000 to 5000 l/hr (0.83 to 1.38 ℓ/s). The Tweefontein boreholes (TW 1 to TW 4) had a total capacity to yield of 60m^3/hr. Boreholes drilled within the Tweefontein farm and neighbouring Annex Grootboom farm, in 1991, were reported to yield approximately 99 m^3/hr (Holland and Witthüser, 2012).

Aquifers

Different authors have identified two main aquifer units: the weathered bedrock aquifer and the fractured zone aquifer (Golder Associates, 2006; Titus et al., 2009).

The weathered aquifer is developed in the weathered bedrock profile (derived from prolonged *in-situ* decomposition of bedrock), with a thickness ranging from insignificant to approximately 20 m. At close proximity of the Dwars River, the weathered aquifer is absent or overlain by alluvial sediments, so creating a distinct intergranular aquifer (Titus et al., 2009).

Fracturing occurs at shallow to moderate depth along the contact zones of the dykes. Within the fault and fractured zone, a series of moderately interconnected horizontal and vertical conduits are assumed to occur, where zones of higher permeability are commonly developed (Golder Associates, 2006).

CHAPTER 4

MATERIALS AND METHODS

4.1. Introduction

Understanding of how geological features influence groundwater flow in structurally complex mining environments is of importance, thus the study employs a multi-approach method to gain an understanding of the prevailing groundwater regime. Field observations, geological maps and cross sections, water level maps, water chemistry, and environmental isotopes will be used to achieve the objectives of the study.

4.2. Desktop Research

During this phase, existing literature on basement aquifers in Southern Africa \were reviewed. Furthermore, the geology and hydrogeology of Tweefontein farm and surrounding areas was assessed. This included geophysical data, aerial photographs, and also reviewing the structural data of the Tweefontein farm. Geophysical maps and field mapping data were used to create geological maps of the area under investigation. Topographical maps were also used to characterise the topography and drainage of the study area.

4.3. Field Work

The geological field mapping included identification of rock outcrops, whereby the orientation of joints, faults, dykes and infill types were investigated. In addition, different aquifer units were mapped and their physical characteristics were discussed.

A total of 11 boreholes were visited through various well maintained access routes within the farm. These boreholes were sampled as part of the quarterly sampling programme that the mine is currently undertaking, and water levels were also recorded.

4.4. Geological Cross Sections

Cross sections were prepared in order to understand subsurface geology and hydrogeological conditions. Three cross sections were constructed: one was drawn on the northern side, another in the middle, and the third was drawn in the southern side of the farm. The cross sections were generally drawn along the true dip of the strata, and thus perpendicular to the strike of the rock units, faults and dykes. This was done to produce as accurate information as possible, thus allowing reasonable interpretation.

4.5. Borehole Data

A total of 67 boreholes were used to create water-level contours within the wider Tweefontein area. Fifty-three of these were drilled and managed by Groundwater Resource Information Project (GRIP), Limpopo, which is managed by the Department of Water and Sanitation of the Republic of South Africa. Sixteen of the boreholes within the Tweefontein farm are managed by Samancor Eastern Chrome Mines, and also by private owners within the farm.

Water depths below ground level (m.g.b.l.) were subtracted from the surface elevation above the mean sea levels (m.a.m.s.l.), to get groundwater elevation. All the borehole co-ordinates (latitude and longitude) and groundwater elevations (m.a.m.s.l.) were imported into ArcGIS 10.4, where a grid was generated. Surface water-level contours were then interpolated.

A selected number of surface exploration boreholes were logged to gain a better understanding of the prevailing geological structures (faults and dykes), fracture patterns and ultimate influence on the groundwater system.

4.6. Water Chemistry

Boreholes were first purged and samples were taken at depth using a bailer sampling device, and this includes lowering the bailer in the hole and waiting for it to fill up with water at a known depth, and then slowly pulling it out. Thereafter the water was transferred into a sealable container.

Samples were collected with 350ml plastic containers and were stored in a cooler box for sample preservation. Seven of the boreholes sampled belong to Samancor Chrome and form part of the monitoring network, while six boreholes are privately

owned, also three samples were collected both from upstream and downstream of Dwars River. The samples collected by Samancor Chrome were then transported to a SANAS accredited laboratory Aquatico Scientific (Pty). Ltd. in Pretoria for analysis. While the privately owned boreholes were sent to a SANAS accredited laboratory Water Lab (Pty). Ltd. in Pretoria.

A major element analysis was conducted for 17 samples from both surface water and boreholes. Cations were analysed using an ICP-OES instrument according to standard specifications, while the anions were analysed using an automated photometric analysis also according to standard specifications. The following major elements were analysed: Calcium (Ca^{2+}), Magnesium (Mg^{2+}), Sodium (Na^{+}), Potassium (K^{+}), Iron (Fe^{2+}), Manganese (Mn^{2+}), Aluminium (Al^{3+}), Total Alkalinity, Chloride (Cl^{-}), Nitrate as N (NO_3^{-}), Sulphate (SO_4^{2-}) and Fluoride (F^{-}), also the total dissolved solids (TDS), pH and electrical conductivity (EC) were measured as part of the quarterly sampling programme currently being conducted by the mine.

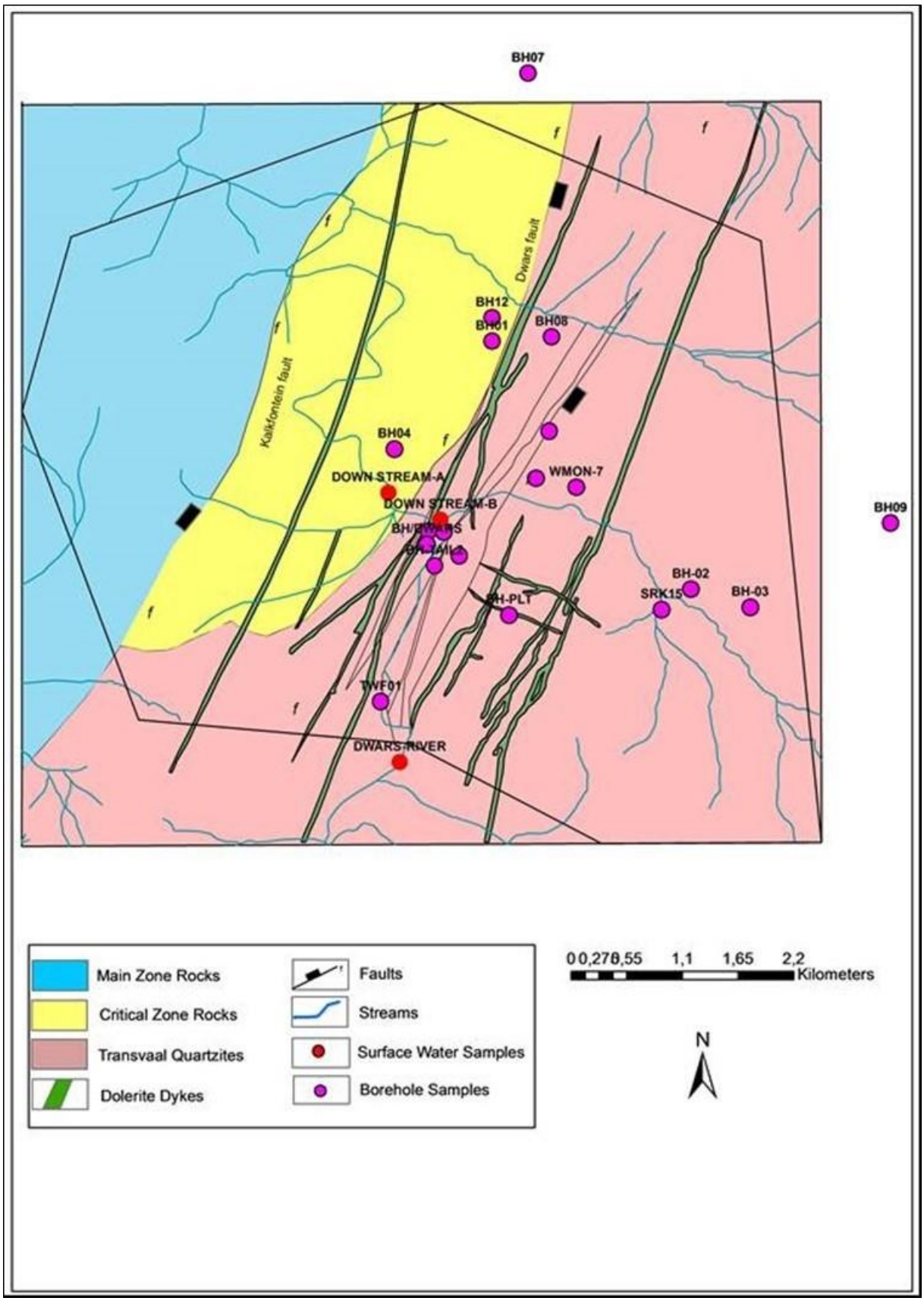


Figure 18: Borehole and stream sampling sites within Tweefontein farm.

4.7. Environmental Isotopes

Samples were collected at depth using a manual bailer, and this included lowering the instrument into the borehole and allowing it to fill with water at a known depth, and then gradually pulling it out. The water samples were then transferred into a 100ml saleable glass container and stored in a cooler box to avoid exposure to the sun.

A total of 17 samples were collected from underground seepages, monitoring boreholes, surface water bodies and streams. The samples for stable isotopes of oxygen 18 and deuterium (^{2}H) were collected during the months August and September, 2017. The samples were analysed at the Hydrogeology laboratory at the School of Geosciences of Wits University, Johannesburg by using the Los Gatos Research Liquid (LGR) Water Isotope Analyser calibrated according to standard specifications.

CHAPTER 5

RESULTS AND DISCUSSION

5.1. Field Work

Dykes

Field observations show that most dykes occur in swarms that are orientated in a NE-SW direction and dip steeply at 75°- 85° NW – with relatively few dykes orientated in a NW-SE direction. The dykes vary in thickness (10 m–40 m). Dolerite dykes located along the fairly flat areas show a high degree of weathering with much scree visible in their vicinity (Figure 19). Furthermore, the degree of weathering appears to be aggravated in the vicinity of the Dwars River. Petzer (2009) recognised weathering within dolerite dykes as one of the main factors that improve the hydraulic conductivity. Such an observation suggests that the highly weathered dykes form part of the local weathered zone aquifer, even though the degree of weathering tends to be much less than that of the country rocks.

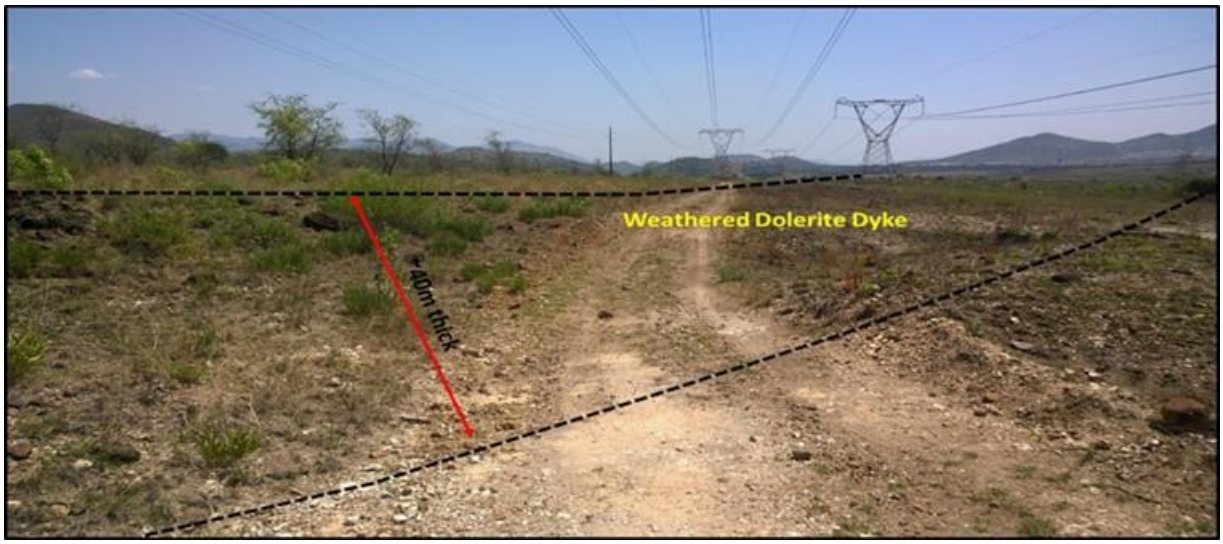


Figure 19: A highly weathered dolerite dyke located in the central portion of Tweefontein farm.

Highly fractured dolerite outcrops were identified in the field in one of the small tributaries east of the main course of the Dwars River (Figure 15). These dykes have a thickness of 8 to10 m. The main joint fractures are orientated in an E-W direction, with cross cutting discontinuous joints of varying orientations that terminate against the E-W striking joints – creating connected blocky fractures (Figures 20 and 21). Furthermore, field observations also show that fractured dolerites coarsen away from

the contacts with the country rock, with the coarsest portion in the middle of the dyke. This signifies rapid cooling at the edges during emplacement, and slower cooling at the centre. The high frequency and interconnectedness of fractures within the dykes strongly suggests that these dykes act as conduits to flow. Bromely et al. (1994) also stated that joints and fractures that form due to cooling of dykes, and which are less than 10 m, tend to have a good hydraulic conductivity – and this observation seems to hold true for the study area.



Figure 20: Highly jointed and fractured dolerite dyke outcrop in the Tweefontein farm.



Figure 21: Highly fractured dolerite dyke outcrop in the Tweefontein farm.

Faults

The major faults within the study area have a similar orientation as the dykes. Several faults were identified in the field, even though most major fault zones are sub outcropping and thus could not be examined in the field. Most faults dip steeply between 70° and 85° towards the NW – with the dominant strike of the faults being to the NE. There are fewer faults which are striking in a NW direction and dip in a NE direction.

Some faults observed in the field have calcium carbonate infilling along the fault planes possibly from leaching from the overlying rocks, and this infill has potential to act as cement, thus restricting flow. However, due to extensive weathering, this barrier effect can be greatly compromised at shallow depths. The thickness of the infill varied from 10 cm for minor faults to 70 cm for major faults (Figure 22). Some fracturing was observed on either side of the faults in the form of joints that tend to strike and dip in the same direction as the faults. Thus, the observed joints coupled with weathering make the area around the faults favourable for water to pass through, which is in line with the observation by Freeze and Cherry (1979) in basement aquifers that weathered infill will probably be permeable to groundwater flow.



Figure 22: A major fault with calcium carbonate infill, observed in the field at Tweefontein farm.

Joints

Mapping within the farm has revealed two main orientations for the major joints – the NE-SW and NW-SE striking joints. The NE-SW striking joints are more prominent and widespread and tend to increase in frequency closer to faults, shear zones and dykes. Such joint orientation has been attributed to previous deformational events (Sami, 2009).

Furthermore, fewer N-S and NNW-SSE orientated joints are associated with the extensional regime. These joints were also found to be favourable water targets, while the NE-SW and NNE-SSW joints were less favourable groundwater targets since they are related to a compressional regime (Sami, 2009). Field observations on the N-S striking joints show that they tend to have open apertures compared to the NE-SW striking joints. However, these joints also displayed the presence of secondary infill (biotite, chlorite and serpentine), which would tend to limit groundwater flow along the structures (Figure 23).

According to Anna (1986), compressional features tend to lead to lower secondary porosity and permeability, and thus could lead to such features forming barriers to groundwater flow or minimizing groundwater flow. Since the more prevalent joints (NE-SW striking) are associated with a compressional regime and have fewer apertures, this would make them less likely to vertically transmit water. This could be one of the reasons why there are no major mine fissure inflows when mining through these NE-SW orientated joints.



Figure 23: Major joints striking in an N-S direction on the Tweefontein farm, the joint on the right has secondary mineral infill (biotite and chlorite).

Other features (folds)

The stratigraphic contact between the Bushveld and the Transvaal quartzite inclusion, is characterised by intense faulting and folds. Even though it is beyond the scope of this research, it is worth noting that there are folded quartzites further north of the farm, and the fold hinge has been eroded and subsequently overlain by regolith. These folds can influence the flow of groundwater at a local scale (Figure 24).



Figure 24: A fold structure near the contact with Bushveld rocks on a road cut north of Tweefontein farm.

Aquifer Units

Field observations reveal three aquifer units within Tweefontein Farm: the alluvial aquifer on certain parts near the Dwars River, the weathered overburden aquifer, and the fractured zone/rock aquifer.

Alluvial aquifer

Chimphamba (2009) described alluvial aquifers as fluvial or lacustrine sediment sequences that tend to vary both vertically and laterally. Sami (2009) noted that in the wider Steelpoort area the clayey alluvium in the valley floors is 20–30 m in thickness. Along the valleys towards the stream channels the alluvial deposits gradually increase in thickness. Furthermore, within the Tweefontein farm, on the

upper reaches of Dwars River, the alluvium has a thin, primarily brownish medium to fine-crystalline sandy soil near the banks of the Dwars River – with hard, less weathered anorthosites occurring beneath it. The soils were evidently transported, as it appears to be very different from the underlying rocks (Figure 25).



Figure 25: The upper reaches of the Dwars River, with transported alluvium on top of anorthosites.

Within the middle section of the farm, the alluvium is much thicker near the reaches of the river. The alluvial aquifer is a mixture of medium- to fine-crystalline soil and poorly sorted sand, with clay is present in other localities. Within the river bed, there are well rounded boulders of varying sizes in the middle portion of the river (Figure 26).



Figure 26: The middle portion of the Dwars River, showing alluvium on the river banks.

Weathered overburden aquifer

The weathered overburden aquifer has been described by Titus et al. (2009) as consisting of saprolite to saprock zones. The authors termed the combination of saprolite with soil as regolith. The saprolite forms due to lengthy *in-situ* weathering of the crystalline rocks (Chimphamba, 2009). The less weathered saprock lies below the saprolite. The saprolite and saprock combined, form the weathered overburden aquifer (Titus et al., 2009).

Within the central section of Tweefontein farm, the regolith aquifer can be seen from the erosional surfaces. The top soil is generally dark with a medium- to fine-crystalline texture, with thicknesses up to 2 m. The saprolite is generally yellowish white in colour, while the overlying soil is darker yellow to brown, with a thickness of up to 4 m. These units tend to be sandy with silt, and the regolith profile formed due to weathering of the underlying norites. The underlying saprock is less weathered, with calcrete occurring in between the highly weathered saprolite and the less weathered saprock (Figure 27).

A trench west of the Dwars River shows the regolith layer of varying thickness – which is generally thicker where the rocks are less competent and prone to weathering. The aquifer within the trench extends further deeper below surface (Figure 28).



Figure 27: Regolith seen from the erosional surfaces on the central part of the Tweefontein farm.

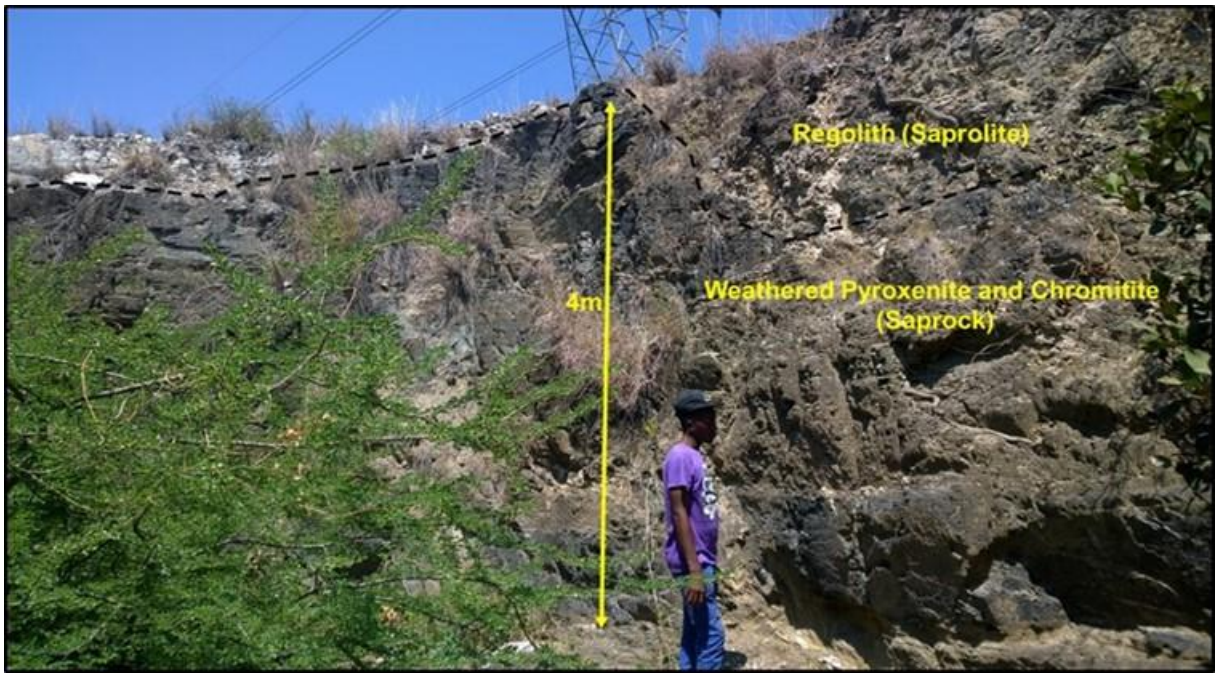


Figure 28: A trench showing the regolith and weathered aquifers in the Tweefontein farm.

Presence of calcrete

There is widespread occurrence of calcrete within the farm, and this is easily identifiable in erosional surfaces. In these erosional surfaces, it is located at the base of the regolith zone. Nash (2012) noted that for calcrete to form, there should be a source of calcium carbonate, a means of moving this carbonate to the area where calcrete is formed, and a means of initiating precipitation. Mazor (2004) explained the formation of calcrete in the Kalahari, whereby water from precipitation is enriched with CO_2 from soil and the CO_2-enriched water interacts with feldspars which introduce high calcium and magnesium – and once saturation is reached, the calcium carbonate precipitates, so forming calcrete. Nash (2012) further noted that in Southern Africa, most calcretes form by illuviation, where there is a gradual transfer of material from one soil horizon to the other by infiltrating water, until it precipitates.

Furthermore, the shallow water table fluxes can contribute to the formation of calcrete in arid and semi-arid areas through capillary action (Gomo and Tonder, 2013). The same authors also suggested that loss of water through evapotranspiration would most likely contribute to the saturation of calcium-rich water, which, in turn, would form calcretes.

In the study area, the source of calcium and magnesium could be from the weathering of anorthosites and norites that are widespread in the area. The calcrete is greyish white in colour, and in most places is hard and consolidated, while in other areas it contains clasts. It mostly occurs in the interface between the saprolite and saprock zones (Figure 29) However, far north of the farm closer to the Dwars River, the observed calcrete is more iron-rich, forming a ferricrete which shows much resistance to erosion. The ferricrete is also underlain by norites (Figure 30).

The calcrete and ferricrete layers within the weathered overburden aquifer in areas where they are present, can continuously act as a barrier to the vertical flow of groundwater or can lead to the formation of preferential flow paths. This can then lead to lessened vertical movement of groundwater from the overlying aquifer to the underlying fractured zone aquifer.



Figure 29: Regolith, calcrete and norite in the vicinity of Dwars River, in the Tweefontein farm.

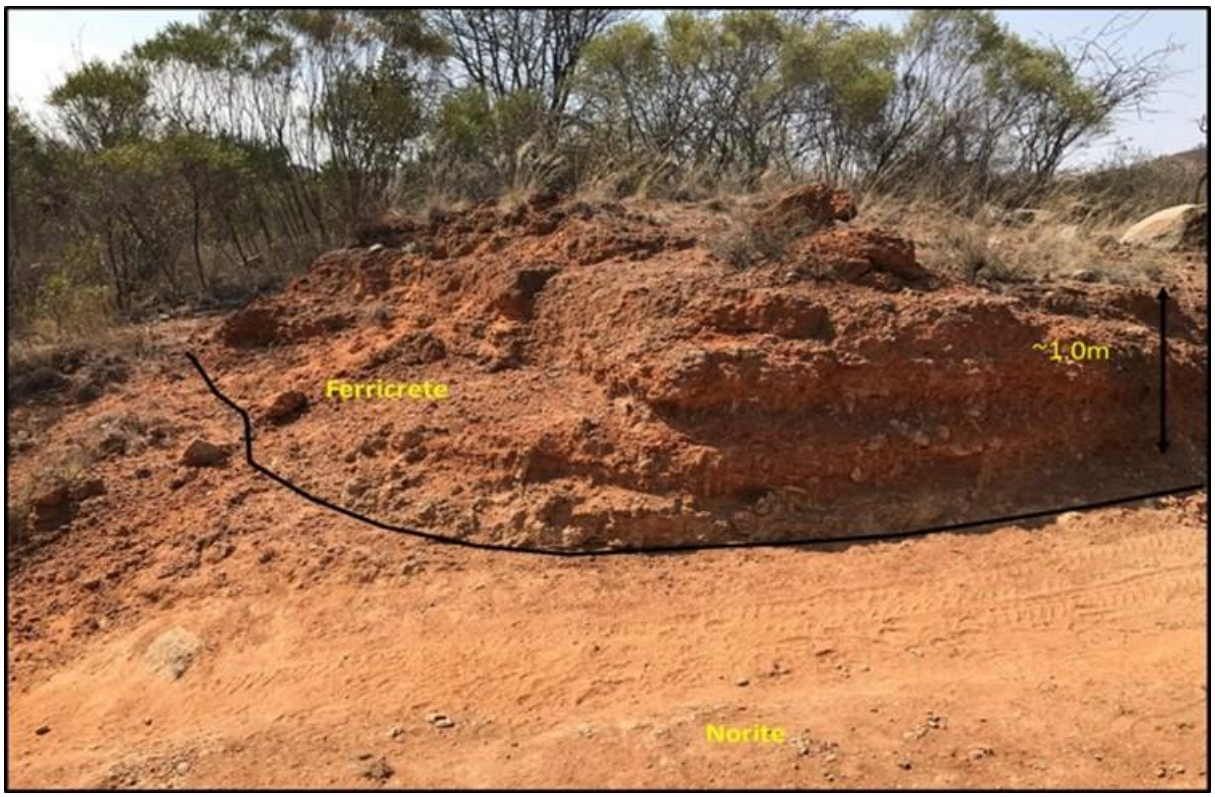


Figure 30: Shows ferricrete exposed to the surface on the reaches of the Dwars River in the extreme north of the Tweefontein farm.

Fractured zone aquifer

The fractured zone aquifer lies under the weathered overburden aquifer. The lower part of the saprock is slightly weathered with a yellowish brown colour, while the unweathered fractured zone norites are more greyish white in colour.

Within the Tweefontein opencast mine, there is groundwater seepage from the interface between the weathered overburden aquifer and the underlying fractured zone, at about 20 m below the surface. The fractured zone aquifer is highly jointed, with most steeply dipping joints orientated in a NE-SW to NNE-SSW direction (Figure 31).

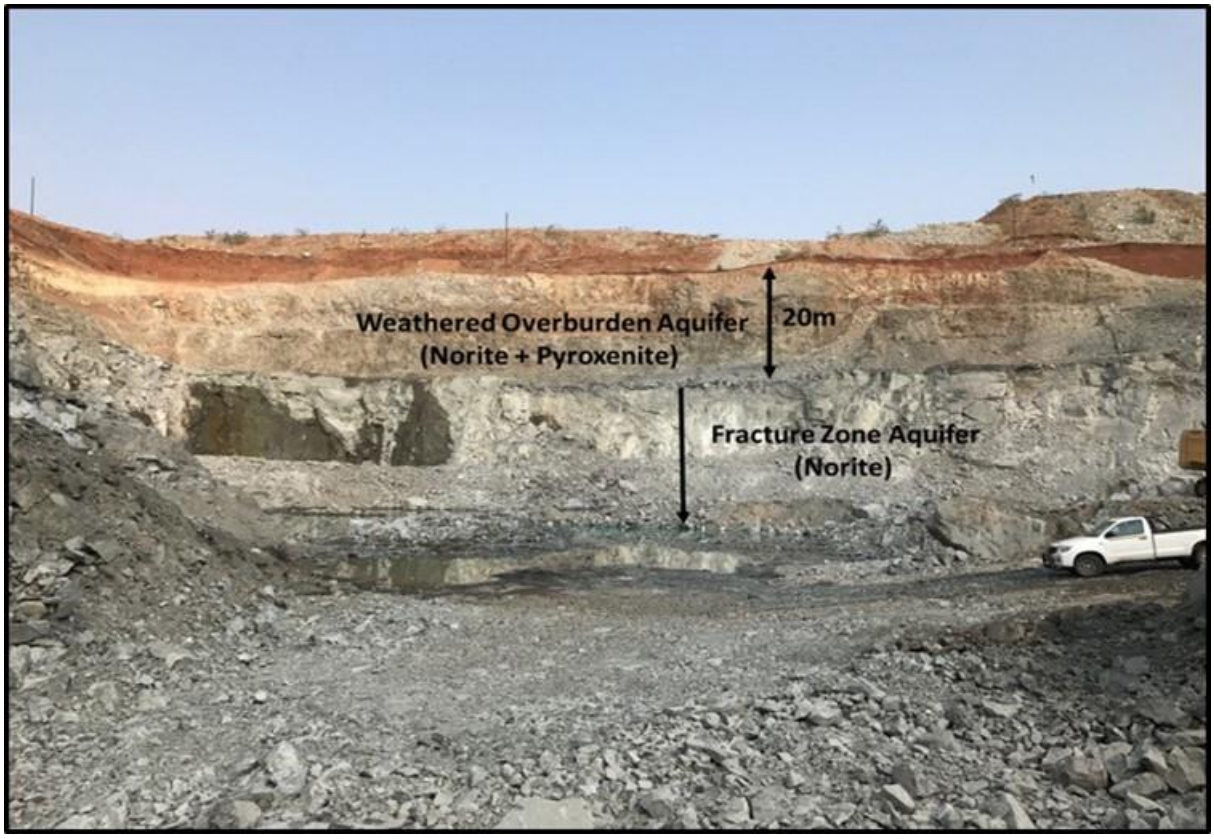


Figure 31: Aquifer units exposed in an opencast high wall in Tweefontein farm.

5.2. Borehole Data

Water levels from boreholes in the wider Tweefontein area were used to create groundwater elevation maps, and thus determine the local and regional groundwater flow. Water-elevation data from different databases were used and the mean water levels were imported into ArcGIS 10.4. The water levels for the weathered zone aquifer were used to create water-level contours. The natural neighbour interpolation method was used, since it provided fitting results for regional flow. Furthermore, 67

measured groundwater elevations within the greater Tweefontein area were used in an attempt to determine the regional flow direction and the depth of the water table.

Based on the collected data, the groundwater levels range from 2.35 m.b.g.l. near the Dwars River to 38.4 m.b.g.l. However, borehole (H35-202 and H35-0211), which is located SW of the project area, groundwater levels of 44.8 m.b.g.l. and 41.78 m.b.g.l were recorded. This can be attributed to unquantified abstractions within a farmland by the community. The average depth to the water table is 15.03 m.b.g.l. within the study area. The interpolated groundwater flow direction in the area is toward the NW and towards the Steelpoort River (Figure 32).

Tóth (1963) noted the importance of understanding locations and the size of recharge and discharge zones, and the direction and velocity of groundwater when seeking to understand groundwater movement. From the data presented in this work, recharge zones should be in the high-lying mountains east and south of the study area. According to Holland and Witthüser (2012), groundwater elevation within the weathered zone aquifer tends to mimic surface topography and groundwater recharge areas coincide with high ground, and the main discharge zone should be the Steelpoort River NW of the study area (Figure 32). There is also no visible influence of faults and dykes on the regional flow regime.

Generally, local groundwater flow can differ from regional flow, and Tóth (1963) stated that most groundwater flow occurs at a local scale compared to regional groundwater flow. Furthermore, Tóth (1963) noted that local groundwater flow tends to be more transient in nature, since it is greatly affected by seasonal changes. Within the farm, it is evident that local flow is in different directions – even though the same major NW flow is still discernible. On the central part of the farm there is a cluster of boreholes where groundwater flow is both from the east and the west towards the river (Figure 33). However, there can be bias, since there are no boreholes in much of the western half of the farm. At a local scale, there is still no evidence of faults and dykes compartmentalising the aquifer. Instead, it seems that these features freely allow water to pass through – possibly due to multiple fractures and weathering.

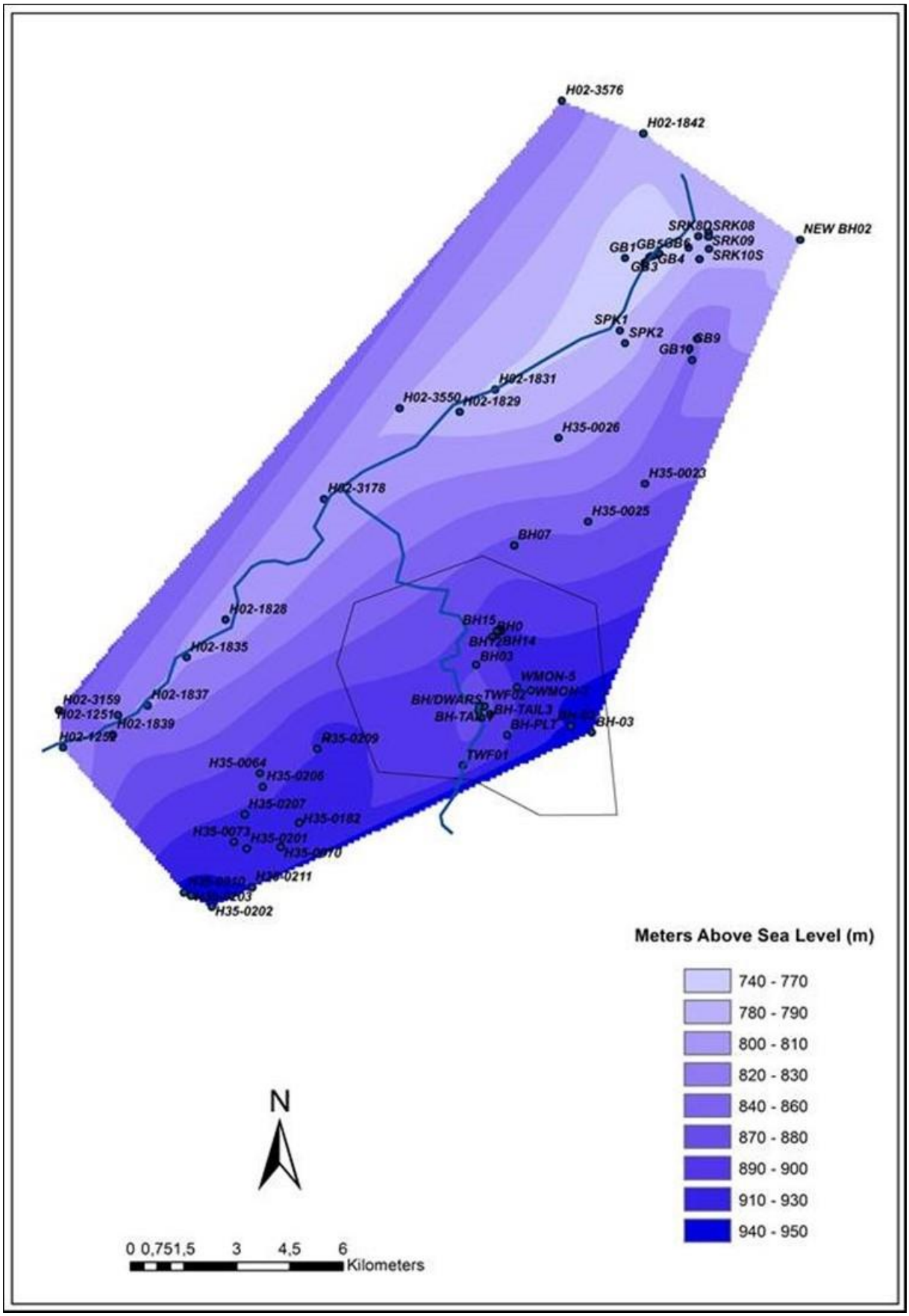


Figure 32: Water-level contours and flow direction within the wider Tweefontein area.

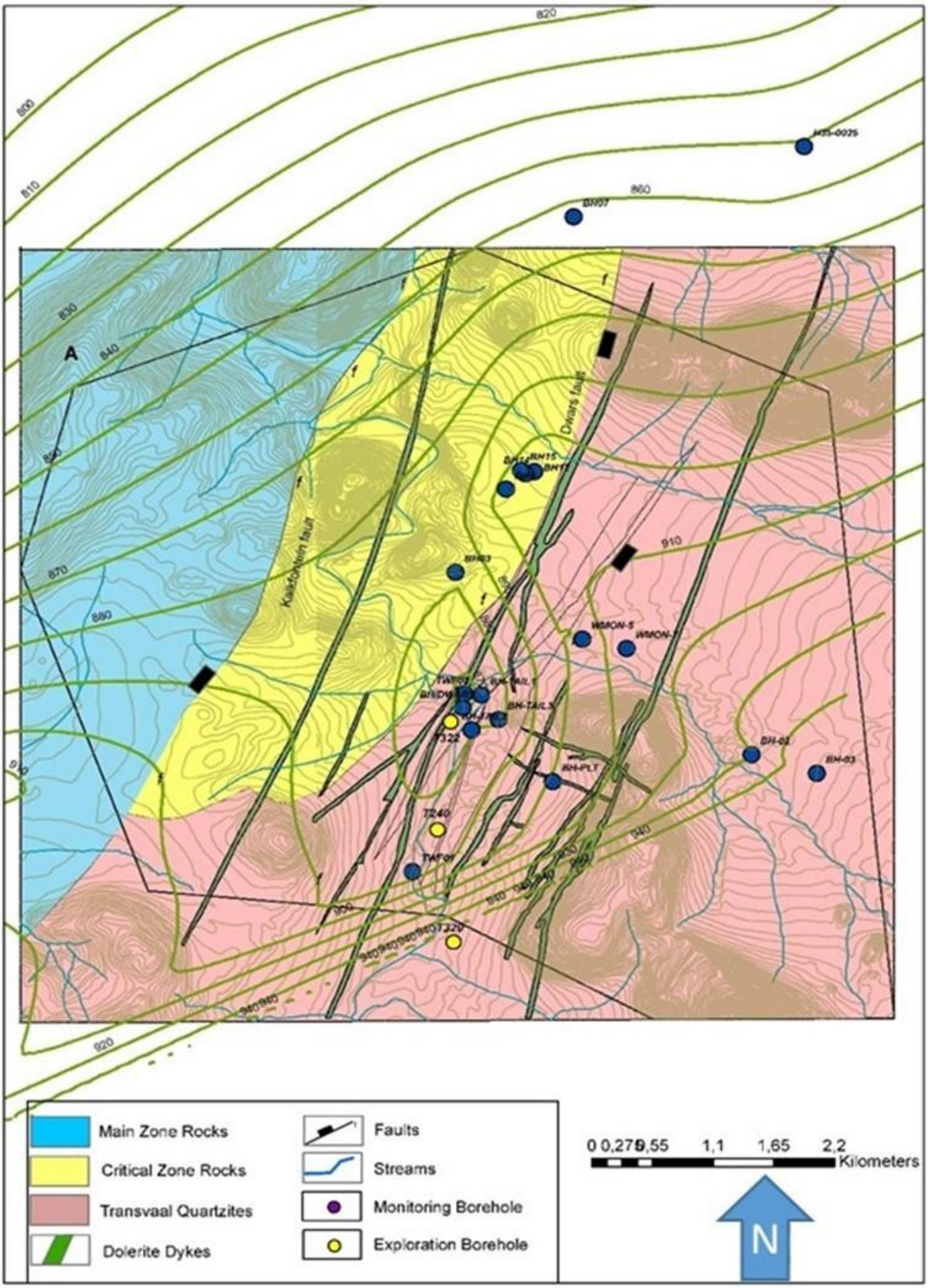


Figure 33: Water-level contours and localised flow direction within the Tweefontein farm.

Core Samples

Three surface exploration boreholes (T240, T320, and T322) and one underground cover drilling core (TWF029) were examined. The surface borehole logs were classified into either aquitards or aquifers based on weathering and fracture prevalence. The unweathered crystalline rocks with minimal fractured would tend to form aquitards while the weathered and fractured rocks would tend to form aquifers.

Borehole T240 was drilled on the reaches of the Dwars River and the main lithologies intersected were norites, anorthosites and a dolerite dyke. A fine crystalline regolith with a thickness of 1.13 m, followed by a medium to coarse crystalline norite to 37.58 m. The norite makes a sharp contact with a fine-crystalline dolerite dyke which extends some metres below. An increase in the frequency of jointing occurs within the dolerite dyke, compared to the country rock.

The regolith aquifer is made of loose soil and is 1.13 m thick. The weathered zone aquifer extends to 17.5 m. From 17.5 to 37.58 m, an aquitard is intersected, with prominent fractures (conduits) visible. Then a dolerite dyke initially forming an aquitard is intersected from 37.58 m, with an increased frequency of fracturing (Figure 34).

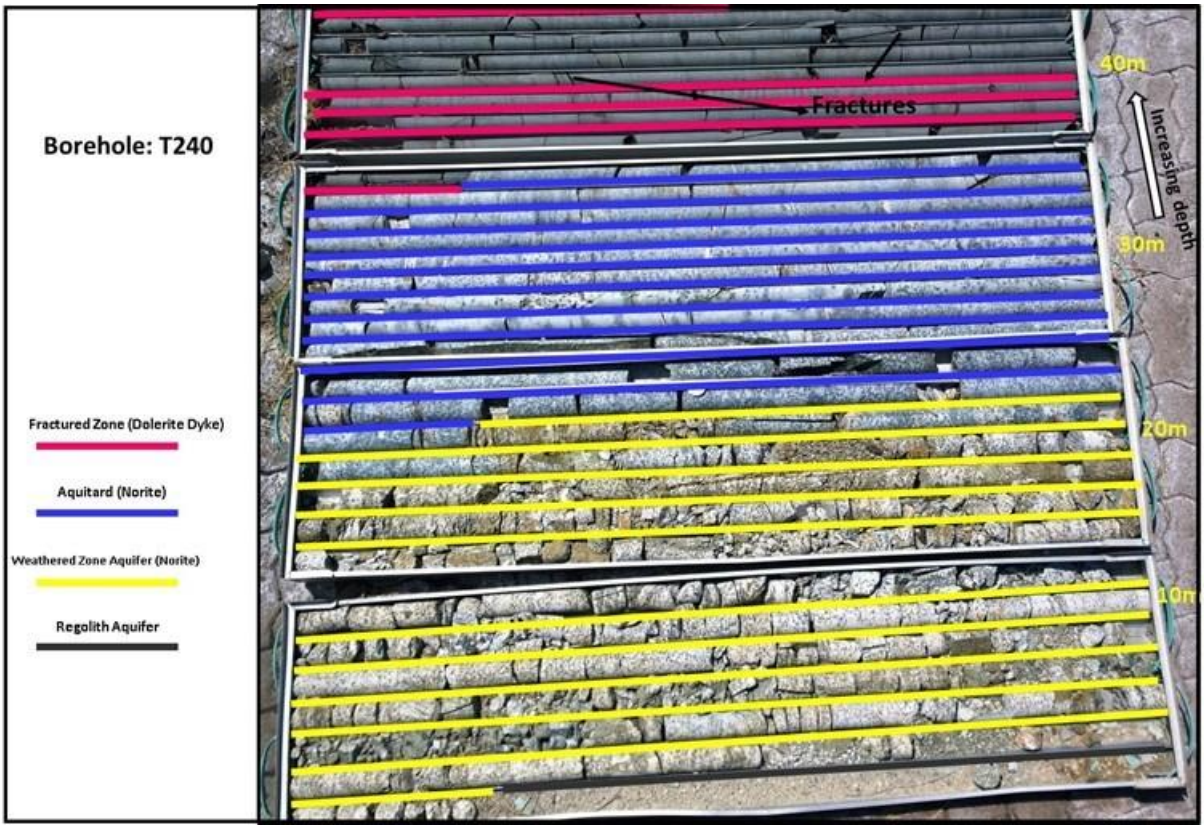


Figure 34: Exploration borehole T240 with lithological and hydrogeological units.

Borehole T322 was drilled west of the Dwars River and the main lithologies intersected are norites, anorthosites and a dolerite dyke. The regolith is about 2.0 m thick and is composed of fine-crystalline clay, followed by medium course-crystalline norite to about 25.5 m. The norite displays sharp contact with a fine-crystalline dolerite dyke, which extends some metres below. There is increased frequency of jointing within the dolerite dyke compared to the country rock – suggesting that the dyke contacts would be favourable water-bearing features.

The regolith aquifer is made of clay with impurities and is 2.0 m thick. The weathered zone aquifer extends to just 10.43 m. From 10.43m to 25.5m an aquitard is intersected with few prominent fractures (conduits) visible. Then a dolerite dyke forming an aquitard in areas with little or no fractures is intersected from 25.5 m, then there is an increased frequency of fracturing (Figure 35).

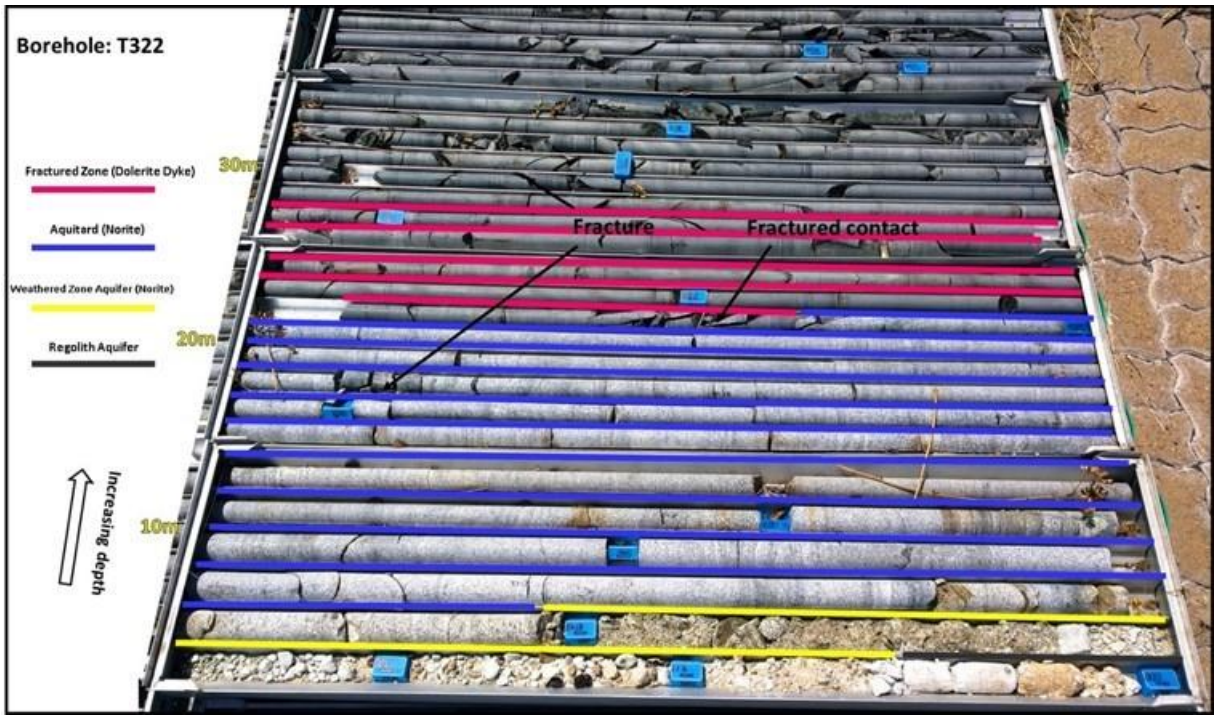


Figure 35: Borehole T322 with lithological and hydrogeological units.

Borehole T320 was drilled within a fault zone, with a combined displacement of 5 m. Prominent water-bearing structures were intersected at 12.5 m, 20 m and 24 m, with thicknesses varying from 0.3 m to 1.0 m. These fractured zones are highly weathered and friable. Some interspersed, prominent joints were intersected – with coating on the surfaces suggestive of water flow (Figure 36).

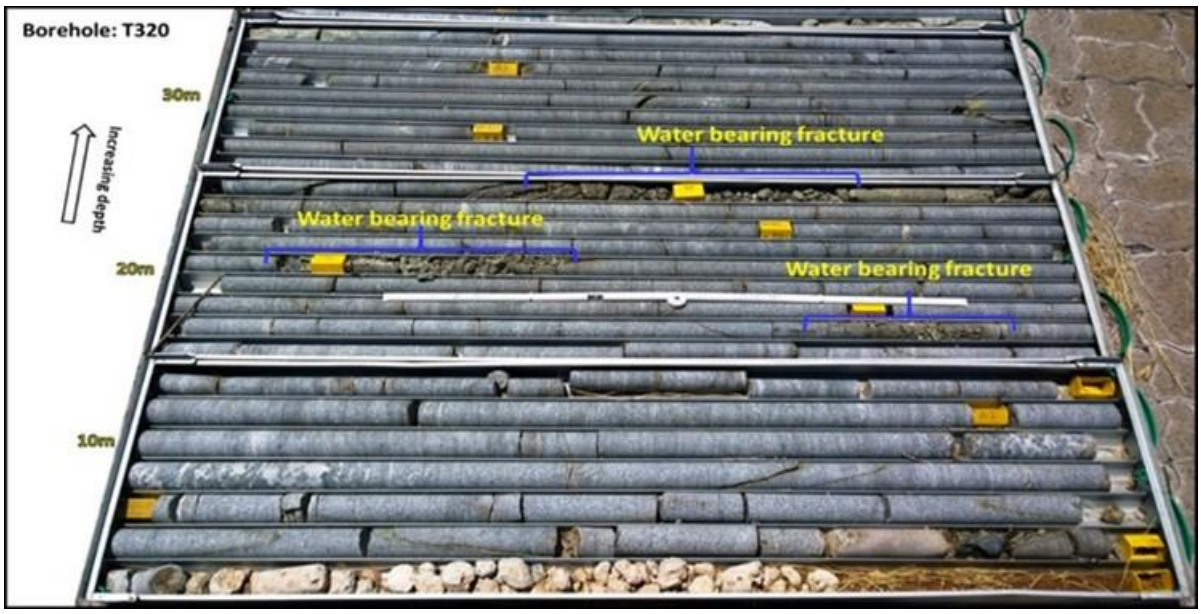


Figure 36: Borehole T320 with lithological and hydrogeological units.

The fractures intersected within the boreholes (at shallow depth ~40m) do not have infill material. However, there is a thin coating of $CaCO^3$ on fracture surfaces indicative of water activity. However at mining depth (~150 m) prominent joints within pyroxenites have serpentinite infill, which is friable, so causing poor cohesion between joint planes.

The fracture frequencies show some variation for all the boreholes. However, all the boreholes show a gradual increase in the number of fractures (10 m interval) with increasing depth to around 40m. This observation was greatly noticeable in boreholes that intersected dolerite dykes where fracture frequencies go up to 49.53% between 20n and 30m depth in borehole T322, whereby the number of fractures sharply increases once the dyke is intersected (Figure 37 and Table 2) – and thus these joints make favourable water flow paths. However, at greater depth the fracture frequencies tends to decrease with increasing depth within the bedrock, where between 70 and 80m depth fracture frequencies vary between 1% and 7% in all the boreholes.

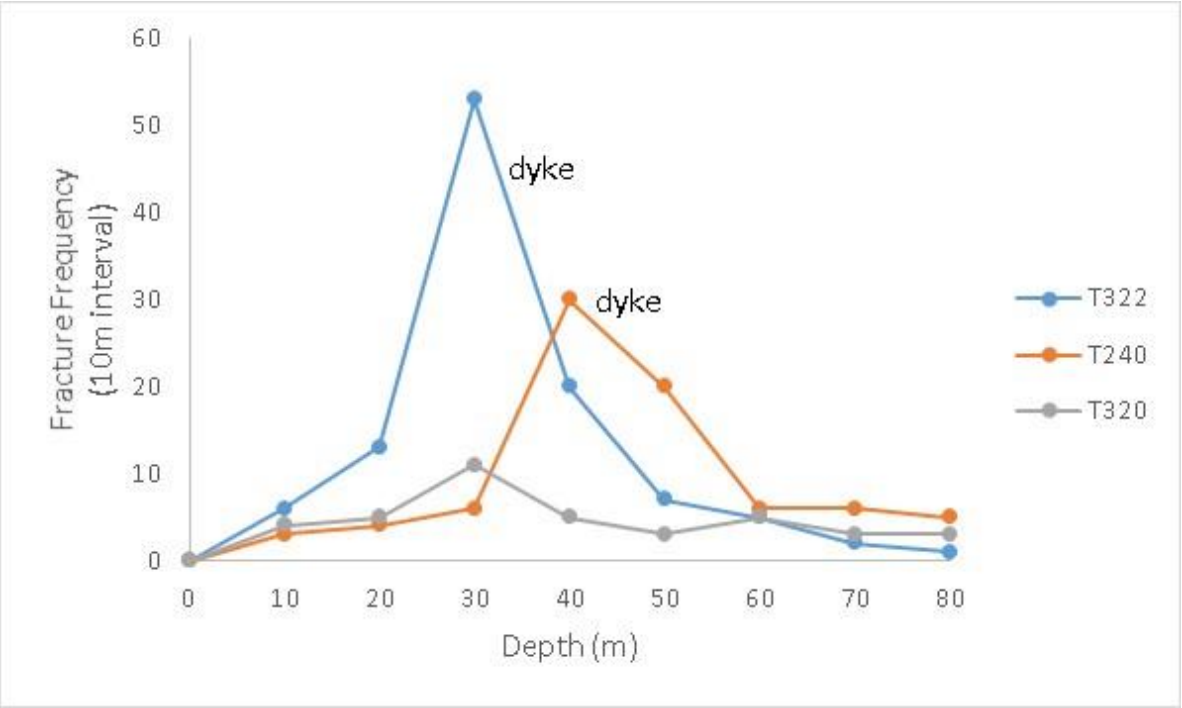


Figure 37: Fracture frequencies within the core samples (boreholes T240, T320 and T322) from Tweefontein farm.

Table 1:Fracture frequencies in percentages for surface exploration boreholes.

Depth(m)	T322	T240	T320
0-10	5.61%	3.75%	10.26%
10-20	12.15%	5.00%	12.82%
20-30	49.53%	7.50%	28.21%
30-40	18.69%	37.50%	12.82%
40-50	6.54%	25.00%	7.69%
50-60	4.67%	7.50%	12.82%
60-70	1.87%	7.50%	7.69%
70-80	0.93%	6.25%	7.69%
	100.00%	100.00%	100.00%

Field mapping and exploration drilling revealed a faulted shear zone in the direction of mining (NW). The Dwars River in the area ahead of mining flows over the faulted shear zone. This prompted the drilling of an underground horizontal borehole (TWF029), in order to ascertain the position of the shear zone and to investigate if the shear zone and associated faulting and jointing were water bearing – since that can lead to mine ingress. The underground mine workings are about 150 m below surface (Figure 38).

The borehole was drilled through the faulted shear zone, and the following observations were made from the drill core: the faulted shear zone was 20 m thick, and the shear zone consisted of highly serpentinised pyroxenite that is highly weathered. The core is extensively fractured and friable within the shear zone (Figure 39). The entire zone has a combined vertical displacement of 30 m.

The shear zone with the associated joints and faults was found to be not water bearing, and subsequent boreholes that have been drilled through the shear zone in different directions were also not water bearing.

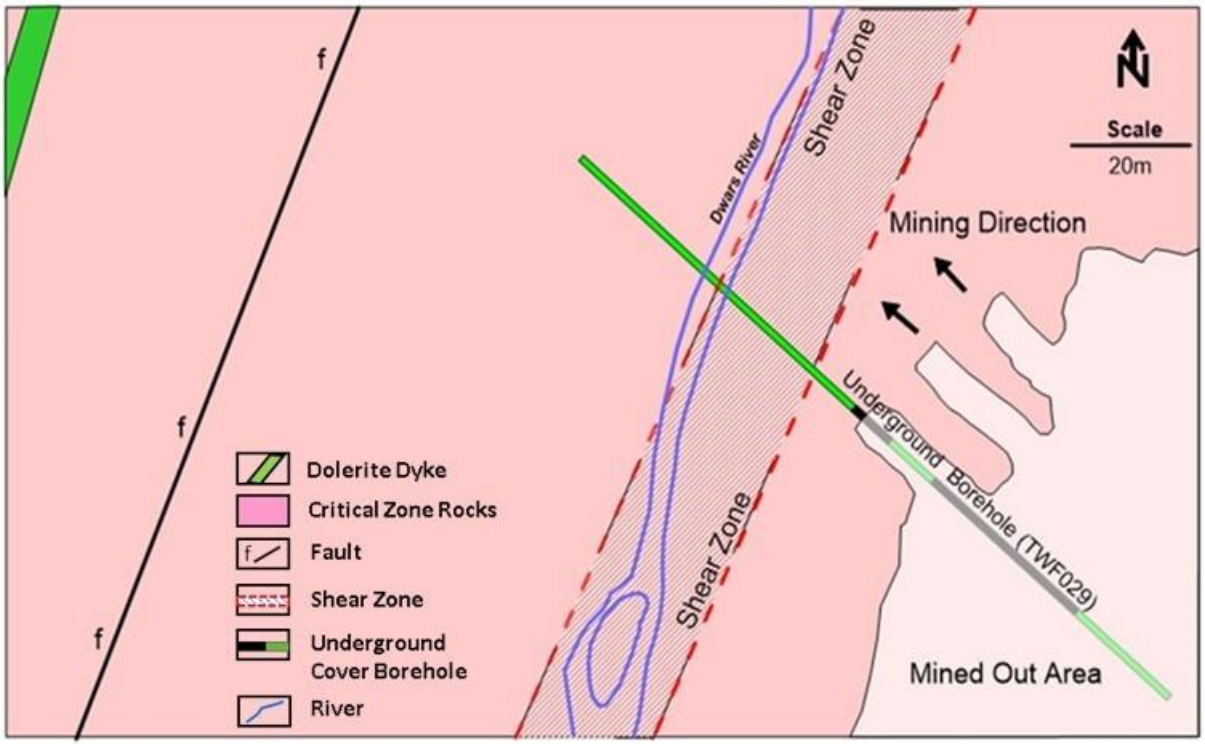


Figure 38: Underground borehole TWF029 drilled horizontally through the shear zone, showing intersected geological units and structures.

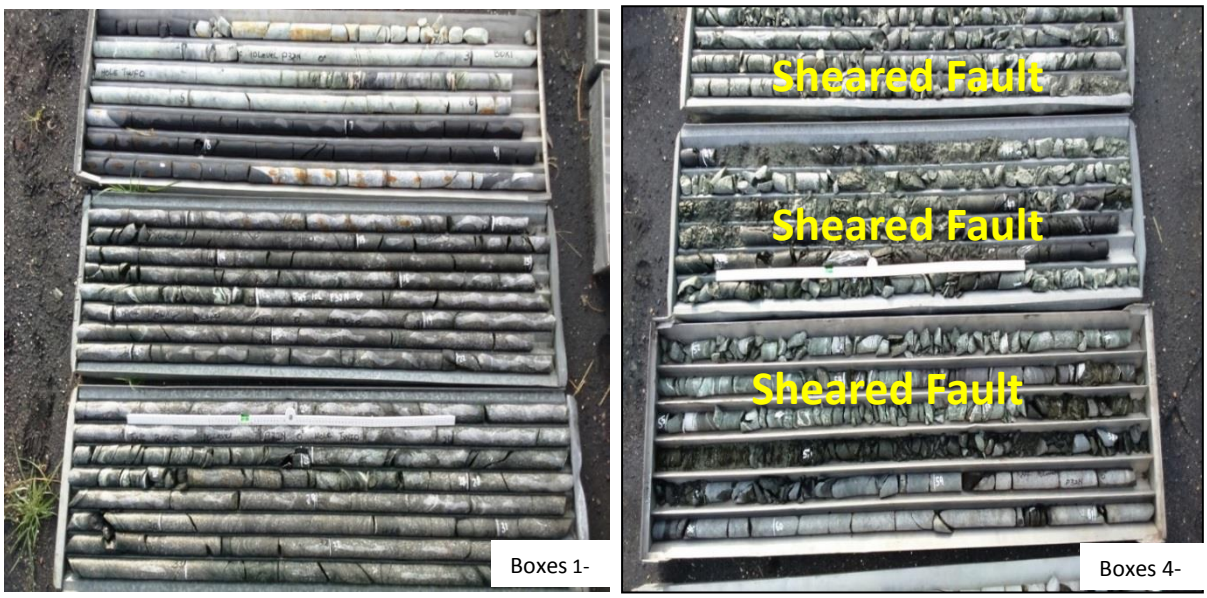


Figure 39: Borehole TWF029 core sample showing intersected geological units and structures.

The results from borehole TWF029 suggests limited vertical hydraulic connection between the overlying Dwars River and the underlying faulted shear zone and joints in the immediate vicinity of the river. The reason for the lack of mine ingress from the river through the faulted shear zone, is not sufficiently understood. However, the depth below the surface (150 m) can contribute to limited hydraulic connection, as the fracture permeability decreases with depth. Furthermore, the core displays clay material from the weathering of the norites and anorthosites, and the clay can also form a barrier to vertical flow within the shear zone.

Surface exploration boreholes drilled also confirm the existence of the weathered zone aquifer and the fractured zone aquifer. The frequency of joints tends to increase with increasing depth, and thus the capacity of fractures to transmit water within the fractured zone is much higher, since there no infill material. Multiples joints occurred near the contacts of the dykes with the country rocks. This would doubtlessly make these dykes preferential channels for water to pass through.

Cross Sections

The central and eastern portions of the Tweefontein farm are located on the Lower and Upper Critical Zone which is composed of ultra-mafic rocks. Mining on this farm is restricted within these zones. The Critical Zone rocks gently dip between 10° and 12° towards the west and north-west. On the central portion towards the west lies Transvaal quartzite, which is bounded by two major faults: the Kalkfontein fault in the west with an estimated vertical displacement of 1000 m and the Dwars River fault in the east (van Rensburg, 1965). Beyond the Kalkfontein fault lie the rocks of the main zone towards the far west. The area has also been intruded by dolerite dykes, which are striking NE-SW. These dykes steeply dip between 75° and 85° NW.

Three geological cross sections have been drawn within the Tweefontein farm, and all the cross sections were drawn on the true dip of the rocks. One section was drawn on the northern parts, one in the middle, and one on the southern portion. The cross sections were drawn in order to understand the subsurface hydrogeological condition within the farm (Figure 40).

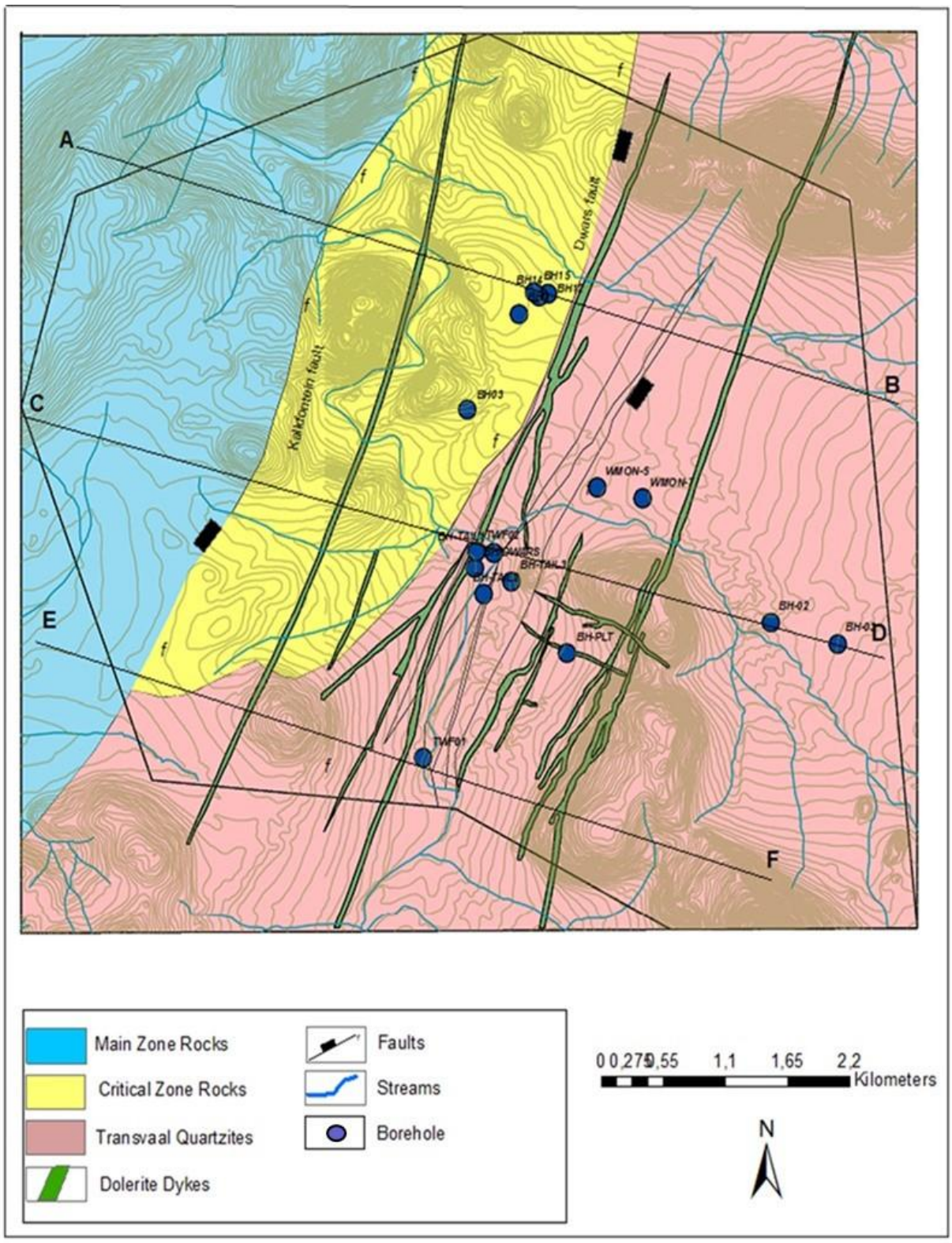


Figure 40: Tweefontein geology map, with cross-section profiles.

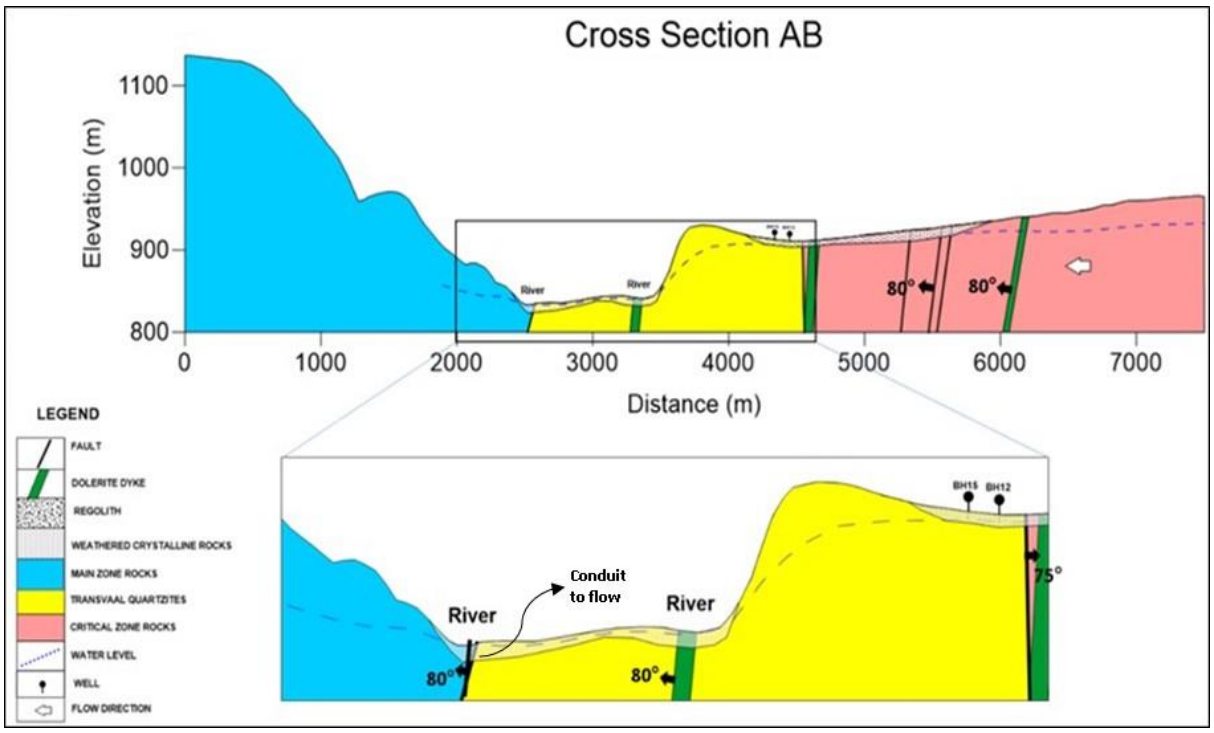


Figure 41: A cross section A-B, showing flow directions and geological units within Tweefontein farm.

The cross section in Figure 41 was drawn from east to west, and the section starts within the critical zone rocks (norites, anorthosites and pyroxenites), which then terminate against the Dwars River fault. Beyond the Dwars River fault zone is a Transvaal quartzite, and the fragment terminates in the west against the Kalkfontein fault. Beyond the Kalkfontein fault are the main zone rocks (grabbro-norites), which stretch to the far west. The main lithologies are intersected by steeply dipping dolerite dykes and faults striking NE-SW, and dipping between 75° and 80° NW. The faults in the eastern portion vary in displacement between 2 m and 30 m (Figure 41).

Eastwards, the weathered zone aquifer is the main aquifer, while the alluvial aquifer is very thin to absent. The thickness of the weathered zone aquifer reaches up to 25 m, while in places the regolith layer only measures up to 0.6 m. Deep weathering occurs within the pyroxenite (located eastwards) compared to the more rigid quartzites and main zone rocks located in the central and western halves of the farm. Two boreholes in the section line exist, and are located in the central portion within the quartzites (BH15 and BH12); the boreholes have water levels averaging 20m below ground level. This suggests that they may extend to the fractured zone aquifer (Figure 41).

In the vicinity of the river, the weathering is increased within the weathered zone aquifer, but beyond that on the highly mountainous rocks westwards there seems to be minimal weathering.

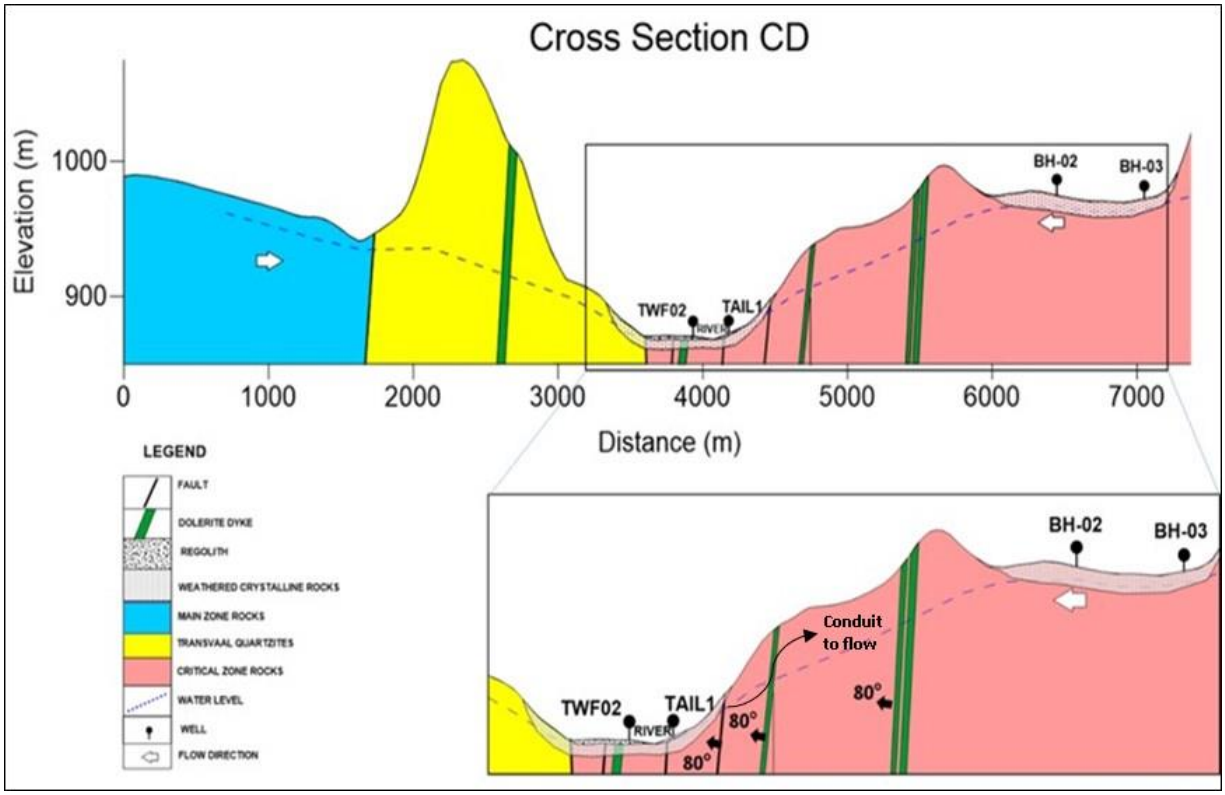


Figure 42: A cross section C-D showing flow directions and geological units within Tweefontein farm.

The section in Figure 42was drawn from the critical zone pyroxenites in the east, and these pyroxenites show some deep weathering towards the east. The critical zone rocks terminate against the Dwars River fault. Beyond the fault are the Transvaal quartzites, which are bounded by the Dwars River fault in the east and the Kalkfontein fault in the west – forming a horst-like structure. West of the Kalkfontein fault lie the main zone composed of gabbro-norites. From east to west the area is intruded by dolerite dykes with thicknesses that vary from10 to40 m, and all the dykes are steeply dipping westwards. Also present are faults that are steeply dipping westwards with vertical displacements of about 30 m (Figure 42).

There are two boreholes located in highly weathered pyroxenites, and water levels average 30 m below ground level in boreholes BH-02 and BH-03. Sami (2009) also found similar conditions in the area where proneness to weathering increases with an increase in pyroxene minerals.

The regolith aquifer increases in thickness to about 3 m on the reaches of Dwars River and to 4 m east of the river. The weathered zone aquifer reaches a thickness of 27 m near the river and 16 m east of the river. There are two boreholes that fall on the section line – TWF02 and BH-TAIL1 – and the water levels in these boreholes is quite shallow at 6.8 m and 2.4 m.

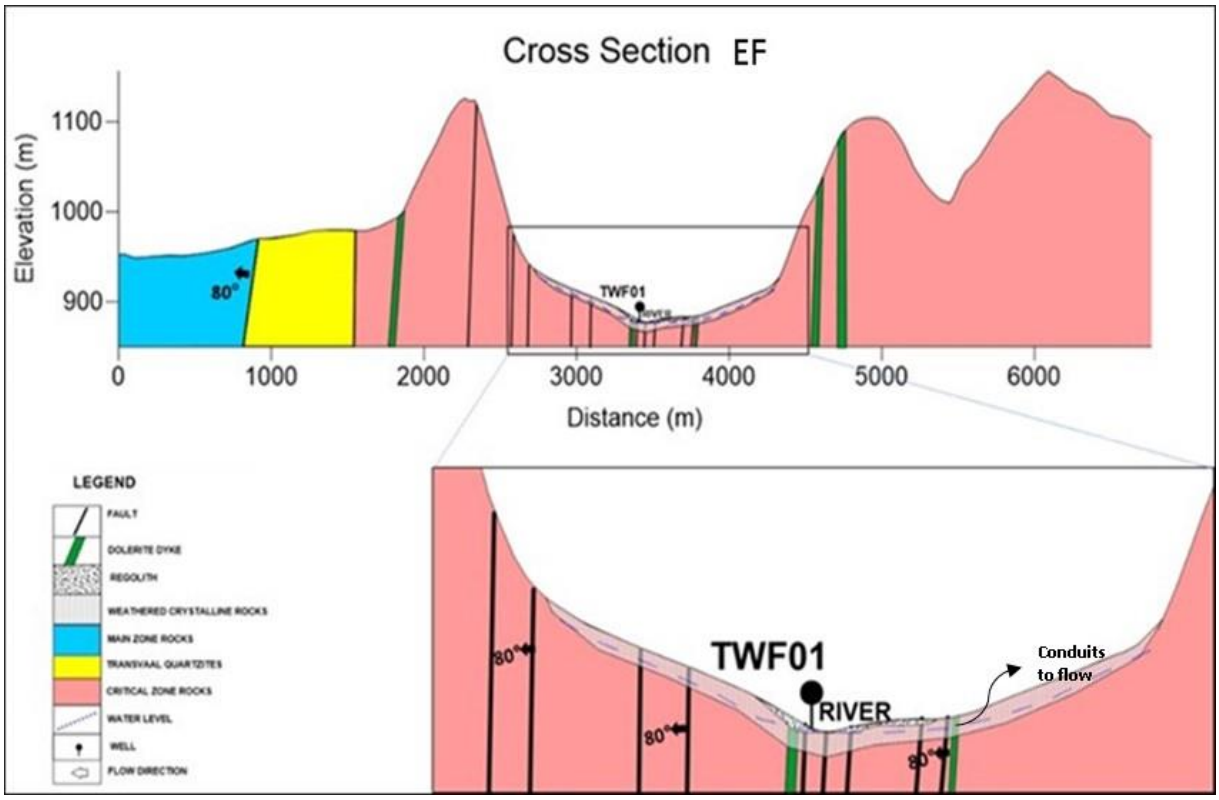


Figure 43: A cross section E-F showing flow directions and geological units within Tweefontein farm

The section in Figure 43 was drawn on the southern portion of the farm from the critical zone pyroxenites which show resistance to erosion, so forming “koppies”. The critical zone rocks terminate against the Dwars River fault on the banks of the River. Beyond the fault are the Transvaal quartzites, which are bounded by the Dwars River fault in the east and the Kalkfontein fault in the west – forming a horst structure. West of the Kalkfontein fault lies the main zone composed of gabbro-norites. From east to west the area is intruded by dolerite dykes with thicknesses of 10–40 m, where the

dykes are steeply dipping westwards. Also present are faults that are steeply dipping westwards, and with vertical displacements of 2–30 m. The area has multiple faults and associated shear zones, with most of them located near the river.

On the southernmost part of the farm the prominent lithologies are anorthosites, where the weathered zone aquifer is replaced by a regolith that is fine to medium crystalline and brownish-reddish in colour, and up to 2 m thick. However, downstream the weathered zone aquifer becomes pronounced with thicknesses of 16–18.5 m near the river, while the overlying regolith reaches up to 2.3 m. Water levels from TWF01 were measured to be 7.51 m below ground level, and the borehole is tapping into the weathered zone aquifer.

From all the cross sections drawn, it is evident that locally groundwater flows towards the Dwars River – indicating that the shallow aquifers are locally recharging the stream. This can also be deduced from water level elevations.

These cross sections were drawn to determine if there is any visible influence on the movement of groundwater caused by geological structures. The lack of noticeable water elevation difference between faults and dykes, tends to suggest that water is flowing through these structures due to them being weathered, and also fractured in the case of dykes (Figure 43).

5.3. Hydrogeochemistry

Samples were collected from monitoring boreholes within the farm and from the Dwars River. Major element analysis was conducted for Calcium (Ca^{2+}), Magnesium (Mg^{2+}), Sodium (Na^{+}), Potassium (K^{+}), Iron (Fe^{2+}), Manganese (Mn^{2+}), Aluminium (Al^{3+}), Total Alkalinity, Chloride (Cl^{-}), Nitrate (NO_3^{-}), Sulphate (SO_4^{2-}), Fluoride (F^{2+}), Total Dissolved Solids (TDS), pH, and EC (Table 1). All samples were taken either from boreholes or from surface water; there were no samples taken from underground mine fissures. The water quality parameters from the project area are presented in Table 1.

The pH ranges from 7.7–9.03, and the groundwater can be classified as slightly alkaline. The total dissolved solid values range between 101 and 1094 mg/ℓ. TDS values are generally elevated in borehole samples, while lower values have been

noted in stream samples. Elevated values in the borehole samples can be attributed to water rock interaction within the shallow weathered zone aquifer. Furthermore, boreholes TWF01 and TWF02 located near the river have lower TDS values, which are similar to stream samples (DWARSRIVER and DOWN STREAM A) – suggesting surface and groundwater interaction.

Boreholes located on the central part of the farm where most mining activities occur (BH-PLT, BH-TAIL1, BH-TAIL2, BH-TAIL3) have elevated TDS values. These boreholes are used to monitor the movement of contaminat plumes from mine tailings and waste rock dumps, and so higher TDS values can be linked to the movement of plumes in the NW direction.

Electrical conductivity (EC) varies from 14.2 to 155 mS/m. In the samples, EC was generally high in boreholes in the central portion of the farm. These boreholes are located west of the mine tailings and groundwater generally flows towards the west to north-west. Therefore, higher EC values are due to high salinity, which has been linked to the movement of the contaminat plume from the mine tailings and waste rock dumps. Boreholes located towards the east and south of the farm generally have lower EC values that are similar to those in the stream water – also suggesting surface and groundwater interaction.

The concentration of calcium and magnesium varies between 9.77–139 mg/ℓ and 11.3–131.8 mg/ℓ, respectively. The high magnesium and calcium concentrations are probably derived from the host rocks, as the Bushveld Igneous Complex comprises a suite of igneous rocks containing abundant magnesium, iron and silicates, and when these rocks weather they tend to release calcium and magnesium minerals.

Nitrates within the samples vary from 0.2–78.2 mg/ℓ. The source of high nitrate concentrations in samples BH-PLT, BH-TAIL1, BH-TAIL2, BH-TAIL3, VOID, BH1, BH4 and BH12 is not known. However, highest concentrations are noted in boreholes near waste rock dumps and mine tailings. Remains from explosives within the waste rock dumps and tailings' materials could contribute to higher nitrate values within the study area. However, since many samples show elevated nitrate values, it would be appropriate to investigate the possible sources of higher nitrates, both locally and regionally.

Chloride levels in the samples vary from 1.58–88.7 mg/ℓ. Boreholes BH07, BH01, BH-TAIL1 and BH-TAIL2 all show high chloride values. Chloride is a well-known conservative anion, and, in the absence of Cl-bearing minerals such as halite, it is neither added nor removed from solution through rock–water interactions (Mazor, 2004). Since the study area is generally dry with evaporation levels exceeding precipitation, elevated chloride levels can be expected.

Total alkalinity is defined as a measure of the buffering capacity of water against acidification, and therefore it has a tendency to pH changes and is expressed by carbon species in water: CO_2^-, HCO_3^-, and CO_3^{2-} (Mazor, 2004). Waters with a neutral pH (~7) tend to be dominated by bicarbonate and the occurrence of carbonate is uncommon, while water with high pH ~9 has contribution from carbonates. In the study area, alkalinity is entirely dominated by bicarbonate anions – even though some pH values are high.

Table 2: Surface and borehole water samples collected in Tweefontein farm.

SAMPLE	Latitude	Longitude	pH	EC (mS/m)	TDS (mg/ℓ)	Ca (mg/ℓ)	Mg (mg/ℓ)	Na (mg/ℓ)	K (mg/ℓ)	Total alkalinity (mg/ ℓ)	Cl (mg/ℓ)	SO^4 (mg/ℓ)	NO^3 (mg/ℓ)
BH-PLT	-24.8928	30.1192	8.16	155	1094	139	91	56.2	1.74	455	40.3	121	78.2
BH-TAIL2	-24.8884	30.1126	9.03	122	885	34.3	96.5	129	1.5	488	63.1	116	28.2
TWF01	-24.9005	30.1078	7.93	66.1	387	61.7	45.3	22.4	0.232	402	11.5	0.141	0.205
BH-TAIL1	-24.8854	30.1134	8.52	121	833	60.3	86.3	115	0.46	493	88.7	125	9.92
TWF02	-24.8853	30.11202	7.95	64.1	395	80	24.6	32.5	1.86	342	11.7	31.7	0.794
BH-TAIL3	-24.8875	30.1148	8.01	109	725	48.2	71	87.2	1.54	425	43.1	106	9.24
SRK15	-24.8923	30.1328	8.18	14.2	112	9.77	11.3	2.87	1.02	82.1	1.58	1.19	0.996
DWARS-RIVER	-24.9061	30.1058	8.45	53.5	366	46.3	34.9	16.6	2	188	15.1	45.7	13
DOWN STREAM-A	-24.8809	30.1093	8.4	63.3	449	49.1	38.6	27.9	2.4	229	22.8	52.7	17.7
DOWN STREAM-B	-24.8819	30.1137	8.18	17.8	101	11.7	13.7	3.25	3.36	92	1.61	8.12	0.675
VOID	-24.8764	30.1228	8.75	102	690	22.3	91.6	48.3	6.49	338	41.3	40.2	41.6
BH01	-24.8684	30.1177	8.1	139	766	53.33	131.8	31.76	3.97	512	157	44	9.3
BH04	-24.878	30.109	8.3	114	732	24.32	100.5	69.29	1.63	436	51	49	29
BH07	-24.8445	30.1209	7.7	140	860	99.44	109.1	39.46	3.53	424	168	102	4.7
BH08	-24.868	30.123	8.2	93.3	606	49.24	79.51	51.15	2.2	472	36	25	6.8
BH09	-24.8846	30.1532	8.2	90.6	548	22.97	97.18	28.65	2	500	20	37	3.3
BH12	-24.8663	30.1177	7.9	110	678	40.28	92.9	50.22	3.02	500	56	43	9.4

Sample points in the Piper diagram (Figure 44) can be categorised into 6 different fields: 1. Ca-HCO_3^-; 2. Na-Cl; 3. Ca-Mg-Cl; Ca-Na-HCO_3; 5. Ca-Cl; and 6. Na-HCO_3^-. The data under consideration fall within field one, which is Ca-HCO_3^-dominated water.

Samples BH01, BH07, BH-PLT, DWARS, VOID and DOWNSTREAM-A, marginally trend toward a chloride-dominated facies showing the strong effect of evaporation within the shallow weathered zone aquifer and surface waters.

Samples TWF01, TWF02, SRK15, BH09, BH08 and DOWNSTREAM-B, are dominated by bicarbonate – suggesting a fresh, recently recharged groundwater that has not been highly evolved. The prevalence of calcium and magnesium within the samples can be attributed to the weathering of silicate minerals of the Bushveld Igneous Complex that are high in calcium and magnesium.

Samples BH04, BH-TAIL1, BH-TAIL2 and BH-TAIL3, are dominated by both calcium, magnesium and the bicarbonate. However, samples seem to be slightly evolving toward a sodium chloride-dominated facies signifying some cation-exchange process between calcium and sodium. Sodium and chloride enrichment can also be due to irrigation return flows associated with farming in the area.

There seems to be no discernible chemical variations between the faults and dykes – suggesting the predominant movement of water between the geological structures. Furthermore, similar chemical signatures of the shallow groundwater and surface water suggest that there is some groundwater–surface water interaction.

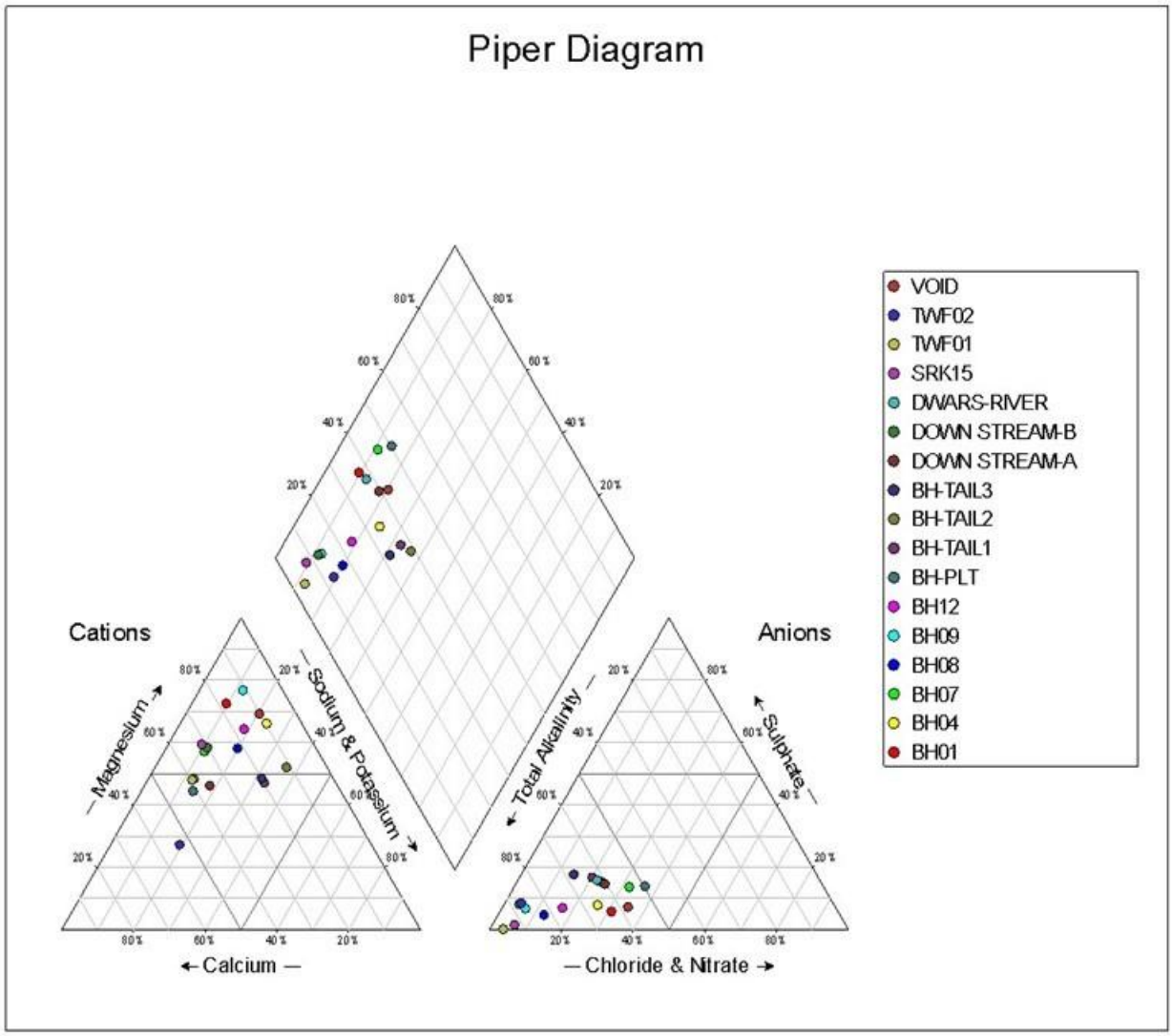


Figure 44: A Piper plot for both surface and borehole water samples collected in Tweefontein farm.

5.4. Environmental Isotopes

The use of isotopes of hydrogen and oxygen in groundwater investigation focuses on the change in the isotopic signature in precipitation, and its subsequent infiltration and forming part of the groundwater system. The changes in isotopic signatures are due to various physical processes – with the most prominent being evaporation and condensation (Aggarwal et al., 2006).

Environmental stable isotopes (deuterium and oxygen 18) are useful in differentiating different sources of groundwater. In this project, stable isotopes were used to investigate whether samples collected within and around the faults and dykes, have similar signatures or not – thus permitting a concise deduction of weather there is an influence of geological structures on such signatures.

A total of 17 samples were collected for stable isotope analysis (oxygen 18 and deuterium) from different parts of the project area. Eleven of the samples were from monitoring boreholes, four from underground seepages from fissures associated with the NE-SW trending shear zones, one from an opencast, and one from the Dwars River. The Pretoria Local Meteoric Water Line of $\delta^2H = 6.7 \times \delta^{18}O + 7.2$ ‰ (IAEA-GNIP), was used in the interpretation (Figure 45).

The stable isotope results for δ^2H vary between -4.28‰ and 0.52‰, while for $\delta^{18}O$ the range is -17.14‰ to 7.21‰. Most of the samples plot below the local meteoric water line (LMWL), while a substantial number plotted in the close proximity to the LMWL. One sample plotted above the LMWL (TM3/SHAFT) (Table 2).

Most samples from both shallow groundwater in the alluvial and weathered zone aquifer and surface waters, show enrichment of with respect to δ^2H and $\delta^{18}O$. These are plotted along the evaporation line – suggesting that the water was subjected to evaporation prior to infiltration. The evaporation effect is further ratified by an increase in salinity in samples that plot on the evaporation line (e.g. BH-DWARS, BH-TAIL2, BH-TAIL1, and BH-PLT).

Samples collected from the seepages along the mine-fissures (TM3 BH/01, TM3 BH/02, TM3-SHAFT) are highly depleted in δ^2H and $\delta^{18}O$, and tend to fall close to the LMWL, suggesting recharge prior to evaporation, and that the water could be recharged during summer months through high rainfall. This suggests that the water was recharged rapidly along preferential flow paths, whereby rain water is recharged

during periods of short and heavy rainfall through geological structures such as joints and faults that outcrop on the surface. Thus these waters would retain the same isotopic composition as rain water. This concurs with Vogel and Van Urk (1974), that in arid and semi-arid regions of Southern Africa, groundwater tends to be depleted of δ^2H and $\delta^{18}O$ stable isotopes compared to rainfall. However, short and rapid heavy rainfalls compare well with groundwater – suggesting that short, heavy rainfall events are responsible for much recharge.

Samples BH-TAIL3, TM3/TRAVEL and WMON-5 also fall within the LMWL, but are significantly enriched in δ^2H and $\delta^{18}O$, suggesting that the water is also of atmospheric origin, and is recharged during the winter months. The water was recharged into the shallow weathered zone aquifer, before it was subject to evaporation.

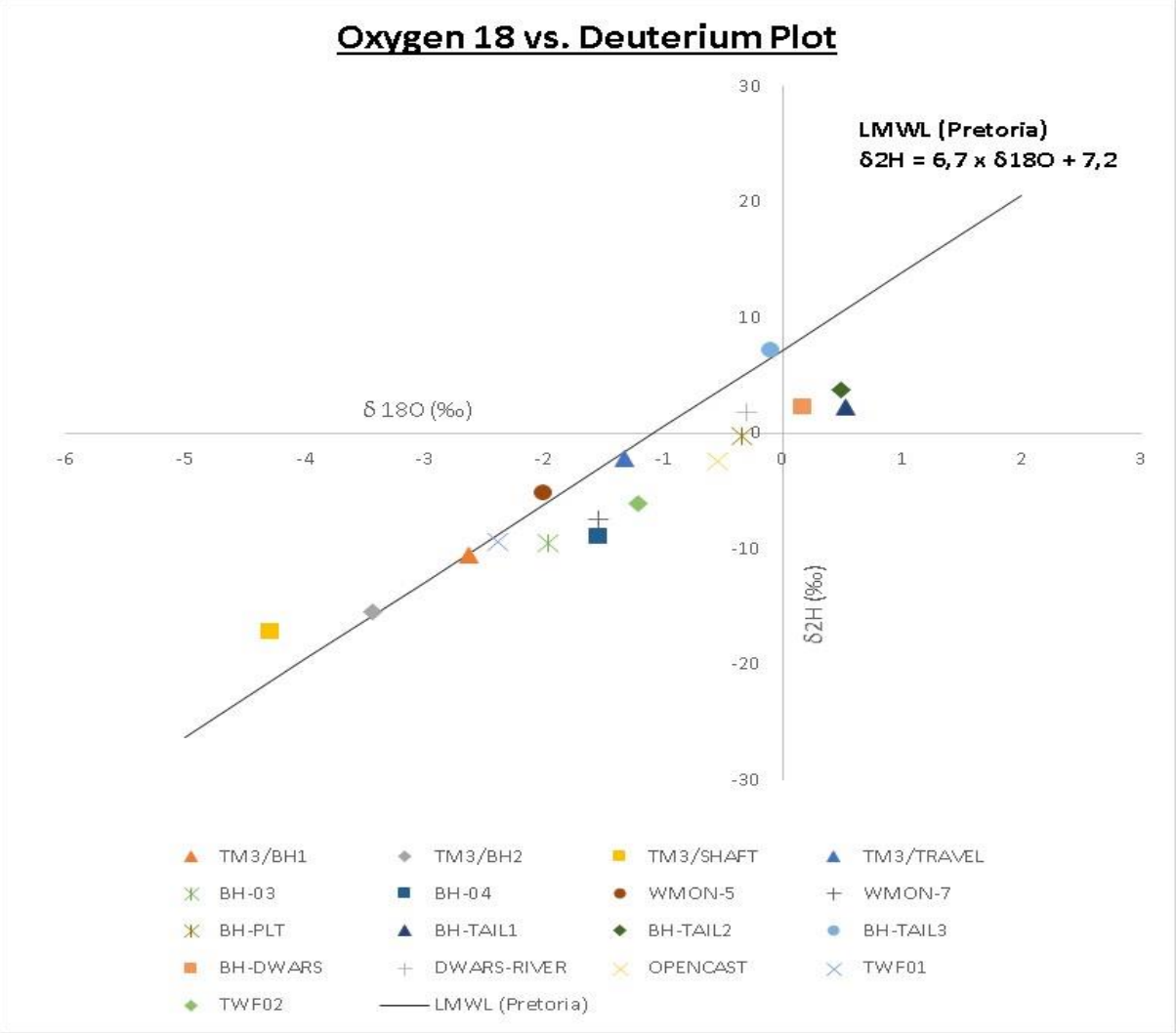


Figure 45: The oxygen 18 vs deuterium plot for the Tweefontein samples.

Table 3: The oxygen 18 vs deuterium isotope results for Tweefontein farm.

Number	Sample ID	Latitude	Longitude	Sampling Date	δ^2H (‰)	δ^2H (‰) StDev	δ^{18}O (‰)	δ^{18}O (‰) StDev
1	TM3/BH1	-24.9063	30.1116	15/08/2016	-10.53	0.17	-2.63	0.06
2	TM3/BH2	-24.9063	30.1116	15/08/2016	-15.45	0.00	-3.43	0.00
3	TM3/SHAFT	-24.9082	30.1113	15/08/2016	-17.14	0.04	-4.28	0.03
4	TM3/TRAVEL	-24.8931	30.1183	15/08/2016	-2.24	0.00	-1.32	0.00
5	BH-03	-24.8921	30.1406	25/08/2016	-9.52	0.03	-1.97	0.07
6	BH-04	-24.8925	30.1428	25/08/2016	-8.88	0.10	-1.54	0.02
7	WMON-5	-24.8806	30.1216	25/08/2016	-5.21	0.00	-2.00	0.00
8	WMON-7	-24.8814	30.1252	25/08/2016	-7.46	0.00	-1.54	0.00
9	BH-PLT	-24.8928	30.1192	25/08/2016	-0.27	0.30	-0.34	0.04
10	BH-TAIL1	-24.8854	30.1134	25/08/2016	2.25	0.00	0.53	0.00
11	BH-TAIL2	-24.8884	30.1126	25/08/2016	3.74	0.19	0.49	0.03
12	BH-TAIL3	-24.8875	30.1148	25/08/2016	7.21	0.00	-0.10	0.00
13	BH-DWARS	-24.8865	30.1119	25/08/2016	2.25	0.00	0.18	0.00
14	DWARS-RIVER	-24.9057	30.1062	25/08/2016	1.81	0.32	-0.30	0.07
15	OPENCAST	-24.8741	30.1215	25/08/2016	-2.39	0.85	-0.54	0.04
16	TWF01	-24.9005	30.1078	25/08/2016	-9.42	0.00	-2.39	0.00
17	TWF02	-24.8853	30.112	25/08/2016	-6.08	0.13	-1.21	0.04

In summary, samples plotting below the LMWL signify evaporation prior to infiltration, and these samples are all from surface and shallow groundwater system. The other group are samples (depleted δ^2H and δ^{18}O) that plot on the LMWL, signifying recharge prior to evaporation during the summer months and associated with short and heavy rainfalls (these are samples from mine fissure seepages). Then another group is represented by samples which also plot within the LMWL (enriched in δ^2H and δ^{18}O) – signifying recharge prior to evaporation during the winter months.

The data also suggest that shallow groundwater is not directly linked hydraulically with mine-fissure water in the underground workings. This is deduced from the fact that shallow groundwaters in the weathered zone show significant enrichment of oxygen 18 and deuterium associated with extensive evaporation before infiltration, while water from seepages associated with mine fissures are significantly depleted of oxygen 18 and deuterium recharged prior to evaporation.

Samples from surface water and shallow boreholes have similar isotopic signatures – even though these boreholes are separated by faults and dykes. This suggests that there is some interaction/lateral flow through these structures; in other words, the structures act as conduits to flow – thus allowing free interaction of waters. This is further confirmed by the chemical composition of the samples, which is very similar in the shallow boreholes.

5.5. Conceptual Model

A conceptual hydrogeological model was constructed from various inputs – such as geological setting, weathering, fracturing and cross-sections (Figure 46).

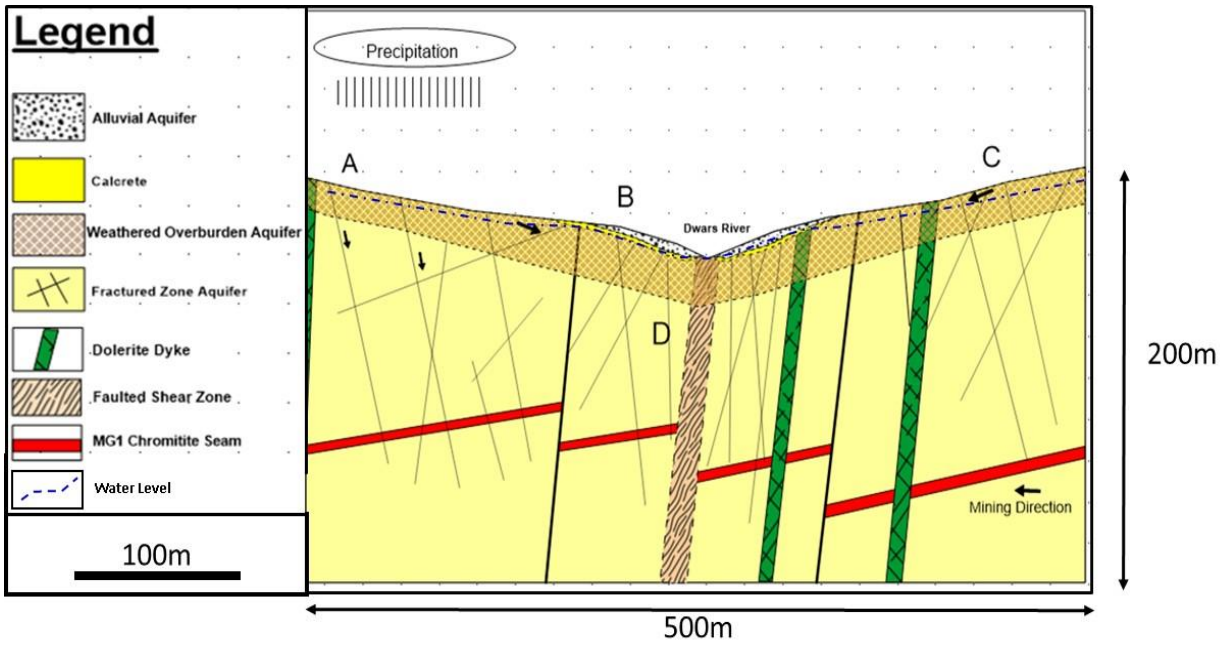


Figure 46: A conceptual model showing the aquifer system and groundwater flow directions.

The developed conceptual groundwater model was divided into four main domains that sought to explain the processes that affect groundwater movement in the mining area of the Tweefontein farm (Figure 46):

(A) Water available in mine fissures that is highly depleted in ^{2}H and ^{18}O isotopes falling within the local meteoric water line, is due to rainfall recharge during periods of heavy rainfall, through geological features acting as preferential flow paths – such as joints and faults that outcrop on surface. As a result, these waters would be quickly recharged and would retain the same isotopic composition as the rain water. These water-bearing geological features, when intersected by mining, lead to temporal ingress of water into underground workings.

(B) Field observations on the low-lying areas of the reaches of the Dwars River revealed extensive calcretes and ferricretes. The calcrete and ferricrete layers exist within the weathered overburden aquifer in areas where they act as a barrier to the vertical flow of groundwater, or could result in the formation of

later preferential flow paths. This can lead to the formation of other features like springs. The presence of calcretes and ferricretes would tend to minimise the hydraulic link with the underlying fractured aquifer, and this can lead to limited mine ingress – even when major structures are intersected.

(C) The outcrops of dolerite dyke are highly fractured with cross-cut joints, thus creating connected blocky fractures. The high frequency and interconnectedness of the fractures within the dykes strongly suggests that these dykes act as conduits to flow, even though the frequency of fracturing decreases with an increase in depth. The dykes show some degree of weathering – meaning they also form part of the local weathered zone aquifer, even though their degree of weathering tends to be less than the country rocks.

Faults mapped in the field have calcium carbonate infilling along the fault planes, and this infill has potential to act as cement, thus restricting the flow of water. However, due to extensive weathering observed the infill does not create a barrier effect making these faults conduits to flow. Field evidence shows that fracturing and weathering are major contributing factors to lateral flow between geological structures.

The lateral hydraulic link between geological features is further confirmed by the fairly uniform isotopic and chemical signatures in shallow boreholes that are located between the faults and dykes – suggesting the lateral movement of water between the geological structures within the weathered zone.

(D) The reason for the lack of mine ingress from the river through the faulted shear zone, is not sufficiently understood. However, the depth below the surface (150 m) can contribute to limited hydraulic connection, since the fracture frequency decreases with depth.

Also due to the shallow nature of the main aquifer (weathered zone aquifer), which only extends to less than 30 m, most of the major fractures probably underwent sealing by some infill mineral – thus reducing permeability and hydraulic connection between the weathered zone aquifer and the deep fractures.

CHAPTER 6

CONCLUSION AND RECOMMENDATIONS

Conclusion

The hydrogeology of the geological features of Tweefontein farm was investigated by considering geology and various aspects of hydrogeology. Geological features (faults, joints and dykes) allow lateral movement of groundwater due to the presence of interconnected, cross-cutting joints. Furthermore, due to the shallow nature of the aquifers, weathering of dykes and faults favours flow within these structures. Thus lateral flow between geological features can be attributed to both weathering and fracturing of rocks in the area.

The current study has shown that the prominent NE-striking shear zone is not linked with underground mine ingress. The reason for this phenomenon is not adequately understood, but factors such as depth below surface, clay mineral content with the fault zone and infilling are believed to contribute for low vertical hydraulic conductivity within the shear zone. Also the decrease in fracture frequency with increasing depth in and around dykes and faults could also limit seepage of water into the mine working.

Furthermore groundwater samples from the shallow alluvial and weathered zone aquifer and from surface waters, show an enrichment of both $\delta^{2}H$ and $\delta^{18}O$. The plot in the evaporation line suggests that the shallow groundwaters were subjected to evaporation prior to infiltration. However, samples from mine fissures are highly depleted with deuterium and oxygen 18, suggesting no direct hydraulic link between the shallow groundwater and the water in mine fissures, and that water from mine fissures was recharged prior to evaporation and are deep circulating water. This could be due to rainfall recharge during periods of high rainfall through geological features such as joints and faults that outcrop on the surface.

The low lying parts of the study area are also covered with calcrete and ferricrite within the aquifer units, these found to act as a barrier to the vertical flow of groundwater besides their role in generating preferential flow paths, which can then lead to water being discharged as springs. These presence of these would obstruct vertical movement of groundwater from the overlying aquifer to the underlying fractured zone aquifer. Thus the presence of calcrete and ferricrete, to some extent

leads to minimal mine ingress through fissures into underground workings – since water would be redirected due to their barrier characteristics.

The groundwater flow net revealed that groundwater, on a regional scale, flows in a NW direction towards the Steelpoort River (discharge), with the recharge zones being the high-lying areas located east and south of the study area. The lack of noticeable water elevation differences between faults and dykes tends to suggest that water is flowing through these structures, as a result of weathering, fracturing and dykes.

The groundwater is mainly bicarbonate dominated, suggesting a fresh, recently recharged groundwater that has not highly evolved which could be linked to infiltrating water through soil horizon. The predominance of calcium and magnesium within the samples has been attributed to the weathering of silicate minerals of the Bushveld Igneous Complex, which are high in calcium and magnesium. Other samples trend marginally towards a chloride-dominated facies, and show the strong effect of evaporation within the shallow weathered zone aquifer and within surface waters. In addition, some samples seem to be slightly evolving towards a sodium chloride-dominated water facies – signifying a cation exchange process between calcium and sodium, or these can be due to irrigation related return flows associated with domestic farming in the area.

The study shed light on the hydrogeology of geological features in the Tweefontein farm that the major geological structures such as the Dwars River fault system are not associated with mine inflows, but mine inflows are due to minor faults and joints that are recharged during periods of heavy rainfalls, and these findings can add insight to future mine design and planning in the structurally complex Tweefontein farm.

Recommendations

The influence of geological features on the groundwater system was investigated. However, more research is needed to improve or validate the research findings. This can be done through:

- A detailed study of the structural analysis of the area, as not much work has been done on the structural setting of the area. This would enable better understanding of how the structural setting affects the distribution and movement of groundwater in the wider Tweefontein area.
- A detailed investigation of the permeability of the NE-striking faulted shear zone is recommended, as this would enable better planning and mitigation when mining through this feature.
- More boreholes are needed – mostly in the northern and western portions of the farm. A wider and more uniform distribution of boreholes would enable better understanding of the groundwater system of the farm. This would then also enable informed mine planning and design.
- Sampling of water from mine fissures for chemical analysis is needed, in order to confirm observations made from isotopic data.
- Pilot underground boreholes are strongly recommended before any virgin ground is mined near the river. This is to determine if there are any water-bearing fissures ahead of mining. Also, since the weathered and fractured aquifers are likely not hydraulically linked, mine fissure inflows when intersected would not have sustained flows.

REFERENCES

Acworth, R.I. (1987). The development of crystalline basement aquifers in a tropical environment. Quarterly Journal of Engineering Geology, 20, 265-272.

Adams, S. (2009). Basement aquifers of Southern Africa: Overview and research needs. In: Basement Aquifers of Southern Africa, WRC Report No. TT 428-09. p. 1-4.

Aggarwal, P.K., Tanweer, A., Groening, M., Gupta, M., Owano, T. and Baer, D. (2006). Laser spectroscopic analysis of stable isotopes in natural waters: A low-cost, robust technique for the use of environmental isotopes in hydrological and climate studies, Eos Trans. AGU, 87(52), Fall Meet. Suppl., Abstract H51D-504.

Alley, W.M., Hearly, W.H., LaBough, J.W., and Reilly, T.E. (2002). Flow and storage in groundwater systems. Science, 296, 1985.

Anna, L.O. (1986). Geologic framework of the ground-water flow system in Jurassic and Cretaceous rocks, northern Great Plains. U.S. Geological Survey Professional Paper 1402- B, 36 p.

Bense, V.F., Gleeson, T., Loveless, S.E., Bour, O. and Scibek, J. (2013). Fault zone hydrogeology. Earth-Science Reviews 127.171–192.

Beukes, J.J., Gauert, C. and Kotze, E. (2013). Reef distribution of Critical Zone rocks of the eastern Bushveld Igneous Complex in the vicinity of the Steelpoort fault, South Africa – petrogenetic implications. Department of Geology, University of the Free State, Bloemfontein, South Africa.

Braune, E. and Mutheiwana, S. (2009). Towards sustainable utilization of basement aquifers in southern Africa. In: Basement aquifers of Southern Africa, WRC Report No. TT 428-09. 104 -113.

Bromley, J., Manstrom, B., Nisca, D. and Jamtlid, A.A. (1994). Airborne geophysics: Application to ground-water study in Botswana. Ground Water, 32, 79-90.

Cameron E.N. (1964). Chromite deposits in the eastern part of the Bushveld Igneous Complex. In: The geology of some ore deposits in southern Africa, Haughton, S.H. (ed.), Geol. Soc. S. Afr., Pretoria, II, 739 p.40

Cawthorn, R.G., Merkle, R.K.W. and Viljoen, M.J. (2002). Platinum-group element deposits in the Bushveld Igneous Complex, South Africa. In: Cabri, L.J. (ed.), The geology, geochemistry, mineralogy and mineral beneficiation of platinum-group elements. Canadian Institute of Mining, Metallurgy and Petroleum, Special Volume 54, 389-429.

Cawthorn R.G. (2002). Delayed accumulation of plagioclase in the Bushveld Complex. Min. Mag. 66, 881-893

Cawthorn, R.G. (2003). Genesis of magmatic oxide deposits – a view from the Bushveld Igneous Complex. Norges Geologsike Undersokelse, Special Publication 9, pp. 11-20.

Cawthorn, R.G., Eales, H.V., Walvaren, F., Uken and Watkeys, M.K. (2006). The Bushveld Complex. In: Johnson, M.R., Anhaeusser, C.R. and Thomas, R.J. (Eds.). The Geology of South Africa. Geol, Soc, South Africa, Council for Geosciences, Pretoria pp 261-281.

Chilton, P.J. and Smith-Carington, A.K. (1984). Characteristics of the weathered basement aquifer in Malawi in relation to rural water supplies. IAHS Publication no. 144, p. 57-72.

Chilton, P.J. and Foster, S.S.D. (1995). Hydrogeological characteristics and water-supply potential of basement aquifers in tropical Africa. Hydrogeology Journal, 3(1), 36-49.

Cook, P.G. (2003). A guide to regional groundwater flow in rock aquifers. CSIRO, Australia. 108 pp.

Eales H.V. and Cawthorn R.G. (1996). The bushveld Complex. In: Cawthorn R.G. (Ed.), Layered Intrusions, Elsevier, Amsterdam. p. 181-230.

Engel R., McFarlane D.J. and Street G.J. (1989). Using geophysics to define recharge: Discharge areas associated with saline seeps in south-western Australia. In: Sharma, M.L. (ed.), Groundwater recharge. A.A. Balkema, Rotterdam, p. 25–39.

Evans, J.P., Forster, C.B. and Goddard, J.V. (1997). Permeability of fault related rocks, and implications for hydraulic structure of fault zones. Journal of Structural Geology, 19, 1393-1404.

Freeze, R.A. and Cherry, J.A. (1979). Groundwater. Prentice- Hall, Englewood Cliffs, New Jersey.

Gebrekristos, R. and Cheshire, P. (2012). Hydrogeological properties of the UG2 pyroxenite aquifers of the Bushveld Igneous Complex. The Southern African Institute of Mining and Metallurgy Platinum 2012, p. 143-152.

Golder Associates (2006). Amendment to the approved environmental management programme report (EMPR) for Tweefontein, Eastern Chrome Mine. Unpublished.

Gomo, M., Tonder, G.V. (2013). Development of a preliminary hydrogeology conceptual model for a heterogeneous alluvial aquifer using geological characterization. J. Geol. Geosci., 2, 128. doi: 10.4172/2329-6755.1000128

Gudmundsson, A., Gjesdal, O. and Brenner, S.L., et al. (2003). Effects of linking up of discontinuities on fracture growth and groundwater transport. Hydrogeol. J., 11, 84–99. doi:10.1007/s10040-002-0238-0.

Hammond, K.J. and Evans, J.P. (2002). Geochemistry, mineralization, structure and permeability of a normal fault zone, Casino Mine, Alligator Ridge District, north central Nevada. Journal of Structural Geology, 25, 717-736.

Hatton, C.J. and von Gruenewaldt, G. (1987).The geological setting and petrogenesis of the Bushveld chromitite layers. In: Stowe, C.W. (ed.), Evolution of chromium ore fields. Van Nostrand Reinhold, New York, pp. 109-143.

Holzer, L., Barton, J., Paya, B. and Kramers, J. (1999). Tectonothermal history of the western part of the Limpopo Belt: Tectonic models and new perspectives. Journal of African Earth Sciences, 28, 383-402.

Hulbert, L.J. and von Gruenewaldt, G. (1985). Textural and compositional features of chromite in the lower and critical zone of the Bushveld Igneous Complex south of Potgietersrus. Eco. Geol., 80, 872-895.

Kinnaird, J.A., Kruger, F.J., Nex, P.A.M. and Cawthorn, R.G. (2002). Chromitite formation – a key understanding process of platinum enrichment. Transactions of the Institute of Mining and Metallurgy, 111, 23-35.

Lea, C.A. (1996). A review of mineralisation in the Bushveld Igneous Complex and some other layered intrusions. In: Cawthorn, R.G. (ed.), Layered intrusions. Elsevier, pp. 103-145.

Linn, F. (2009). Groundwater exploration and development of basement aquifers in Botswana. In: Basement aquifers of Southern Africa, WRC Report No. TT 428-09. p.31-38.

Lloyd, J.W. (1999). Water resources of hard rock aquifers in arid and semi-arid areas. In: Lloyd, J.E. (ed.), Water resources of hard rock aquifers in arid and semi-arid areas. Unesco Publishing, Studies and Reports in Hydrology, 58, 13-19.

Maynard, A.J. (2007). Independent geological evaluation, Spitskop 333KT Project, Bushveld Igneous Complex, Republic of South Africa.

Mazor, E. (2004). Chemical and isotopic groundwater hydrology (3rd Ed.). Marcel Dekker, Inc, p. 61. ISBN: 0-8247-4704-6.

Midgley, D.C., Pitman, W.V. and Middleton, B.J. (1994). Surface water resources of South Africa 1990. Vol IV. Appendices. 1st ed. Rep. No. 298/4.1/94. Water Research Commission, Pretoria.

Mills, P.J. (1980). Detailed ground magnetic survey – Tweefontein chrome mine. Samancor Chrome, unpublished data.

Nakhwa, R.A. (2005). Structural controls on groundwater flow in the Clanwilliam area. Unpublsihed MSc thesis, Department of Earth Sciences, Faculty of Natural Sciences, University of the Western Cape, Cape Town. p.7

Nathan, R.J. & McMahan, T.A., 1990. Evaluation of automated techniques for baseflow and recession analyses. Water Resources Research, 26(7), pp.1465–1473.

Petzer, K.J. (2009). Structural geological controls on the flow and occurrence of groundwater in the basement lithologies of the Limpopo Province, South Africa. Unpublished M.Sc Dissertation, University of Pretoria, South Africa. p. 34-35.

Rashleigh, B., Hardwick, D. and Roux, D. (2009). Fish assemblage patterns as a tool to aid conservation in the Olifants River catchment (East), South Africa. Vol.35, n.4, pp.517-524. ISSN 1816-7950.

Roberts, J.L. (1982). Geological maps and structures. Pergamon Press.

Samancor ECM (2013). Geology mapping archives, unpublished reports. Unpublished.

Sami, K. (2009). Groundwater exploration and development. In: Titus, R.A., Adams S. and Strachan, L. (eds), The basement aquifers of Southern Africa. WRC Report Nr. TT 428/09, Water Research commission, Pretoria. p. 19-30.

Scoon, R.G. and Teigler, B. (1995). A new LG6 chromite reserve at Eerste Geluk in the boundary zone between the central and southern sectors of the eastern Bushveld Igneous Complex. Econ. Geol., 90, 969-982

Seabrook, C.L. (2005). The Upper Critical and Lower Main Zones of the eastern Bushveld Igneous Complex. PhD thesis, Department of Geosciences, University of the Witwatersrand, South Africa. p. 9-10.

Silver, P.G., Fouch, M.J., Gao, S.S. and Schmitz, M. (2004). Kaapvaal Seismic Group, 2004. Seismic anisotropy, mantle fabric, and the magmatic evolution of Precambrian southern Africa. South African Journal of Geology, 107, 45-58.

Taylor, R. and Howard, K. (2000). A tectono-geomorphic model of the hydrogeology of deeply weathered crystalline rock: Evidence from Uganda. Hydrogeology Journal, 8, 279-294.

Tessema, A. and Nzotta, U. (2014). Multi-data integration approach in groundwater resource potential mapping: A case study from the North West Province, South Africa. Council of Geosciences, Pretoria. p.1.

Titus, R., Witthüser, K., and Walters, B. (2009). Groundwater and mining in the Bushveld Igneous Complex. Proceedings of the International Mine Water Conference, Pretoria, South Africa, 19-23 October 2009. Water Institute of Southern Africa and International Mine Water Association.

Tóth, J. (1963). A theoretical analysis of groundwater flow in small drainage basins. J. Geophys. Res., 68(16), 4795- 4812.

UNEP and WRC. (2008). Freshwater under threat: Vulnerability assessment of freshwater resources to environmental change. UNEP-WRC publication. Water Research Commission, South Africa.

UNESCO. (2004). Groundwater resources of the world and their use. IHP-VI, Series On Groundwater, no 6.

Van Rensburg, W.C.J. (1965). The geology of the Dwars River Fragment, Lydenburg District, Transvaal. Annals of the Geological Survey of South Africa, 4, 74.

Viljoen, M.J. and Schürmann, L.W. (1998). Platinum-group metals. In: Wilson, M.G.C. and Anhaeusser, C.R. (eds), The mineral resources of South Africa. Handbook 16, Council for Geoscience, Pretoria, pp. 532-568.

Vogel, J.C. and Van Urk, H. (1974). Isotopic composition of groundwater in semi-arid regions of Southern Africa. Journal of Hydrology, 25 (1975), 23-36.

APPENDICES

Appendix A – Groundwater Levels

BH ID	Latitude	Longitude	Z	WL (mamsl)	WL (mbgl)
H02-1251	30.02017	-24.88762	821.16	814.15	7.01
H02-1252	30.00618	-24.89595	828.5	805.9	22.6
H02-1828	30.04759	-24.86334	801.82	788.04	13.78
H02-1829	30.10704	-24.81053	776.66	770.14	6.52
H02-1831	30.11611	-24.80479	770.05	762.5	7.55
H02-1835	30.0377	-24.87303	813.79	809.57	4.22
H02-1837	30.02772	-24.88521	819.45	807.99	11.46
H02-1839	30.01899	-24.89265	869.23	849.83	19.4
H02-1842	30.15376	-24.73961	781.3	773.3	8
H02-3159	30.00522	-24.88646	869.23	863.06	6.17
H02-3178	30.07264	-24.83269	805.1	790.86	14.24
H02-3550	30.09181	-24.80958	802.23	787.82	14.41
H02-3576	30.13306	-24.7313	838.89	829.79	9.1
H35-0023	30.15415	-24.82885	861.42	847.9	13.52
H35-0025	30.13968	-24.83848	870.01	851.02	18.99
H35-0026	30.13217	-24.81714	820.35	799.64	20.71
H35-0064	30.05628	-24.90255	915.66	895.95	19.71
H35-0070	30.06151	-24.9213	955.72	921.49	34.23
H35-0073	30.04974	-24.92004	945.35	915.95	29.4
H35-0080	30.07331	-24.89317	925.1	914.38	10.72
H35-0182	30.06632	-24.9151	958.03	922.73	35.3
H35-0201	30.05296	-24.92169	945.21	911.41	33.8
H35-0202	30.04407	-24.93651	980.96	936.16	44.8
H35-0203	30.03873	-24.93367	968.88	930.48	38.4
H35-0206	30.05708	-24.90591	920.76	894.06	26.7
H35-0207	30.05245	-24.91298	932.07	906.4	25.67
H35-0209	30.07092	-24.89628	915.6	901.4	14.2
H35-0210	30.03697	-24.93281	968.28	933.02	35.26
H35-0211	30.05429	-24.9315	967.92	926.14	41.78
BH0	30.1154	-24.8678	939	906.38	32.62
BH03	30.1113	-24.8749	907	881.36	25.64
BH07	30.1209	-24.8445	890	863.6	26.4
BH12	30.1177	-24.8663	930	909.43	20.57
BH14	30.117	-24.8665	925	902.16	22.84
BH15	30.1166	-24.8662	925	900.92	24.08
SPK1	30.1478	-24.7898	782.7362	768.9762	13.76
SPK2	30.14909	-24.7931	794.8145	773.0145	21.8
GB1	30.14909	-24.7714	752.4025	743.4225	8.98

GB7	30.1541	-24.7725	751.1086	744.2786	6.83
GB8	30.15401	-24.77306	752.8715	743.2915	9.58
GB2	30.1552	-24.7712	752.9049	746.0249	6.88
GB3	30.1557	-24.7709	752.2009	744.8709	7.33
GB4	30.1564	-24.7709	751.8414	746.4714	5.37
GB5	30.1571	-24.7706	750.9224	742.4624	8.46
GB6	30.1579	-24.7703	751.1497	746.4597	4.69
NEW BH03	30.1653	-24.7687	775.3406	768.9406	6.4
GB9	30.1655	-24.7945	846.3975	834.5875	11.81
GB10	30.1662	-24.7973	853.0911	841.3111	11.78
NEW BH02	30.1936	-24.7667	773.3593	769.8693	3.49
GB11	30.1674	-24.7919	844.7079	833.2879	11.42
NEW BH01	30.1677	-24.7658	775.0507	765.3107	9.74
NEW BH04	30.16803	-24.7717	791.9342	783.3042	8.63
SRK09	30.1703	-24.7648	787.1334	779.1534	7.98
SRK8D	30.1702	-24.7659	789.0435	782.0435	7
SRK08	30.1704	-24.7659	789.5757	780.8757	8.7
SRK10S	30.1704	-24.76901	789.2233	778.1233	11.1
BH-02	30.1354	-24.8905	963	928.71	34.29
BH-03	30.1407	-24.8921	977	950.05	26.95
BH-PLT	30.1192	-24.8928	924	900.98	23.02
BH-TAIL2	30.1126	-24.8884	884	881.48	2.52
TWF01	30.1078	-24.9005	891	883.48	7.52
WMON-7	30.1252	-24.8814	925.5	914.45	11.05
WMON-5	30.1216	-24.8806	916.5	904.91	11.59
BH-TAIL1	30.1134	-24.8854	873.5	871.1	2.4
BH/DWARS	30.1119	-24.8865	870.4	868.05	2.35
TWF02	30.11202	-24.8853	873	866.2	6.8
BH-TAIL3	30.1148	-24.8875	881.3	877.3	4